THE ALLOSTERIC NAD-SPECIFIC ISOCITRATE DEHYDROGENASE FROM NEUROSPORA CRASSA

by

Robert A. Cook

A thesis

submitted to

the Faculty of Graduate Studies and Research

University of Manitoba

In partial fulfilment

of the requirements for the degree

Doctor of Philosophy

1967

To my late father, Adolf W. Cook and my mother, Bernice Cook, whose early advice and continued encouragement made this work possible.

ACKNOWLEDGEMENTS

The author is grateful to Dr. B. D. Sanwal for his encouragement, advice and patient guidance throughout this work and in the preparation of this manuscript. Thanks are due to Dr. I. Suzuki, Peter Maeba, and F.W.J. Davis for their stimulating discussions, advice and aid concerning various aspects of this investigation.

ABSTRACT

The NAD-specific isocitrate dehydrogenase of Neurospora crassa has been examined both by steady-state kinetic studies and equilibrium binding studies.

The kinetic data indicated that the reaction mechanism is Random in the absence of AMP and it changes to either Rapid Equilibrium Random or Ordered in its presence.

Equilibrium binding studies indicated that isocitrate dehydrogenase has two binding sites for NAD, AMP and citrate, but four binding sites for isocitrate.

A model for isocitrate dehydrogenase, consistent with the data, is proposed. The enzyme is considered to consist of two non-identical subunits only one of which is productive, i.e., releases the substrates.

TABLE OF CONTENTS

TABLE OF CONTENTS CONT'D

TABLE OF CONTENTS CONT'D

TABLE OF CONTENTS CONT'D

LIST OF TABLES

LIST OF FIGURES

LIST OF FIGURES CONT'D

LIST OF FIGURES CONT'D

LIST OF FIGURES CONT'D

LIST OF FIGURES CONT'D

ABBREVIATIONS

ADH	- alcohol dehydrogenase
AMP	- adenosine-5'-monophosphate
ATP	- adenosine-5'-triphosphate
3'5'-AMP	- cyclic adenosine monophosphate
CTP	- cytidine-5'-triphosphate
dCMP	- deoxycytidine-5'-monophosphate
dCDP	- deoxycytidine-5'-diphosphate
dCTP	- deoxycytidine-5'-triphosphate
DEAE	- diethylaminoethyl
EDTA	- ethylenediamine tetracetic acid
F-1,6-P	- fructose-1,6-diphosphate
IDH	- isocitrate dehydrogenase
Mg^{++}	- divalent magnesium
MDH	- malic dehydrogenase
NAD	- nicotinamide-adenine dinucleotide
NADH	- reduced nicotinamide-adenine dinucleotide
dTTP	- deoxythymidine triphosphate
TRIS	- trihydroxymethylaminomethane
UDP	- uridine-5'-diphosphate

INTRODUCTION

INTRODUCTION

Two trends in the kinetic analysis of allosteric enzymes (Monod et al., 1965) have been evident in recent years. Based on the general theory proposed by Monod et al., (1963, 1965), a number of workers (see Atkinson, 1966; Stadtman, 1966) have attempted to explain their findings in terms of 'allosteric transitions', i.e., on the assumption that the peculiar kinetic properties of allosteric enzymes are due to the displacement of equilibria between two accessible states of the protein brought about by the binding of allosteric ligands. On the other hand, the mechanism of reactions catalyzed by allosteric enzymes has been explained by various workers on the basis of an extension of the 'induced fit' theory of Koshland (Koshland et al., 1966; Atkinson et al., 1965) which in its present generalized form maintains that binding of effectors or substrates creates 'active' sites or new enzyme forms (hybrids) very similar to the kind discussed by Adair (1925) for hemoglobin.

Mathematical descriptions of both models (Monod et al., 1965); Koshland et al., 1966), however, have relied entirely,

or very heavily, on the assumption of a real thermodynamic equilibrium during catalysis. This assumption while true in the case of oxygen binding to hemoglobin is, of course, untenable for a vast majority of enzymes which both *in vivo* and *in vitro* function in a steady-state. If the thermodynamic equations are applied to actual binding of ligands to allosteric enzymes, it is almost impossible to distinguish between the "allosteric transition" or "induced fit" models, (Anderson and Weber, 1965; Daniel and Weber, 1966) unless methods are available to find the 'function of state' (Monod *et al.*, 1965) of the enzyme, or stable 'hybrid' enzyme forms (Koshland *et al.*, 1966) are demonstrated by physico-chemical techniques.

A survey of literature on allosteric enzymes shows that with a few exceptions (Frieden, 1964; Lowry *et al.*, 1967) no serious attempts have been made to apply steady-state kinetic theory to these enzymes, although it has witnessed sophisticated developments in recent years (King and Altman, 1956; Reiner, 1959; Dalziel, 1957; Cleland, 1963a,b,c). Together with the equilibrium binding data, steady-state theories could very easily be used to support or discard mechanisms of action proposed for allosteric enzymes so far.

It was with this aim in view that the work presented here was undertaken with the regulatory NAD-specific isocitrate dehydrogenase of Neurospora crassa.

HISTORICAL

HISTORICAL

General

One of the most remarkable features of living organisms is their ability to coordinate cellular activity so that a constant balance is maintained between various catabolic processes and biosynthetic reactions essential to survival. The elucidation of numerous pathways of intermediary metabolism and the characterization of the enzymes that catalyze the multistep reaction sequences involved, has set the stage for current investigations of the regulatory mechanisms.

The early observation of Dische (1940) that the phosphorylation of glucose in erythrocyte hemolyzates was specifically inhibited by phosphoglycerate indicated that end products could regulate their own synthesis. A similar observation was made by Roberts *et al.* (1955), who working with *E. coli*, noted that *de novo* synthesis of various amino acids were supplied exogenously in the growth medium. The demonstration that end products had the capacity to inhibit the early steps unique to their biosynthesis (Umbarger, 1956)

and also to curtail the synthesis of one or more of the enzymes in the biosynthetic pathway (Cohen et al., 1953; Gorini and Mass, 1956) indicated that two separate mechanisms of regulation were present. These mechanisms were referred to as feedback inhibition and repression, respectively. The enzymes which were susceptible to activation or inhibition by metabolite effectors other than the catalytically active substrates were termed "regulatory enzymes". Since there was normally no structural similarity between the effector metabolites and the catalytically active substrate, it was assumed that modulation of the enzyme activity was achieved through the binding of the metabolite effectors at specific regulatory sites that were distinct from the catalytic sites. Due to this structural dissimilarity between substrate and effectors, Monod, Changeux and Jacob (1963) proposed that the latter be called allosteric effectors and their binding sites, allosteric sites. Accordingly, the regulatory enzymes are commonly referred to as allosteric enzymes.

Properties of Allosteric Enzymes

Allosteric enzymes are characterized by several distinctive features as compared to non-regulatory "classical

enzymes".

A. One of these features is the initial velocity pattern obtained in a kinetic analysis of the enzyme. The initial velocity data obtained in the case of non-regulatory enzymes is normally a rectangular hyperbola defined by the Michaelis-Menton equation:

$$v = \frac{VS}{K_m + S} \qquad \ldots\ldots\ldots (1)$$

The presence of inhibitors or activators does not change the shape of the rectangular hyperbola, but does however alter the parameters associated with the Michaelis-Menton equation, i.e., V_{max} or K_m. Inhibitors are, therefore, classed as competitive, noncompetitive or uncompetitive depending upon whether only the K_m is changed or V_{max} or both of the parameters. (See, Cleland, 1963a,b,c,d).

In the case of regulatory enzymes, however, a variety of plots are obtained when velocity is measured as a function of substrate concentration alone. In the presence of allosteric effectors these plots generally change their shape. In the literature three main types have been described which can be conveniently described under the following headings:

Fig. 1. Plot of velocity versus substrate concentration exhibited by Class I allosteric enzymes. (Sigmoid Response).

O is in the absence of effectors

A is in the presence of activators

I is in the presence of inhibitors

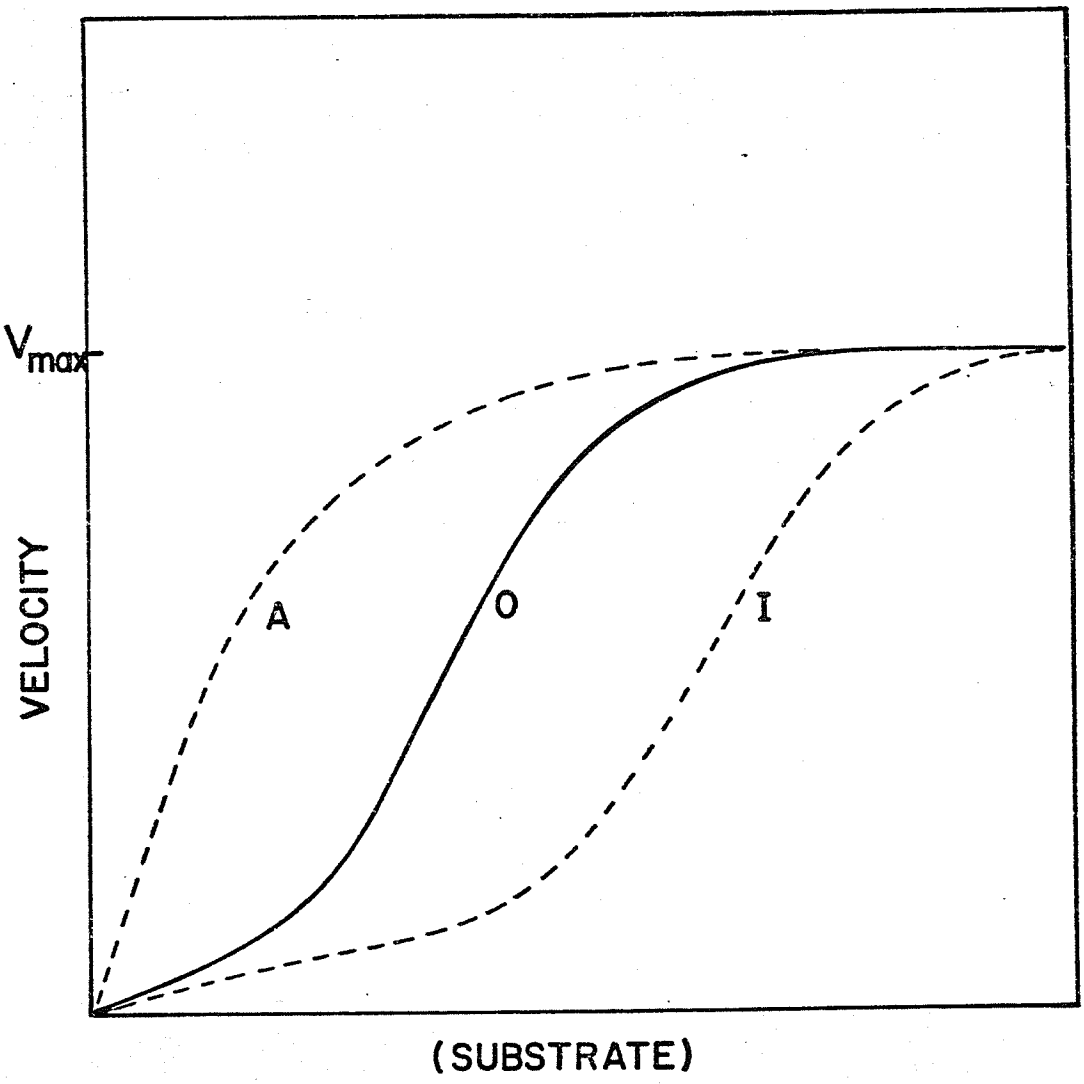
V_{max}
VELOCITY
A
O
I
(SUBSTRATE)

1. Sigmoid Response (Fig. 1)

With this class of enzymes, the rate-substrate concentration curve is sigmoid, i.e., it shows a cooperative behaviour. The shape of this curve (Fig. 1) is changed fundamentally in the presence of activators or inhibitors in direct contrast to the non-regulatory enzymes. Thus, in the presence of saturating concentrations of activator or inhibitor, the originally sigmoid curve is converted to a hyperbola. In the presence of less than saturating concentrations of an inhibitor, the curve becomes more cooperative or more sigmoid in nature. For a bireactant enzyme, i.e., an enzyme having two substrates, both substrates may or may not show cooperativity. One of the best understood allosteric enzymes, Aspartate Transcarbamylase (ATCase) from E. coli (Gerhart and Pardee, 1962, 1964), demonstrates this behaviour. A velocity versus aspartate concentration curve is sigmoid in this case. In the presence of ATP, the specific activator, the curve becomes hyperbolic, but in the presence of a specific inhibitor, CTP, it becomes more sigmoidal. The second substrate, carbamyl phosphate in contrast, does not exhibit any sigmoid response, although it is essential for the binding of aspartate (Changeux, Gerhart and Schachman,

1967). Similar results, barring details, have been obtained for several other allosteric enzymes as shown in Table 1.

It is important to point out that exceptions to this behaviour have been noted by Atkinson et al. (1965) in the case of isocitrate dehydrogenase from yeast and phospho-fructokinase from E. coli (Atkinson and Walton, 1965). In both cases the allosteric activators are unable to convert the cooperative curve for substrates into a hyperbola. However, in most cases it is clear that both negative as well as positive effectors change the apparent affinity of the substrate without changing the V_{max}.

The saturation curves of the effectors are significantly different for allosteric enzymes when compared to the non-regulatory enzymes. In the case of non-regulatory enzymes, the velocity of the enzyme decreases in a hyperbolic manner with the increasing concentration of inhibitor at any concentration of substrate. The behaviour with allosteric enzymes is fundamentally different depending upon the concentration of substrate. At low substrate concentrations the inhibitor shows a hyperbolic response but at high substrate concentration the response is sigmoid. The opposite holds for activators. Therefore, the saturation functions for

substrate, inhibitor and activator are sigmoid. Monod et al. (1965), whose theory will be discussed at length later, has classified these interactions into two categories:

1) Homotropic interactions, where a single ligand shows cooperative behaviour in the absence of all others.

2) Heterotropic interactions where interaction is seen only in the presence of two ligands.

2. Hyperbolic Response

a) Substrate non-cooperativity (V system of Monod et al., 1965).

The enzymes of this class show no homotropic interactions of the substrate, i.e., the rate-concentration curves are hyperbolic as in the case of non-regulatory enzymes. In the presence of an inhibitor or activator, the curves do not change shape. However, very importantly, the inhibitor or activator show homotropic or cooperative interaction. This behaviour is typified by the enzyme fructose diphosphatase from beef liver (Taketa and Pogell, 1965) and from frog muscle (Salas et al., 1964). In this case, the velocity versus fructose diphosphate concentration curves are hyperbolic and in the presence of a specific inhibitor, AMP, the curves remain hyperbolic. The K_m is unaltered in the presence of the

effector but a change in V_{max} occurs. However, the inhibitor saturation curve is sigmoid. Several other examples of this class of enzymes are given in Table 1.

b) Effector (inhibitor or activator) dependent substrate cooperativity.

In this class of enzymes, the substrate curve is hyperbolic as in the (2a) class of enzymes, but unlike the latter, these curves become sigmoid in the presence of inhibitors or activators, with a resultant K_m change for substrate with or without a concomitant change in V_{max}. In addition, both activators and inhibitors show cooperativity. Several enzymes exhibit this behaviour as indicated in Table 1.

3. Substrate Activation

A few enzymes are known (Table 1) where the substrate exhibits two K_m values. Generally, the effectors do not cause a change in the rate-concentration curves.

B. Desensitization and Dissociation

A second peculiarity of allosteric enzymes is the phenomenon of desensitization. The term desensitization refers to a change of enzyme brought about by environmental factors which lead to the loss of both homotropic and heterotropic

Table 1. General properties of some allosteric proteins from various organisms. (-) represents inhibitors and (+) represents activators.

Enzyme	Allosteric effectors	Class	References
aspartate transcarbamylase	CTP (-) ATP (+)	I	Gerhart and Pardee (1962, 1964) Changeux et al. (1967)
threonine deaminase	valine (+) L-isoleucine (-)	I	Freundlich and Umbarger (1963) Changeux (1961, 1963) Cennamo et al. (1964) Maeba and Sanwal (1966)
phosphofructokinase	3'-5'AMP (+) ATP (-)	I	Mansour and Mansour (1962) Atkinson and Walton (1965) Passonneau and Lowry (1962) Blangy (1967)
phosphorylase b	5'AMP (+) ATP (-)	I	Helmreich and Cori (1964) Madsen (1964) Ullman et al. (1964)
isocitrate dehydrogenase	citrate (+) AMP (+)	I	Hathaway and Atkinson (1963) Atkinson et al. (1965) Sanwal et al. (1964, 1965, 1966) Chen et al. (1963, 1964)
deoxycytidylate aminohydrolase	dCTP (+)	I	Scarano et al. (1963, 1964) Maley and Maley (1964)

Table 1 (continued)

Enzyme	Allosteric effectors	Class	References
fructose diphosphatase	AMP (-)	IIa	Takata and Pogell (1965) Salas et al. (1964) Krebs (1964)
aspartokinase (lysine)	lysine (-)	IIa	Stadtman et al. (1961) Patte and Cohen (1964)
ATP-PRPP pyrophosphorylase	histidine (-)	IIa	Martin (1962)
α-isopropylmalate synthetase		IIa	Gross et al. (1963)
glycogen synthetase	glucose-6-PO_4 (+)	IIa	Traut and Lipmann (1963) Algranati and Cabib (1962)
L-glutamine D-fructose-6-phosphate transaminase	UDP-N-acetyl hexosamine (-)	IIa	Kornfield et al. (1964)
dTDP-D-glucose pyrophosphorylase	d-TDP-L-rhamnose (-)	IIb	Melo and Glaser (1965)
UDP-d-glucose dehydrogenase	UDP-D-xylose (-)	IIb	Neufeld and Hall (1965)
PEP-carboxylase	CDP (+) aspartate (-) F-1-6-diP (+) acetyl-CoA (+)	IIb	Maeba and Sanwal (1965) Sanwal and Maeba (1966a, 1966b)

Table 1 (continued)

Enzyme	Allosteric effectors	Class	References
homoserine dehydrogenase (R. rubrum)	L-threonine (-)	III	Sturani et al. (1963) Datta et al. (1964)
aspartokinase (Rps. capsulatus)	threonine (-) + lysine	III	Datta and Gest (1964)

effects caused by substrate, inhibitors or activators.

Examining the case of aspartate transcarbamylase, for instance, Gerhart and Pardee (1962) noted that if the enzyme was heated to 60° C, or treated with urea or thiol-reagents such as PCMB or other mercurials, it became desensitized to the effect of the activator ATP and the inhibitor, CTP. The cooperativity or homotropic interactions of the substrate were simultaneously lost. This effect was found to be due to the dissociation of the enzyme into subunits. Gerhart and Schachman (1965) have shown that the native enzyme has a molecular weight of 300,000 corresponding to an S value of about 12. In the presence of desensitizing agents the enzyme dissociates into two types of subunits, one regulatory (2.8S) and one catalytic subunit (5.8S). Both the regulatory as well as the catalytic subunits carry four binding sites (Changeux, Gerhart and Schachman, 1967). The regulatory subunit binds only CTP and ATP while the catalytic subunit binds the substrates or substrate analogues. This remarkable construction of an allosteric enzyme is uniquely restricted so far to ATCase, despite claims to the contrary for some other allosteric enzymes (Rosen et al., 1966). Several other enzymes have been desensitized to the action of the effectors

such as phosphoribosyl-ATP pyrophosphorylase (Martin, 1962), threonine deaminase of E. coli (Changeux, 1961, 1963), homoserine dehydrogenase of R. rubrum (Sturani et al., 1963; Datta et al., 1964) fructose diphosphatase (Rosen et al., 1966) and PEP carboxylase (Sanwal et al., 1966).

In nearly all cases of desensitization, the catalytic activity is preserved, but the allosteric property is lost which suggests a separate effector binding site on the enzyme. Normally, desensitization is not accompanied by changes in the sedimentation velocity and molecular weight of the enzyme. In some cases, however, the binding of allosteric ligands do cause changes in sedimentation. This is the case with homoserine dehydrogenase of R. rubrum where the activators methionine and isoleucine as well as the substrate promote dissociation and the inhibitor promotes aggregation (Datta et al., 1964). In the case of deoxycytidylate deaminase (Maley and Maley, 1964), in the presence of substrate dCMP the enzyme exhibits an S value of 1-2, but in the presence of activator dCTP, the enzyme becomes associated (7-8S). Similarly, in the case of acetyl-CoA carboxylase, the activator, citrate, causes the enzyme to polymerize (Vagelos et al., 1963). A protein concentration dependent aggregation-deaggregation

phenomenon brought about by various effectors has been described also for bovine glutamate dehydrogenase (Frieden and Colman, 1967).

It may therefore be concluded that desensitization is a general phenomenon and must be accounted for by any kinetic theory. Aggregation-deaggregation phenomenon do not appear to be universal and may or may not be connected with allostery proper.

Theories of Allosteric Action

Several molecular mechanisms have been proposed to explain all or most of the observed properties of the various classes of allosteric enzymes so far described.

A. Allosteric Theory

The most generalized theory so far proposed has been that of Monod, Wyman and Changeux (1965). The essential points of this theory are:

1) Allosteric enzymes are symmetrical oligomers constituted of identical protomers, which may vary in number from one enzyme to another. A protein may consist of either one monomer (one polypeptide chain) or may be constituted of two or more monomers (different chains) combined together. Thus for an oligomer of

the constitution ($\alpha\alpha\alpha\alpha$) like lactic dehydrogenase, α is at once a monomer as well as a protomer, but for an enzyme like aspartate transcarbamylase which is ($\alpha_4\beta_4$), a protomer is ($\alpha\beta$) constituted of two different monomers. The protomers which may have no symmetry by themselves, however, gain symmetry when associated in a polymer.

2) The protein oligomer exists in two or perhaps more conformations (designated R and T) in solution, and these are in thermodynamic equilibrium (defined by a constant L) with each other in the absence of ligands.

3) In each protomer there is exactly <u>one</u> site corresponding to each ligand it is capable of binding, i.e., if an enzyme has one substrate, one activator and one inhibitor, each protomer carries three distinct and separate sites each binding to its stereospecific ligand. <u>The binding of any one ligand is completely independent of binding of any other</u>. The binding affinity for each ligand is different in each of the two states, but for every protomer is the same in any given state.

4) One of the states, e.g., R is stabilized by substrate and activator and the other state, e.g., T is stabilized by inhibitor. Therefore, each acts by displacing the equilibrium L to favour one or the other state. At saturating concentration

of inhibitor, therefore, all enzyme is in the state T while at saturating concentrations of activator or substrate, the enzyme is all in state R.

5) For an enzyme which largely exists in the T form, for example, binding of substrate to any protomer changes the configuration of all protomers (bound or unbound) to state R. It is thus an all-or-none process and is highly cooperative.

With these basic assumptions, it is possible to analyze the interactions of such a model protein with a single ligand (F) endowed with differential affinity toward the two accessible states. The states R_o and T_o are assumed to be in equilibrium governed by the dissociation constant L, commonly referred to as the "allosteric constant". Let K_r and K_t be the microscopic dissociation constants of a ligand F bound to a stereospecific site, in the R and T states respectively. These dissociation constants are the same for all homologous sites in each of the two states. Assuming n protomers and using the notation R_o, R_1, R_2, etc. -------- R_n; and T_o, T_1, T_2, etc. -------- T_n to designate the complexes involving 0, 1, 2, etc. -------- n molecules of ligand the following equations can be written:

$$R_o \overset{L}{\rightleftharpoons} T_o$$

$$R_o + F \overset{K_r}{\rightleftharpoons} R_1 \qquad T_o + F \overset{K_t}{\rightleftharpoons} T_1$$

$$R_1 + F \rightleftharpoons R_2 \qquad T_1 + F \rightleftharpoons T_2$$

$$R_2 + F \rightleftharpoons R_3 \qquad T_2 + F \rightleftharpoons T_3$$

$$\vdots \qquad\qquad \vdots$$

$$R_{n-1} + F \rightleftharpoons R_n \qquad T_{n-1} + F \rightleftharpoons T_n$$

Taking into account the probability factors for the dissociation of the R_1, R_2, ------ R_n and T_1, T_2, ------ T_n complexes the following equilibrium equations can be obtained:

$$T_o = LR_o$$

$$R_1 = R_o \; n \; F/K_r \qquad T_1 = T_o \; n \; F/K_t$$

$$R_2 = R_1 \frac{n-1}{2} F/K_r \qquad T_2 = T_1 \frac{n-1}{2} F/K_t$$

$$\vdots \qquad\qquad \vdots$$

$$R_n = R_{n-1} \frac{1}{n} F/K_r \qquad T_n = T_{n-1} \frac{1}{n} F/K_t$$

It is now possible to define

a) the fraction of protein in the R state ($\overline{R}$):

$$\overline{R} = \frac{R_o + R_1 + R_2 + \text{-------} + R_n}{(R_o + R_1 + R_2 + \text{-----} R_n) + (T_o + T_1 + T_2 \text{-----} T_n)}$$

Using the equilibrium equations and setting $F/K_r = \alpha$ and $K_r/K_t = c$ by the binomial expansion the following "function of state" is obtained:

$$\bar{R} = \frac{(1 + \alpha)^n}{L\,(1 + c\alpha)^n + (1 + \alpha)^n} \qquad \ldots\ldots\ldots (2)$$

b) The fraction of sites actually bound by the ligand:

$$\bar{Y}_s = \frac{(R_1 + 2\,R_2 + \text{----} + nR_n) + (T_1 + 2\,T_2 + \text{----} nT_n)}{n\left[(R_o + R_1 + R_2 \text{----} + R_n) + (T_o + T_1 + T_2 \text{----} + T_n)\right]}$$

The "saturation function" can then be expressed as

$$\bar{Y}_s = \frac{\alpha\,(1 + \alpha)^{n-1} + Lc\alpha\,(1 + c\alpha)^{n-1}}{(1 + \alpha)^n + L\,(1 + c\alpha)^n} \qquad \ldots\ldots\ldots (3)$$

The presence of the three stereospecific ligands substrate (S), activator (A) and inhibitor (I) will alter these basic equations. Following the assumption given previously, the saturation function for substrate in the presence of activator and inhibitor may be written:

$$\bar{Y}_s = \frac{\alpha\,(1 + \alpha)^{n-1} + L'c\alpha\,(1 + c\alpha)^{n-1}}{(1 + \alpha)^n + L'\,(1 + c\alpha)^n} \qquad \ldots\ldots\ldots (4)$$

or,

$$\bar{Y}_s = \frac{\alpha}{1 + \alpha} \bar{R} + \frac{c\alpha}{1 + c\alpha} (1 - \bar{R}) \qquad \ldots\ldots\ldots (5)$$

where α is defined as before and L' is an "apparent allosteric constant" defined as:

$$L_1 = \frac{\sum_o^n T_I}{\sum_o^n R_A}$$

where $\sum_o^n T_I$ and $\sum_o^n R_A$ stand respectively for the sum of the different complexes of the T state with I and of the R state with A. Following the same derivation,

$$L' = L \frac{(1 + \beta d)^n (1 + \gamma e)^n}{(1 + \beta)^n (1 + \gamma)^n} \qquad \ldots\ldots\ldots (6)$$

with $\beta = I/K_i$ and $\gamma = A/K_a$ where K_i and K_a stand for the microscopic dissociation constants of inhibitor and activator with the T and R states respectively.

Assuming, for example, that L is large ($> 10^5$) so that the enzyme is largely in the T state and that the affinity ratio of the substrate for T and R states is very low ($c < 10^4$), equation (4) reduces to

$$\bar{Y}_s = \frac{\alpha (1 + \alpha)^{n-1}}{L' + (1 + \alpha)^n} \qquad \ldots\ldots\ldots (7)$$

Since the affinity of the T state is very low for substrate, the first molecules bind with difficulty, but this binding converts the protomers to the R state which has a high affinity for substrate. A sigmoid or cooperative curve results; the degree of cooperativity obviously then is dependent upon the values of n, L, and c. The model, therefore, accounts for the homotropic cooperative effects mentioned previously. In the presence of saturating levels of activator, all of the enzyme is converted to the R state and the substrate shows no cooperativity since the substrate binds to only one state having protomers with the same affinity. At low substrate concentrations, the activator shows pronounced cooperativity because it can bind with different affinity to both the R state and T state which are both present.

Similarly, at high substrate concentrations, the enzyme exists in the R state and I shows cooperativity because it binds with difficulty to R, but once bound, converts the enzyme to the T state which binds inhibitor with high affinity. Thus this model explains both the homotropic and heterotropic cooperative effects exhibited by those enzymes giving the sigmoid response mentioned previously (K system).

Similarly, the so called V system (2a) can be explained by this model. The assumption is made that the affinity of the R and T states is the same for the substrate i.e. c = 1 and that only the R state is active i.e. the only state capable of releasing products. Under these conditions the saturation function (4) reduces to

$$\bar{Y}_s = \frac{\alpha}{1 + \alpha} = \frac{F}{K_r + F} \qquad \ldots\ldots\ldots (8)$$

which is the form of the Michaelis-Menton equation (1). Thus initial velocity patterns will be hyperbolic. An effector has, however, differential affinity for the R and T states and will always show cooperativity while the substrate will not.

Although Monod et al., (1965) have not discussed Class 2b enzymes described before, the allosteric model can easily be extended to include these. The only assumption that has to be made is that most of the enzyme is present in the R state (note that in the K system the enzyme is considered to be present primarily in the T state), i.e., a state of high affinity for the substrate. With this assumption it is easy to see that the rate-concentration curve for substrate will

be hyperbolic but will become sigmoid in the presence of an inhibitor for which the R state represents a state of low affinity. The cooperativity would result simply by a displacement of the R to the T state by the inhibitor.

Desensitization can be easily understood by this model and is the only model which does explain this phenomenon. Desensitization as previously described leads to the conversion of sigmoid kinetics to hyperbolic kinetics and to loss of effect of activators and inhibitors. According to this model, loss of interactions would follow from any structural alteration that would make one of the two states (R or T) virtually inaccessible. Thus, limiting the model to only one state would result in loss of both homotropic and heterotropic interactions.

The observations on several allosteric proteins (Atkinson et al., 1965a,b; Atkinson, 1966) appear to be inconsistent with the simple exclusive binding predicted by this model. Further predictions have been derived for the general case in which both the postulated states of an allosteric protein bind a specified ligand with significant but unequal affinity i.e. non-exclusive binding (Rubin and Changeux, 1966). In particular, the non-exclusive binding of

one or more of the ligands i.e., substrate, inhibitor, or activator is expected to introduce limits on:

1) The extent to which the equilibrium between the conformational states of the protein may be shifted in their presence;

2) the degree of cooperativity in the saturation of each ligand (as measured by the Hill coefficient);

3) the extent of cooperative or antagonistic interactions among the various ligands (partial and multivalent effects).

In order to measure the cooperativity of a saturation curve, the equations for characterizing the binding of oxygen to hemoglobin have been generally employed (Brown and Hill, 1923). At any degree of saturation, the binding of a ligand s to a protein is given by an equation of the type

$$E + nS \underset{}{\overset{K}{\rightleftharpoons}} ESn \qquad \ldots\ldots\ldots (9)$$

which by suitable manipulation yields:

$$\log \frac{ESn}{E} = \log \frac{\bar{Y}}{1 - \bar{Y}} = n \log S - \log K \qquad \ldots\ldots\ldots (10)$$

Plotting $\log \bar{Y}/1 - \bar{Y}$ as a function of log P (where P was the partial pressure of oxygen and Y was the saturation function of hemoglobin i.e., $\frac{HbO_2}{Hb + HbO_2}$), Hill obtained an

approximate value for n. By analogy, this equation is applied to any allosteric protein by plotting log α as a function of log $\bar{Y}/1 - \bar{Y}$ from equation (5). The slope of the curve gives "n" (for c = 0):

$$\text{"n"} = \frac{d\left(\log \frac{\bar{Y}}{1-\bar{Y}}\right)}{d(\log \alpha)} = 1 + \frac{(n-1)\,L\alpha}{(1+\alpha)\,L + (1+\alpha)^{n-1}} \qquad \ldots\ldots\ldots (11)$$

It is obvious that n = 1 when α = 0 or . The maximum value of "n" termed n_{max} is obtained from d"n"/dα = 0. This derivative obtains a relation between L and the value α_{max} for which "n" = n_{max}.

$$L = (1 + \alpha_{max})^{n-1} \cdot \left[(n-1) \cdot \alpha_{max} - 1\right] \qquad \ldots\ldots\ldots (12)$$

and,

$$n_{max} = 1 + \frac{L}{(1 + \alpha_{max})^{n}} \qquad \ldots\ldots\ldots (13)$$

Rubin and Changeux (1966) have introduced a further parameter for the measurement of the effects of heterotropic ligands; the substrate concentration required for half saturation ($\alpha_{1/2}$). In terms of the allosteric model, the following relation between $\alpha_{1/2}$ and L' may be derived by

replacing $\bar{Y}_s$ by 1/2 in equation (4).

$$L' = \frac{\alpha_{1/2} - 1}{1 + \alpha_{1/2}c} \left(\frac{1 + \alpha_{1/2}}{1 + c\alpha_{1/2}}\right)^{n-1} \qquad \ldots\ldots\ldots (14)$$

Accordingly, log $\alpha_{1/2}$ is a sigmoid function of log L' when the value of c is greater than 0. By plotting n_{max} as a function of log L', a sigmoid line is obtained if c = 0, i.e., complete exclusive binding. The deviation from this line allows the determination of the degree of non-exclusive binding in a given case. Similarly, the importance of non-exclusive binding can be determined from a plot of n_{max} as a function of log $\alpha_{1/2}$ (12).

The degree of non-exclusive binding may be determined in still another way. The variation of the equilibrium constant L' with the concentration of e.g., activator, conforms to the equation

$$L' = L_o \cdot \frac{(1 + b\beta)^n}{(1 + \beta)^n} \qquad \ldots\ldots\ldots (6)$$

with $\beta = A/K_a$ and $b = K_{r(A)}/K_{t(A)}$

By plotting the nth root of L' as a function of A according to the equation

$$\frac{1}{\sqrt[n]{L'}} = \frac{1}{\sqrt[n]{L_o}} = \frac{1 + \beta}{1 + b\beta} \qquad \ldots\ldots\ldots (15)$$

a straight line is obtained at low values of A if the value of b is negligible, i.e., only exclusive binding is present. This line intersects the abscissa at a point corresponding to $-K_r(A)$ which is a measure of the affinity of a particular state for activator. The deviation of the line from linearity allows the calculation of the factor b, the degree of non-exclusive binding.

Similarly, at a constant substrate concentration, the presence of activator or inhibitor modifies the initial velocity by changing the value of the equilibrium $R \rightleftharpoons T$. In a perfect K system, it was previously shown that

$$\bar{Y} = \frac{V}{Vm} = \frac{\alpha}{1 + \alpha} \cdot \bar{R} + \frac{c\alpha}{1 + c\alpha}(1 - \bar{R}) \qquad \ldots\ldots\ldots (5)$$

In the particular case where c was negligible this equation reduced to

$$\frac{V}{Vm} = \frac{\alpha}{1 + \alpha} \cdot \bar{R} \qquad \ldots\ldots\ldots (8)$$

Defining V as the maximum velocity obtained in the

presence of a given concentration of substrate one obtains $v/V = R$ with $V = \alpha/1 + \alpha$. V_m and

$$\frac{v}{V - v} = \frac{\bar{R}}{1 - \bar{R}} = \frac{(1 + \alpha)^n (1 + \beta)^n}{L \cdot (1 + b\beta)^n} = \frac{1}{L(\alpha)} \cdot \frac{(1 + \beta)^n}{(1 + b\beta)^n} \quad \ldots\ldots\ldots (16)$$

This equation is best represented by plotting the nth root of $v/V - V$ $(= \bar{R}/1 - \bar{R})$ as a function of the affector concentration (A or β) according to the equation

$$\sqrt[n]{\frac{\bar{R}}{1 - \bar{R}}} = \sqrt[n]{\frac{v}{V - v}} = \sqrt[n]{\frac{1}{L(\alpha)}} \cdot (1 + \beta) \quad \ldots\ldots\ldots (17)$$

with the assumption again that b is negligible. If b is not negligible, the lines will become non-linear indicating non-exclusive binding and the factor b may be determined as before. Representation of results by equations (15 and 17) allows a simple determination of the affinity constants for any activator or inhibitor and also the degree of non-exclusive binding involved. Such representation has been attempted in the case of phosphofructokinase of E. coli (Blangy, 1967).

The question may now be asked whether or not the cooperative properties observed in kinetic analysis always reflect an isomerization process of the enzyme, i.e., the

different conformations of the enzyme in equilibrium. In the majority of cases in the literature, the cooperative properties of enzymes are observed by the initial velocity measurements of enzyme reactions. The observed effects of activators and inhibitors thus occurs in a steady-state system rather than an equilibrium state. It may therefore be hazardous to apply an equilibrium scheme such as that of Monod et al. (1965) to interpret a system in a steady-state.

In all steady state systems which deviate considerable from thermodynamic equilibrium, it is possible to obtain a cooperative binding curve of ligand X without it being necessary to consider an interaction between different acceptor sites for X. Consider a macromolecule containing only one site for the ligand X, but existing in two conformational states A and B.

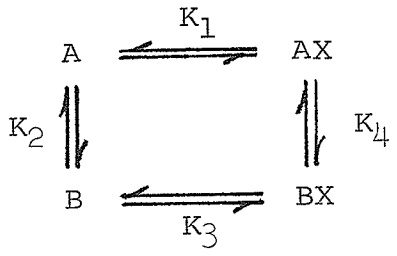

In the case of true equilibrium ($K_1K_2K_3K_4 = 1$), no cooperativity of the binding of X can be observed. If, under the influence of some external force, at least one of

the equilibrium constants is disturbed, the product $K_1K_2K_3K_4 \neq 1$ and the system no longer exhibits <u>any</u> equilibrium. There can be however a steady state in which there is a constant reaction round the square in one sense or the other maintained by a constant supply of energy, by binding of substrate or release of product, for instance. Under these conditions one can demonstrate that the binding of X may be expressed (if the rate constants are suitably chosen) by a Hill coefficient approaching 2, as if the macromolecule had two sites for the ligand X. The expression for the ratio of bound to unbound enzyme forms becomes

$$\frac{\bar{Y}}{1 - \bar{Y}} = \frac{AX + BX}{A + B} \qquad \ldots\ldots\ldots (18)$$

and the resulting equation interms of rate constants has the following form:

$$\frac{\bar{Y}}{1 - \bar{Y}} = \frac{ax + bx^2}{c + dx} \qquad \ldots\ldots\ldots (19)$$

Higher values for the Hill coefficient can moreover be obtained if the number of conformational states of the enzyme are increased or the number of sites are increased. Such a model could be applied to several bimolecular reactions so

far studied. A careful kinetic study of the enzyme with several substrates is then necessary to affirm that the kinetic cooperativity reflects a change in enzyme conformation.

Several alternate mechanisms have been proposed to account for the sigmoidal saturation curves.

B. Induced-fit Theory

For the classical case of oxygen binding to hemoglobin, Adair (1925) suggested a mechanism involving four consecutive bimolecular steps with successively increasing affinity for the ligand. This mechanism may be expressed by the following equilibrium steps

$$P + A \rightleftharpoons QA$$

$$QA + A \rightleftharpoons RA_2$$

$$RA_2 + A \rightleftharpoons SA_3$$

$$SA_3 + A \rightleftharpoons TA_4$$

where A represents oxygen and P, QA, RA_2, SA_3 and TA_4 represent different forms of the enzyme. During each binding a discrete conformational change was assumed to take place. No attempt was made by Adair (1925) to bring in the concept of the subunit

structure of the protein molecule.

Koshland et al. (1966) have applied the "induced fit" hypothesis to explain the cooperative saturation curves obtained in allosteric enzyme systems. This theory postulates that in the free state, the enzyme does not possess active sites, but that the presence of substrate and its interaction with the protein creates these sites.

Assuming a tetrameric free enzyme A_4 (see Fig. 2) the prediction is made that the binding of a molecule of substrate (S) induces the formation of a hybrid structure A_3BS where B represents the subunit (A) having undergone a conformational change by the binding of S. This hybrid now possesses a greater stability than the form A_4 and the binding of the second molecule of substrate giving $A_2B_2S_2$ is found to be easier, the same process being repeated for each of the following states. On the other hand, the stability of structures of the type A_iB_{n-i} and those states of B not having bound substrate are assumed weak, i.e., all of the hybrid states of the type A_3B ------ AB_3, as well as the forms B_4S ------ B_4S_3, are present in negligible quantities. In considering only the sequence

$$A_4 \rightleftharpoons (A_3B)S \rightleftharpoons (A_2B_2)S_2 \rightleftharpoons (AB_3)S_3 \rightleftharpoons (B_4)S_4$$

Fig. 2. Binding of substrate (S) to a tetrameric enzyme. (A) and (B) represent two different conformational states of the subunit.

□ according to the allosteric model of Monod et al., 1965.

▩ according to the "induced fit" model of Koshland et al., 1966.

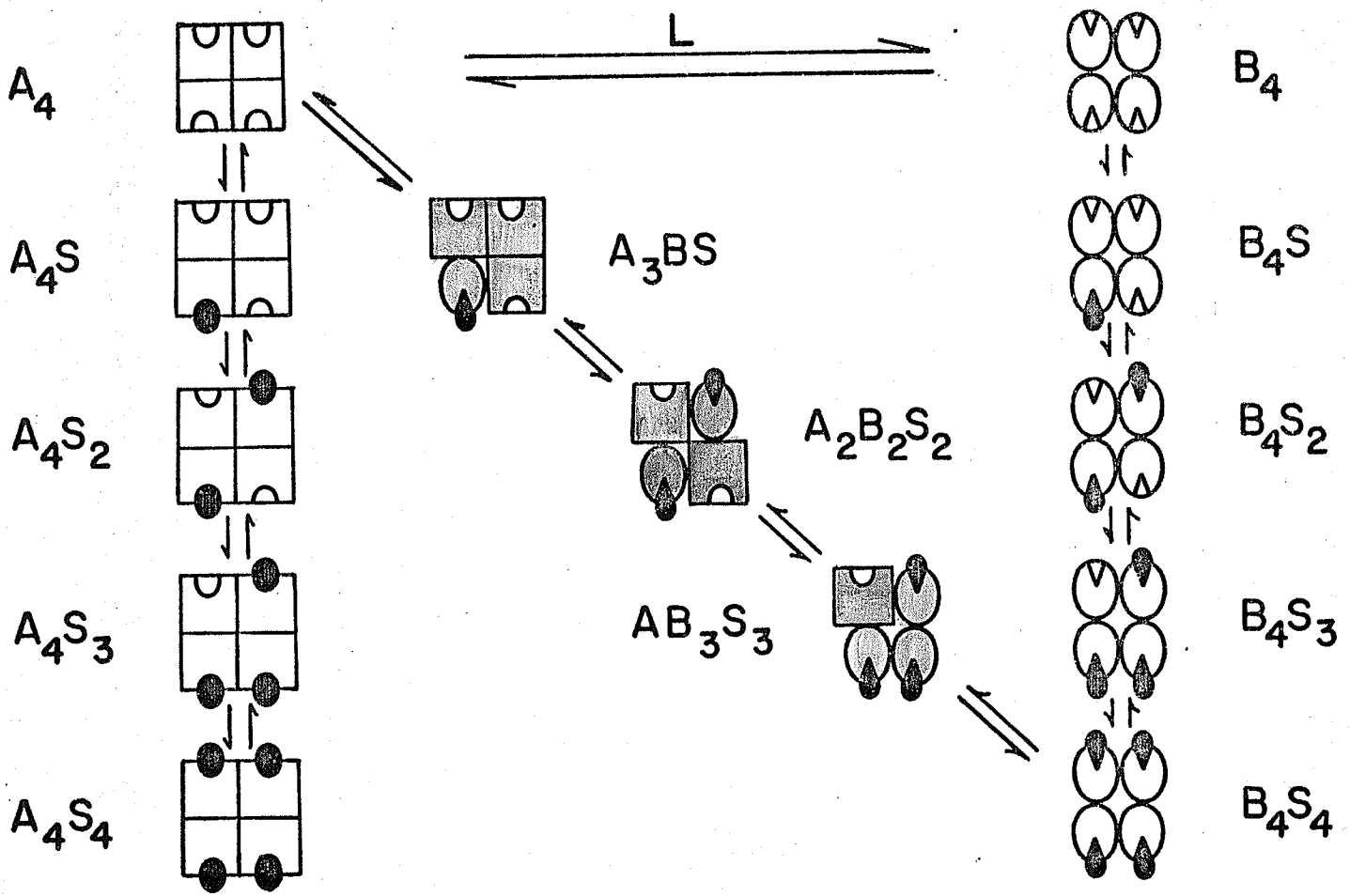
L
A4
A4S
A4S2
A4S3
A4S4
A3BS
A2B2S2
AB3S3
B4
B4S
B4S2
B4S3
B4S4

Koshland et al. (1966) have accounted for the cooperative properties of the hemoglobin-oxygen system.

Atkinson et al. (1965) have proposed an important model for ligand interactions which differs significantly from the model of Monod et al. (1965). The model which may be considered as an extension of the 'induced fit' theory of Koshland et al. (1966) is based on the Hill equation for the binding of oxygen to hemoglobin.

$$y = \frac{K\left[O_2\right]^n}{1 + K\left[O_2\right]^n} \qquad \ldots\ldots\ldots (20)$$

(where y = fraction of sites bound by oxygen, K is a complex dissociation constant, and n is the number of interacting binding sites). An analogous equation derived from equation (9) is utilized.

$$K = \frac{\left[E\right]\left[S\right]^n}{ESn} \qquad \ldots\ldots\ldots (21)$$

(where E is the concentration of free enzyme, S is the substrate concentration, Sn is the complex of n molecules of S per molecule of E and K is a complex dissociation constant, the product of the n dissociation constants of the separate binding steps). It is assumed in this analysis that

a) the reaction $ES_{n-1} + S \rightleftharpoons ES_n$ is the only rate limiting step.

b) the concentration of all ES complexes involving less than n molecules of S are negligibly small (or, in rapid equilibrium). This is shown to be possible mathematically when the binding of S is "sufficiently cooperative", i.e., when the value of the dissociation constants decrease for each successive S molecule bound. Under the above conditions,

$$v = K(ESn)$$

$$V_{max} = (kE_t)$$

(where k is the rate constant, v is the reaction rate, V_{max} is the rate at S saturating and E_t is the total enzyme concentration).

$$\text{Since } E = E_t - ESn$$

$$= \frac{V_{max} - v}{k}$$

$$kE = V_{max} - v$$

$$\text{Then, } \frac{(ESn)}{E} = \frac{v}{V_{max} - v} = \frac{(S)^n}{K}$$

$$\text{and, } \log \frac{v}{V_{max} - v} = n \log S - \log K \qquad \ldots\ldots\ldots (22)$$

Plots of log v/V - v versus log S yield straight lines of slope = n. The slope of the lines is considered to be a function both of the number of interacting sites per molecule and of the "strength" of the interactions.

Calculations of "interaction factors" (measuring the dependence of n on the strength of site interactions) are based on the assumptions:

a) Binding of one substrate molecule facilitates binding of others.

b) The intrinsic dissociation constants for substrate from all sites are equal.

c) Binding at any site has the same effect on all unbound sites.

d) The rate of reaction of each complex is proportional to the number of substrate molecules bound.

The model, in effect, states that the complex relationships found between substrates and modifiers in several enzyme systems are caused by progressive changes in ligand site interaction, i.e., the binding of a ligand at one site could either increase or decrease the affinity of a ligand at a second site, which can in turn affect the binding of a ligand at the third site, and so on.

Some attempts have been made to distinguish between the various proposed models for cooperative ligand binding in several systems. Notably, Kirschner et al. (1966) have attempted temperature-jump relaxation studies on the allosteric transition in the glyceraldehyde-3-phosphate dehydrogenase of yeast. Although the error limits of the method are high (± 25%), the authors have interpreted their results to indicate:

1) The apo-enzyme exists in two tetrameric conformations only.

2) The dissociation constants of the various binding sites on each isomer are identical and independent of each other.

3) The cooperativity between the subunits appears to be so high that the structural transition is an all-or-none phenomenon.

4) Very importantly, no evidence could be found for hybrid states of the type R_3T, etc..

The conclusion was, therefore, reached that only the model of Monod et al. (1965) fitted the results obtained with this enzyme.

Detailed kinetic and physical-chemical studies of allosteric enzymes such as aspartate transcarbamylase (Changeux,

Gerhart and Schachman, 1967) and phosphofructokinase of E. coli (Blangy, 1967) have supported the model proposed by Monod et al. (1965). However, at this time, none of the proposed models can be considered as a general model capable of explaining the kinetics of all allosteric enzymes. Modifications of both major models may be introduced to explain the exceptions in K systems so far observed. For example, the model of Monod et al. (1965) may be amplified by the abandonment of the postulate of the independence of identical binding sites. Similarly the model of Koshland et al. (1966) could be modified by permitting the ligand to bind to both conformations of the enzyme.

On the other hand, the possibility exists that just as "classical" non-regulatory enzymes obey various mechanisms (ordered, random, ping-pong, etc.), different allosteric enzymes may also follow a variety of mechanisms, in which case detailed steady-state kinetic and equilibrium binding study will be necessary to postulate these mechanisms.

Kinetics and Other Properties of Isocitrate Dehydrogenase from Various Sources.

Early studies on isocitrate metabolism in yeast

revealed the presence of two isocitrate dehydrogenases (Kornberg and Pricer, 1951). One of these utilized NADP as the coenzyme whereas the other required NAD as the coenzyme.

The NADP requiring enzyme corresponded in properties to the enzyme then known to occur in various animal tissues, plants and microorganisms. The most popular source of the highly purified enzyme was pig heart (Ochoa, 1948), and as a result the most detailed studies of the properties of the enzyme have been from this source. The NADP-specific isocitrate dehydrogenase catalyzed the oxidative decarboxylation of isocitrate to α-ketoglutarate (Adler et al., 1939) and in the reverse direction, the decarboxylation of oxalsuccinate (Ochoa, 1948) and the reduction of oxalsuccinate to isocitrate (Ochoa, 1948).

The NAD-specific isocitrate dehydrogenase from all sources so far investigated catalyzed the oxidative decarboxylation of isocitrate to α-ketoglutarate. In contrast to the NADP-dependent enzyme, the NAD-requiring enzyme cannot catalyze the decarboxylation or reduction of oxalsuccinate or the reductive carboxylation of α-ketoglutarate. As a result, the NAD-specific isocitrate dehydrogenase is believed to be

primarily responsible for the oxidation of threo-D_s-isocitrate (Ernster and Navazio, 1957; Kaplan et al., 1956). An additional difference between the two enzyme forms was the requirement of the NAD-specific enzyme for an additional cofactor, adenosine-5'-phosphate. The enzymes from yeast (Kornberg and Pricer, 1951) and Aspergillus niger (Ramakrishnan and Martin, 1955) were found to have an absolute requirement for this cofactor. The NAD-requiring enzymes from animal sources, Acetobacter aceti (Rao, 1955) and pea seedlings (Davies, 1955) are apparently not affected by AMP.

A possible regulatory role of AMP was postulated by Hathaway and Atkinson (1963) working with the NAD-specific isocitrate dehydrogenase from yeast. Adenylic acid was found not to be required for enzyme activity but affected markedly the rate of the reaction under some conditions. The authors noted that the AMP effect was a function of isocitrate concentration, i.e., at low levels of isocitrate, the presence of AMP appeared to be an absolute requirement for activity, but at high isocitrate (> 0.7 mM) only slight stimulation by AMP was obtained. The authors also observed that the enzyme was activated by citrate in the absence of AMP. It was concluded that the reaction catalyzed by the yeast enzyme was

unusually complicated in terms of interactions between substrates and activators. In general, an increase in concentration of any component of the reaction appeared to decrease the quantity of one or more other components required for half saturation. The suggestion was made that the enzyme contained two effectively different sites; the reaction site at which the catalysis actually occurred and an activating site which had to be occupied by isocitrate, AMP or citrate in order that the reaction site would be active.

The activity of NAD-specific isocitrate dehydrogenase from Neurospora crassa was found to be controlled by precursor activation and end product inhibition (Sanwal et al., 1963). The enzyme, purified approximately 100 fold, was activated by citrate, a precursor, and inhibited by α-ketoglutarate, the end product. The enzyme was found not to obey classical Michaelis-Menten kinetics at its pH optimum of 7.6. Sanwal et al., (1963) suggested that the enzyme contained two sites for isocitrate, a "regulatory" site and an "active" site. At pH 6.5 the enzyme obeyed classical Michaelis-Menten kinetics in the presence of saturating concentrations of AMP, suggesting that the regulatory site had apparently become "non-functional".

No activation or inhibition by citrate and α-ketoglutarate was found at pH 6.5, suggesting that this effect occurred only at the regulatory site. The authors proposed that since citrate activated the enzyme at low physiological levels, the "precursor activation" could have some importance in the regulation of cell metabolism.

A more detailed study of the NAD-specific isocitrate dehydrogenase from N. crassa was attempted by the same authors (Sanwal et al., 1964). The enzyme was found to be most active at a pH of 7.4-7.8, a pH at which sigmoidal curves of velocity versus isocitrate concentration were obtained. As previously reported, the same curves became hyperbolic at pH 6.4 (Sanwal et al., 1963).

Two possible explanations were presented:

1) At least two molecules of isocitrate participated in the reaction at pH 7.6, but only one molecule of isocitrate at pH 6.4.

2) This was not a true bimolecular reaction, but there was some type of interaction between homologous substrate sites, as in the case of the binding of oxygen to hemoglobin discussed previously.

Normal Michaelis-Menten plots of velocity versus

substrate were observed when NAD was varied, both at pH 7.6 and 6.4 in the presence of AMP.

The effect of AMP on the enzyme was tested and activation was noted, although the Km was dependent upon the concentration of isocitrate as previously reported with the yeast NAD-specific isocitrate dehydrogenase (Hathaway and Atkinson, 1963). From the results obtained, the authors suggested that AMP did not participate in the reaction by direct interaction with substrates or other cofactors. The activator AMP was suggested to function by causing intramolecular changes in isocitrate dehydrogenase.

A more detailed examination of the specificity of the allosteric and active sites was then undertaken (Stachow and Sanwal, 1965), using a highly purified enzyme preparation. The enzyme was found to be activated by citrate, as previously shown, and also by erythro-L_S-isocitrate at pH 7.6; this effect being 'competitive' with the substrate threo-D_S-isocitrate. The enzyme obeyed classical Michaelis-Menten kinetics, and activators had no effect on the velocity of the reaction at pH 6.5.

It was suggested that the enzyme had <u>at least</u> two sites, one specific active site which bound only threo-D_S-

isocitrate and at least one other allosteric site which bound citrate, erythro-L_s-isocitrate, α-ketoglutarate and glutamate. Binding of the latter two compounds led to an inhibition of enzyme activity. As had been shown previously (Sanwal et al., 1964), the requirement for AMP for the activation of the enzyme was dispensable in the presence of high citrate concentrations. Adenylic acid appeared to increase the affinity of both the allosteric and active sites.

It was suggested that citrate could effect the enzyme activity on the basis of conformational changes in the enzyme structure, as opposed to monomer-polymer interactions as reported for other enzymes such as acetyl-CoA carboxylase (Vagelos et al., 1963) and glutamate dehydrogenase (Cole and Frieden, 1967).

NAD-specific isocitrate dehydrogenase was studied from Aspergillus niger and Aspergillus flavus (Chan et al., 1965) and was found in both cases to be allosteric in nature, similar to the case of isocitrate dehydrogenase of Neurospora crassa.

Hathaway, Smith and Atkinson (1965) presented detailed kinetic data on the isocitrate dehydrogenase of yeast and proposed a model for the mode of action of this enzyme, which

is as follows:

a) The results of interaction between substrate and effectors are attributed to modified dissociation constants.

b) Binding of isocitrate at any site decreases the dissociation constant for isocitrate at other sites by a factor of 20.

c) Binding of NAD at a catalytic site decreases the dissociation constant for isocitrate by a factor of 20 at that site only, i.e., NAD interactions are indirect, mediated by the effect of isocitrate binding.

d) Binding of AMP at a regulatory site decreases the dissociation constant for isocitrate at all four sites by a factor of 5. AMP has no effect on isocitrate interactions.

e) Citrate can bind at any isocitrate site, is a competitive inhibitor of isocitrate at catalytic sites, and has the same effect on other parameters as does ^{iso}citrate.

The order of the reaction, n, was determined from the Hill equation as previously described and was found to be 3.9 for isocitrate and 1.7-2.0 for NAD, Mg++ and AMP. The conclusion was reached that the isocitrate dehydrogenase molecule probably has two catalytic sites, binding isocitrate, NAD, and Mg^{++}; two regulatory sites binding isocitrate, and

two regulatory sites binding AMP.

In calculating the overall kinetic order of the reaction, the assumptions of the Hill equation are presumed to hold. Since n = 4,

$$v_1 = k\,(ES_4A_2D_2M_2)$$

$$= \frac{k\,ES^4A^2D^2M^2}{K}$$

(where K is the overall dissociation constant, S is isocitrate concentration, A is AMP concentration, D is NAD concentration and M is magnesium concentration). As predicted by this equation, eleventh order kinetics are obtained in experiments on dilute systems.

Predictions from the model previously described (see Historical, General) appear to correspond to experimental results for the case of isocitrate dehydrogenase from yeast. However, as the authors themselves state, some of the assumptions on which the model is based seem unlikely, i.e., the assumption that both catalytic and regulatory sites have the same dissociation constant for isocitrate. A more serious fault is the questionable validity of the Hill equation as it applied to mechanisms about which few facts are known (see Discussion).

MATERIAL AND METHODS

MATERIALS AND METHODS

Chemicals

Reduced and oxidized NAD, AMP, calcium phosphate gel and DEAE-cellulose were obtained from Sigma Chemical Company. Dithiothreitol and D_sL_s-isocitric acid were obtained from Calbiochem. Corporation. Threo-D_sL_s-isocitric acid and threo-D_s-isocitrate were generous gifts of Dr. H. B. Vickery (Connecticut Agricultural Experiment Station). Crystalline enzymes were purchased from Boehringer and Soehne (Germany). Sephadex resins were obtained from Pharmacia (Sweden). Scintillation grade chemicals were obtained from the Packard Instrument Company and Nuclear Enterprises (Winnipeg, Canada). Reagent grade chemicals were routinely used and were obtained from various commercial sources.

Radioisotopes

Nicotinamide-7-C^{14} and Sodium isocitrate-5,6-C^{14} were obtained from New England Nuclear Corporation (Boston). Sodium citrate-5,6-C^{14} was obtained from Calbiochem. Corporation.

Adenylic acid-H^3 was obtained from Schwartz Bioresearch (Orangeburg, New York).

Genetic Strains

Isocitrate dehydrogenase was isolated routinely from the wild-type strain STA-4 of Neurospora crassa. The strain was originally obtained from the culture collection of the Fungal Genetics Stock Centre located at Dartmouth College, Hew Hampshire. Stock cultures of this strain of Neurospora crassa were maintained on agar slants of Neurospora Culture Agar (Baltimore Biological Laboratories, Inc.).

Growth Conditions

The basic growth medium used for culturing Neurospora crassa was Vogel's medium-N (Vogel, 1956). The stock solution of medium-N contained: Sodium citrate, 120 gm, potassium dihydrogen phosphate (anhydrous), 250 gm, ammonium nitrate, 100 gm, $MgSO_4 \cdot 7H_2O$, 10 gm, $CaCl_2 \cdot 2H_2O$, 5 gm, trace element solution, 5 ml and 0.01% biotin, 2.5 ml dissolved in glass-distilled water to yield a final volume of 1000 ml. Chloroform (5.0 ml/l) was added as preservative. The trace element

solution consisted of: citric acid, 5 gm, $ZnSO_4 \cdot 7H_2O$, 5 gm, $FeSO_4 \cdot 7H_2O$, 1 gm, $CuSO_4 \cdot 5H_2O$, 0.2 gm, $MnSO_4 \cdot H_2O$, 0.05 gm, anhydrous H_3BO_3, 0.05 gm, and $Na_2MoO_4 \cdot 2H_2O$, 0.05 gm, dissolved in 100 ml of glass distilled water. The stock solution was diluted fifty-fold with glass distilled water and supplemented with the appropriate sucrose concentration before inoculation.

Conidia from stock cultures of wild type (STA-4) were grown in 250 ml flasks on medium-N Special Nobel agar at 28° C in the dark until abundant hyphal formation was evident. The cultures were then exposed to light for conidiation. Conidia were washed off the agar with sterile deionized water, passed asceptically through four layers of gauze to remove hyphal fragments and washed three times by alternate centrifugation and suspension in water.

Erlenmeyer flasks of 500 ml capacity, containing 100 ml diluted medium-N, were inoculated with approximately 5×10^8 conidia and grown at 28° C for the required length of time. Vigorous aeration was accomplished on a New Brunswick rotary shaker. The resulting cells were harvested by filtration through two layers of cheesecloth and repeatedly washed with distilled water. The cells were pressed dry between paper towels and used for the preparation of cell-free enzyme

extracts.

Large quantities of mycelia for enzyme purification were obtained by inoculating conidia into fifteen liter carboys containing ten liters of medium-N supplemented with the appropriate carbon source. Aeration was achieved by forcing sterile air through the medium. Carboys were incubated at 28° C for 48 hours. The mycelial mass was harvested in the usual manner, washed, and excess water removed by wrapping the mycelia in cheesecloth and passing it through a washing machine wringer. The squeeze-dried mat was then lyophilized, ground into a fine powder by means of a Waring Blender and stored at -20° C in tightly sealed containers. The lyophilized powder could be stored indefinitely without loss of NAD-specific isocitrate dehydrogenase activity.

Extraction Procedure

In preliminary purification studies utilizing small quantities of mycelia (1-10 gm wet weight), the cells were disrupted and the enzyme was extracted by grinding according to the method of Sanwal and Lata (1961). For the extraction of large quantities of NAD-specific isocitrate dehydrogenase,

the lyophilized cells were suspended in 0.2 M Tris-acetate buffer, pH 7.6 containing 10^{-4} M EDTA and 10^{-4} M dithiothreitol (1 gm of powder in 15 ml of buffer). The suspension was mechanically stirred for one hour at 4^{o} C. The cell debris was removed by centrifugation at 17,000 x g for 15 minutes. The supernatant solution constituted the crude enzyme extract.

Assay Procedure

In crude extracts, the enzyme activity was estimated by coupling the reaction to the reduction of dichlorophenol-indophenol with diaphorase. The following components were added to a cuvette of 1.0 cm light path; 500 μmoles Tris-acetate buffer, pH 7.6, 1.5 μmoles NAD, .53 μmoles dichlorophenol-indophenol, 2 μmoles AMP, 10 μmoles $MgCl_2$, 2.5 μmoles sodium isocitrate, an excess of diaphorase, a suitable diluted enzyme preparation and water to give a final volume of 3.0 ml. The reaction was initiated by the addition of the enzyme and the decrease in absorbancy was measured at 600 mμ over a two minute period.

With purified preparations of the enzyme, the assay mixture contained 500 μmoles Tris-acetate buffer, pH 7.6, 1.5 μmoles NAD, 2 μmoles AMP, 10 μmoles $MgCl_2$, 2.5 μmoles

sodium threo-D_sL_s-isocitrate and enzyme plus water to give a final volume of 3.0 ml. The reaction was initiated by the addition of enzyme and the initial rate of increase of absorbance was measured at 340 mμ. All solutions were initially adjusted to pH 7.6. Assays were carried out on a Gilford Model 2000, recording spectrophotometer. The reference cuvette contained all components of the reaction mixture except isocitrate.

One unit of enzyme activity is defined as the amount causing an increase in absorbance of 0.001 per minute at 340 mμ. Specific activity is expressed as units per milligram of protein. Protein concentration was determined by the colorimetric method of Lowry et al. (1951) using twice crystallized serum albumin as standard.

Kinetic Measurements

All kinetic studies were performed with a Gilford Model 2000 optical density converter connected to a Beckman-DU monochromator and a ten inch self-balancing servo-recorder with a multiple chart drive. Absorbancy changes in the presence of NADH as inhibitor of the enzymatic reaction were recorded

after "blanking-out" the original absorbance. Reduced and oxidized NAD and AMP were prepared just before use and kept at 0° C throughout the experiment. The reaction mixture, lacking enzyme, was preincubated to 25-26° C before the addition of enzyme. The recorder curves were extrapolated to zero time and the slopes were taken as initial velocities. The reaction was linear for at least two minutes. Small velocity changes were recorded using the full scale sensitivity of the recorder between the optical densities of 0.1 and 0.2.

Analysis of Kinetic Data

All kinetic data were processed according to Cleland (1963d), using an IBM 1650 digital computer. The nomenclature of reaction mechanisms and description of kinetic constants used in this work was also that proposed by Cleland (1963a). After preliminary plots were made of the data in the reciprocal form (plots of 1/v versus 1/S), iterative least-square fits were made to equation (23) when the reciprocal plots were believed to be straight lines.

$$v = \frac{VS}{K + S} \qquad \ldots\ldots\ldots (23)$$

When the reciprocal plots were parabolas, equation (24) was used.

$$v = \frac{VS^2}{a + 2bS + S^2} \qquad \ldots\ldots\ldots (24)$$

In some cases where the data indicated a cubic function, equation (25) was used.

$$v = \frac{VS^3}{a + bS + cS^2 + S^3} \qquad \ldots\ldots\ldots (25)$$

Replots of slopes or intercepts obtained from these analysis were made against inhibitor concentration to determine the nature of the inhibition. Also replots of slopes or intercepts were made against the reciprocal of the concentration of the non-varied substrate in initial velocity studies. The replots were fitted, when appropriate (Cleland, 1963d), to a straight line, $y = ax + b$, or a parabola, $y = a + bx + cx^2$, using weighting factors supplied by the first fits to equation (23) or (24). Appropriate fits were then made, wherever possible, to an overall rate equation describing the observed type of inhibition, or the proper initial velocity pattern. In particular, data were fitted in the case of linear competitive inhibition to equation (26):

$$v = \frac{VS}{K\,(1 + I/K_i) + S} \qquad \ldots\ldots\ldots (26)$$

in the case of linear non-competitive inhibition to equation (27)

$$v = \frac{VS}{K\,(1 + I/K_i) + S\,(1 + I/K_{ii})} \qquad \ldots\ldots\ldots (27)$$

in the case of linear uncompetitive inhibition to equation (28)

$$v = \frac{VS}{K + S\,(1 + I/K_i)} \qquad \ldots\ldots\ldots (28)$$

and, finally, in the case of S-parabolic I-linear non-competitive inhibition to equation (29)

$$v = \frac{VS}{K\,(1 + I/K_{ii} + I^2/K_{i2}) + S\,(1 + I/K_{ii})} \qquad \ldots\ldots\ldots (29)$$

The value of inhibition constants were obtained together with standard errors of their estimates from overall fits to these equations.

Disc Electrophoresis

Disc electrophoresis was performed as described by

Ornstein and Davis (preprint from Distillation Products Industry, Eastman Kodak Co., Rochester, N.Y.), using Tris-glycine buffer pH 8.3. Solutions of 100-200 μg of protein were routinely applied onto the polyacrylamide gel. Concentration of protein solutions was achieved by vacuum dialysis or by precipitation of the protein in 80% ammonium sulfate followed by dialysis to remove excess ammonium sulfate.

Molecular Weight Determinations

Molecular weight determinations of the enzyme were carried out by the sucrose density gradient method described by Martin and Ames (1961). A 4-20% sucrose gradient was prepared in 5 ml lusteroid Spinco centrifuge tubes using cold (0-5° C) sucrose solutions dissolved in 0.05 M potassium phosphate buffer, pH 7.6. The sample solutions (0.2 ml) were then carefully layered on the top of the gradients and the tubes were centrifuged for 12 hours at 39,000 rpm in a SW39L rotor (Model L Spinco).

The deceleration of the rotor was not braked. The bottom of the tubes was pierced and two drop fractions were collected. The fractions were then assayed for enzyme activity

as previously described. Marker proteins such as malic dehydrogenase or alcohol dehydrogenase were routinely used.

Analytical Ultracentrifugation

An estimation of homogeneity and size of the purified NAD-specific isocitrate dehydrogenase was attempted by use of a Spinco Model E Analytical ultracentrifuge equipped with Schlieren optics. Protein concentrations ranging from 3-6 mg/ml in 0.05 M potassium phosphate buffer, pH 6.5 were routinely used. All experiments were attempted at 4° C at 60,000 rpm with photographs taken at 8 minute intervals.

Spectrofluorometric Analysis

Spectrophotofluorometric quenching studies were carried out after the method of Velick (1958). The fluorescence of the enzyme was measured in an Aminco-Bowman Spectrofluorometer equipped with a 416-992 Xenon lamp and an Electro Instruments flat-bed X-Y recorder. Purified NAD-specific isocitrate dehydrogenase was concentrated and dialyzed at 4° C for three hours against 0.05 M potassium phosphate buffer, pH 6.5, containing 10^{-4} EDTA and 10^{-4} M dithiothreitol. The dialyzed enzyme, as well as all other reagents (NADH, AMP, citrate,

isocitrate and buffer), were clarified by filtration through a millipore filter (pore size 0.45 μ). All experiments were carried out at a constant enzyme concentration approximately 3×10^{-5} M. The total initial volume of the reaction mixture in a 1 cm cuvette was 1.0 ml. An excitation wavelength of 340 mμ was employed throughout, and the emission spectrum was measured from 400-800 mμ. The enzyme-NADH complex had a fluorescent peak at 440 mμ and free NADH, a fluorescent peak at 460 mμ at this excitation wavelength. The fluorescence of the NADH-IDH complex was corrected for dilution by titration of IDH with buffer only. A correction was also made for the absorption of the exciting light by NADH.

Measurement of Protein-binding by Gel Filtration

The binding of NADH to isocitrate dehydrogenase was measured by filtration of the protein through Sephadex G-25 equilibrated with NADH according to the method of Hummel and Dreyer (1962) as described in detail recently by Fairclough and Fruton (1966). Columns of Sephadex G-25 (0.4 x 100 cm) were prepared and equilibrated with 0.05 M phosphate buffer, pH 6.5, containing an appropriate concentration of NADH and 10^{-4} M EDTA and 10^{-4} M dithiothreitol. Isocitrate dehydrogenase

(2-3 mg suspended in the same buffer) was placed on the column and eluted with the same buffer at an elution rate of 0.3 ml/minute. The effluent solution was continually monitored through a 1 cm quartz micro-flow cell with a Gilford recording spectrophotometer set at 340 mμ and 1-2 ml fractions were collected. The amount of NADH bound to the enzyme was determined from the amount of NADH in the "trough" compared to an equal volume of effluent obtained from the base line. All experiments were performed at 23° C.

Equilibrium Dialysis Analysis

The binding of various substrates to isocitrate dehydrogenase was measured in equilibrium dialysis cells described by Myer and Schellman (1962). To one compartment was added 0.5 ml of enzyme solution in 0.05 M phosphate buffer, pH 6.5, and to the other compartment 0.5 ml of various concentrations of radioactive substrate. The membrane, commercial 20/32 Visking tubing, was washed and soaked for several days in 10^{-2} M EDTA prior to use. The two compartments were brought to equilibrium by rotation (8 rpm) for 12 hours at 4° C. The time required for equilibration was determined

in separate controls in which buffer was substituted for enzyme and the substrate compartment contained the highest substrate concentration employed in the experiment. As a further precaution duplicate samples were removed and analyzed at significantly different times. Routinely, 0.1 ml samples were removed from each compartment (after equilibration) and the radioactivity measured. By employing radioactive substrates, direct analysis of substrate concentration on both sides of the membrane could be achieved.

Determination of Radioactivity

The radioactivity of C^{14}- and H^{3}-compounds was measured in a Packard Tri-Carb Liquid Scintillation Spectrometer, Model 3000 at 4^{o} C. One-tenth ml of each sample was counted in 15 ml of a scintillation solution containing 100 g of napthalene, 7 g of 2,5 diphenyloxazole (PPO), .3 gm of 1,4-bis-2-(5-phenyloxazolyl) benzene dissolved in one liter of dioxane. Polypropylene screw neck vials were used for all determinations. No quenching of the samples was observed when estimated by means of the external standard. In all experiments the counts averaged above 6000 counts/minute with a background of 20 counts/minute.

Analysis of Binding Data

a) Equilibrium Dialysis

The binding of a substrate (S) to a protein (E^o) molecule will always obey the equation:

$$E^o + nS \underset{}{\overset{K}{\rightleftharpoons}} E^oS_n$$

(where n represents the number of molecules of S bound to E^o). The use of radioactive substrates in this technique allows the direct determination of ES_n, the amount of substrate bound to the enzyme and simultaneously, the concentration of free substrate. Knowing the molecular weight of the enzyme, the concentration of E^o can be calculated. The binding data can then be represented by:

$$\frac{1}{r} = \frac{1}{nkA} + \frac{1}{n} \qquad \ldots\ldots\ldots (30)$$

(where r = moles of substrate bound/mole of enzyme, k is the association constant $\frac{EA}{(E)\ (A)}$, and A is the concentration of <u>free</u> substrate).

Plotting 1/r as a function of 1/A, a straight line is obtained if the sites are independent. Deviation from a straight line is indicative of interaction or dissimilarity of

the sites. Equation (30) may be rearranged into the form:

$$\frac{r}{A} = - rk + nk \qquad \ldots\ldots\ldots (31)$$

Plotting r/A as a function of r, a straight line of negative slope is obtained if the sites are independent, and n is determined at the horizontal axis when r/A = 0 (Scatchard et al., 1957). If the sites are not independent (cooperative) or independent but not identical, this line will deviate from linearity as seen in Fig. 3.

b) Spectrofluorometric Analysis

The binding data from spectrofluorometric analysis can be represented by a modified form of equation (30) (Stockell, 1957). In this representation $r = np/E_o$, where p is the fraction of sites bound to substrate x E^o; E^o is the total molar concentration of protein.

(A) = S - np, where S is the total concentration of substrate and np represents the molar concentration of bound substrate.

$k = 1/K_s$ where $K_s = \frac{(E)\ (S)}{(ES)}$ = dissociation constant.

Then, $\frac{1}{r} = \frac{1}{nkA} + \frac{1}{n}$ is equal to $\frac{E^o}{np} = \frac{K_s}{n\ (S - np)} + \frac{1}{n}$

Fig. 3. Theoretical binding curves according to the Scatchard equation (31) (Scatchard et al., 1957).

A - independent, identical binding sites

B - cooperative binding sites

C - anticooperative or non-identical binding sites.

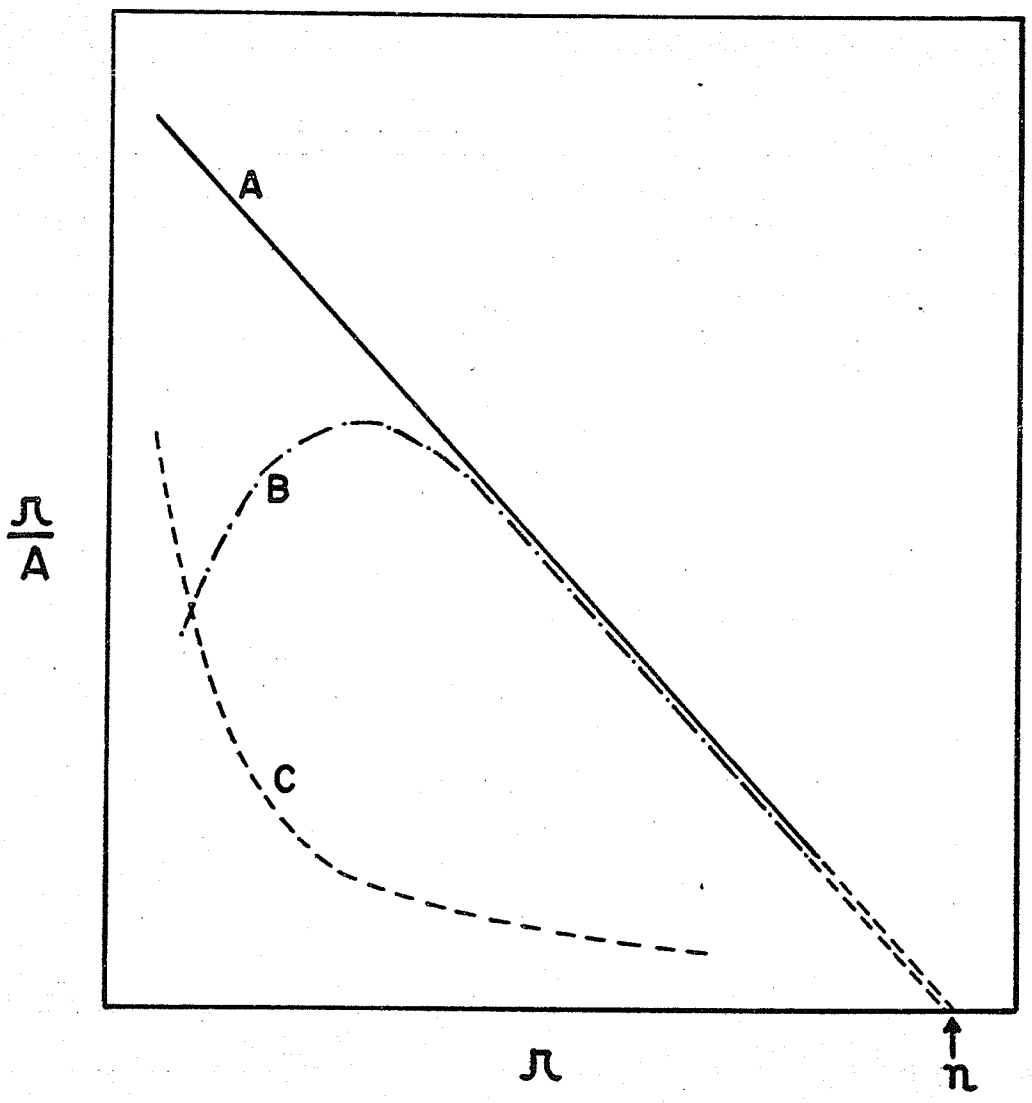
A
B
C
Π/A
Π
π

Rearranging,

$$\frac{S}{p} = \frac{K_S}{E^o - p} + n \qquad \ldots\ldots\ldots (32)$$

(where p = the change in fluorescence in the presence of a

$$\frac{\text{known concentration of S } (\Delta F)}{\text{the change in fluorescence at saturating S } (\Delta F_{max})} \times E^o)$$

The ΔF_{max} is determined from the horizontal asymptote of a plot of ΔF_{max} as a function of S. Thus plotting S/p as a function of $1/E^o - p$ yields a straight line whose vertical intercept yields the value n, if the sites are equivalent and independent. If the sites are not independent, this line will deviate from linearity as seen in Fig. 4.

Fig. 4. Theoretical binding curves according to the Stockell equation (32) (Stockell, 1957).

A - independent, equivalent binding sites

B - cooperative binding sites

C - anticooperative or non-identical binding sites

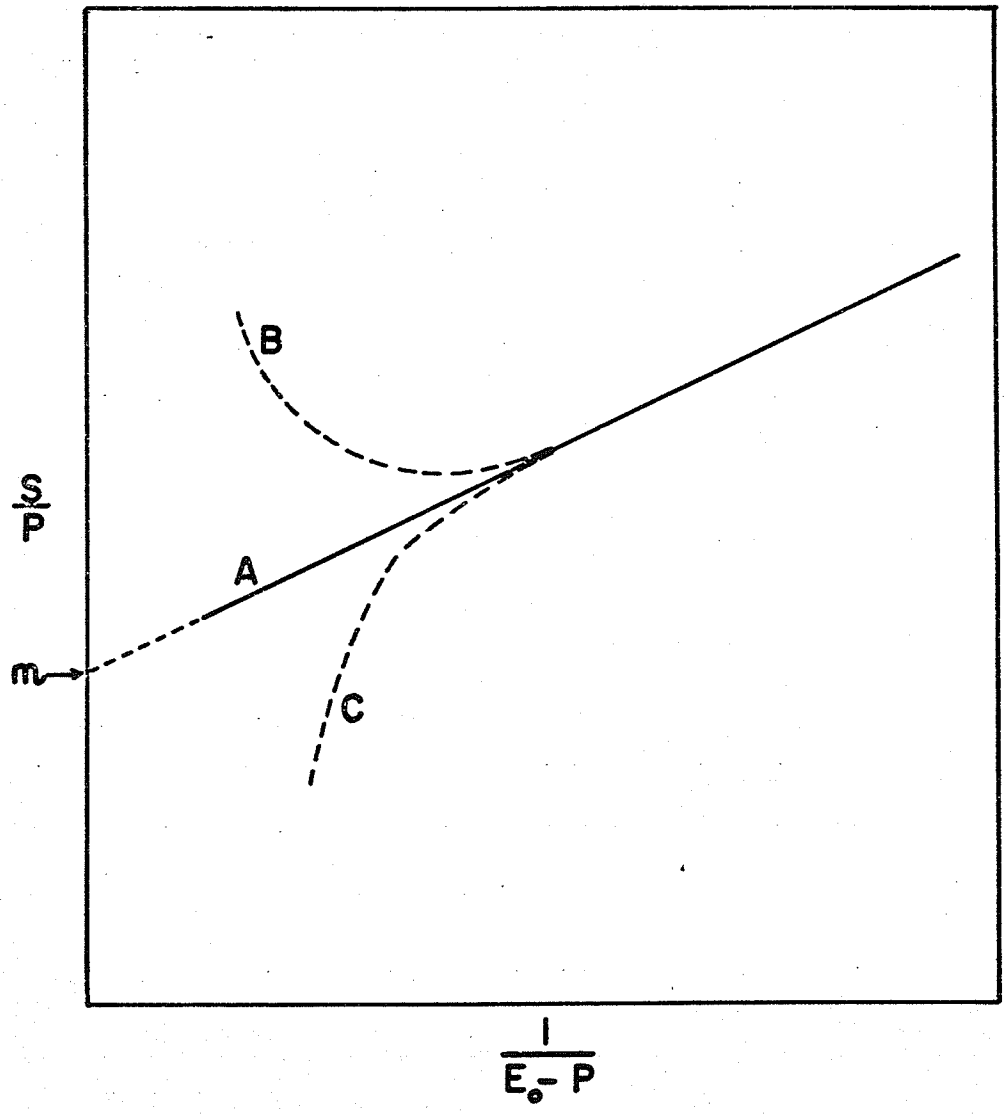
B
A
C
m
S/P
1/(E₀ - P)

RESULTS

RESULTS

Determination of Growth Conditions

Before any attempts were made to purify isocitrate dehydrogenase from Neurospora crassa, the specific activity of the enzyme was determined at various stages of growth. Several 500 ml Erlenmeyer flasks containing 100 ml of Vogel's medium-N were inoculated with washed conidia, allowed to grow for various lengths of time, and the cells treated as previously described. The specific activity of isocitrate dehydrogenase was determined at each time interval as described in Materials and Methods. The results appear in Fig. 5. The specific activity attained a maximum after 18 hours of growth.

Several concentrations of sodium citrate were tested for possible induction of isocitrate dehydrogenase production. The specific activity of isocitrate dehydrogenase was determined as previously described and the results are presented in Fig. 6. A slight induction of isocitrate dehydrogenase was found at a concentration of 0.01 M sodium citrate.

The effect of limiting glucose concentration on the

Fig. 5. Specific activity of NAD-specific isocitrate dehydrogenase versus time of growth.

Strain STA-4 grown in Vogel's minimal medium-N containing 2% sucrose as carbon source at 28° C.

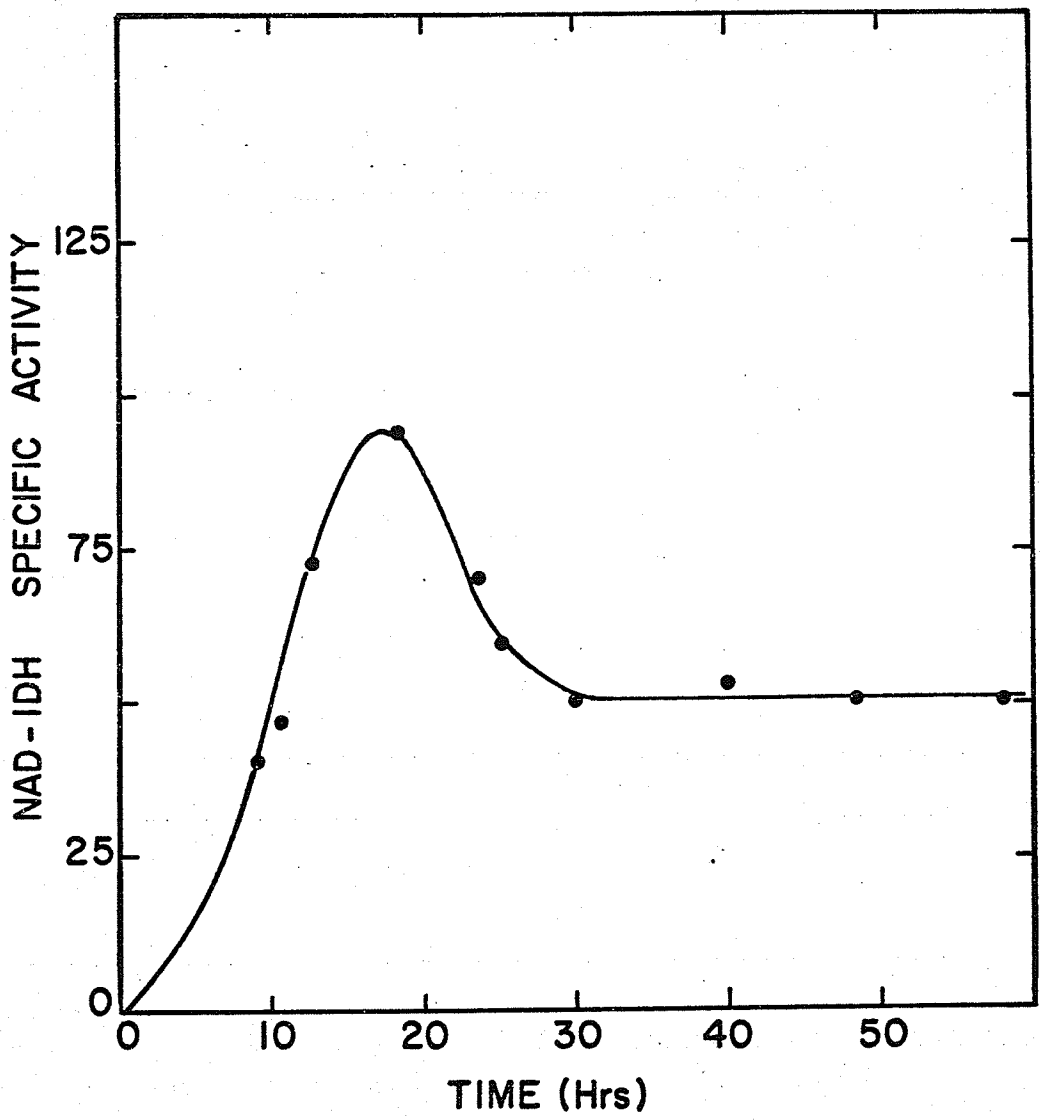
NAD-IDH SPECIFIC ACTIVITY
125
75
25
0
0
10
20
30
40
50
TIME (Hrs)

Fig. 6. Specific activity of NAD-specific isocitrate dehydrogenase grown in the presence of various concentrations of sodium citrate.

STA-4 grown in Vogel's minimal medium-N containing 2% sucrose as carbon source for 20 hours at 28° C.

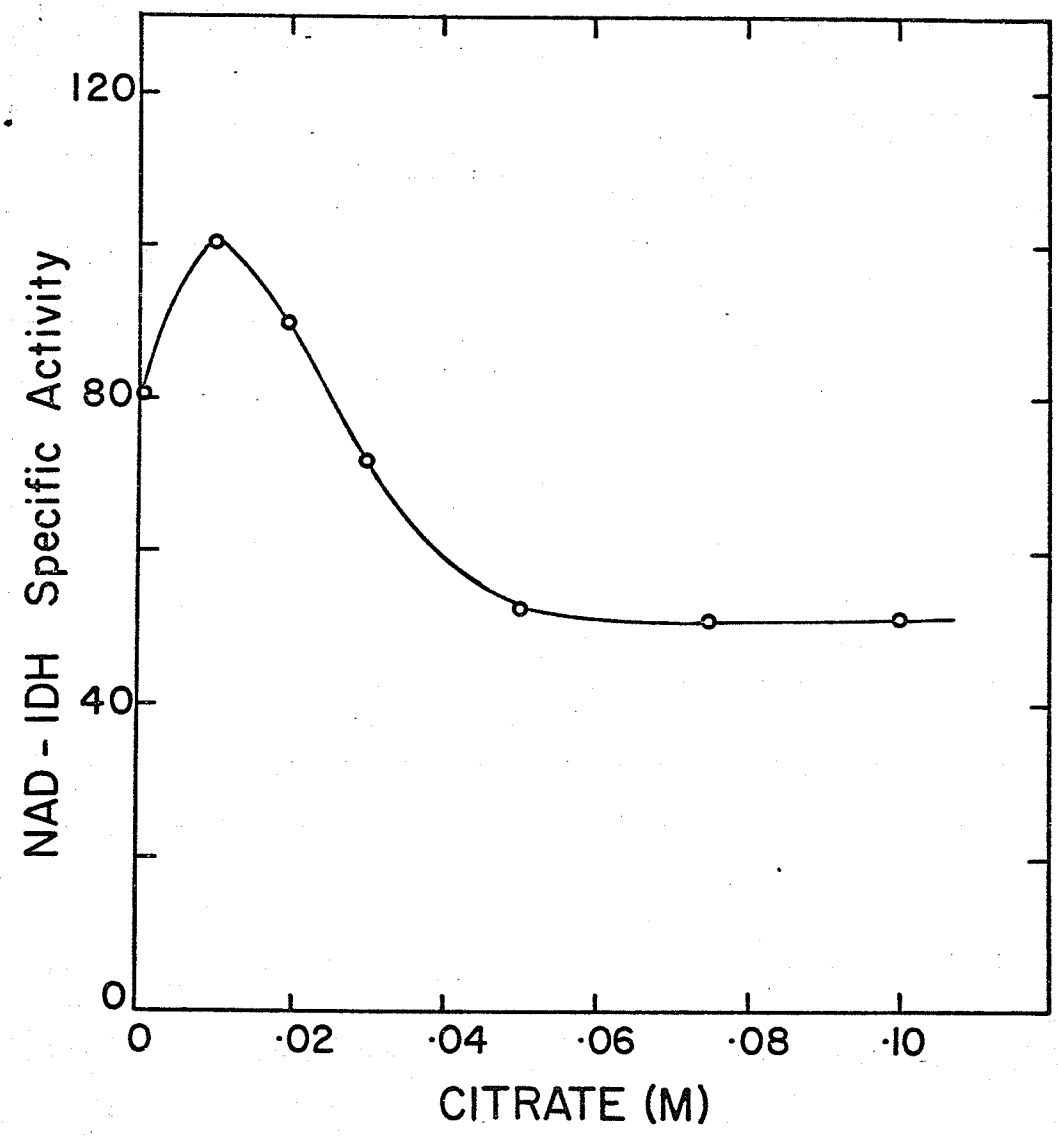
120
80
40
0
NAD - IDH Specific Activity
0
·02
·04
·06
·08
·10
CITRATE (M)

levels of isocitrate dehydrogenase was studied. Three concentrations of sucrose, 2%, 1%, and 0.5% were tested on N. crassa grown for 20 hours in the presence of 0.01 M sodium citrate. The methods of growth, isolation, and determination of specific activity were as previously described. The results appear in Table 2.

The specific activity of isocitrate dehydrogenase was highest in cells grown in 0.5% sucrose although total growth was reduced. Neurospora crassa was normally grown in Vogel's medium-N containing 0.01 M sodium citrate and 0.5% sucrose as the carbon source. Subsequent experiments revealed that the time of appearance of maximum enzyme activity was dependent upon inoculum size, aeration and temperature. Therefore these conditions were kept constant throughout the course of this investigation. For small scale preparations, i.e., Erlenmeyer flasks, maximum activity appeared after 20 hours of growth. For large scale preparations, i.e., 15 litre carboys, maximum enzyme activity appeared after 48 hours of growth.

Purification of NAD-specific Isocitrate Dehydrogenase

All purification procedures were carried out at 0-4° C, unless otherwise stated. All centrifugations were performed

Table 2. Effect of varying glucose concentrations on total growth and NAD-isocitrate dehydrogenase activity. Growth time was 20 hours.

Sucrose	Weight wet of cells (g)	Specific activity
2.0%	4.5	2.76
1.0%	3.4	4.46
0.5%	2.0	4.96

at 17,000 x g for 15 minutes. A crude enzyme extract was prepared from lyophilized mycelia according to the procedure described in Methods. The pH of the crude extract was adjusted to 5.0 with 20% acetic acid and the precipitate was discarded after centrifugation.

Ethanol (precooled to -20° C) was added gradually with stirring to the supernatant solution to give a final concentration of 9%. After standing at -10° C for 15 minutes, the precipitate was removed by centrifugation. Ethanol was then added gradually to this supernatant solution to give a final concentration of 20%, and allowed to remain at -10° C for 1 hour. The precipitate was recovered by centrifugation and dissolved in 0.1 M Tris-acetate buffer, pH 7.6, containing 10^{-4} M EDTA and 10^{-4} M dithiothreitol. The final volume was 1/10 the volume of the original extract.

The pH of this suspension was adjusted to 5.0 with 20% acetic acid and the precipitate was removed by centrifugation. Ethanol was added to the supernatant solution to a final concentration of 9% and allowed to stand for 15 minutes at -10° C. The precipitate was again removed by centrifugation. More ethanol was added to the supernatant solution to give a final concentration of 15% and maintained at -10° C for 2 hours.

The resulting precipitate was recovered by centrifugation and was dissolved in a small volume of 0.02 M potassium phosphate buffer, pH 6.5, containing 10^{-4} M EDTA.

The enzyme preparation was centrifuged at 40,000 rpm in 4.5 ml lots for 1 hour in a swinging bucket rotor (SW39L) of a Spinco Model L ultracentrifuge. The gelatinous precipitate containing nucleoproteins was discarded. The enzyme preparation was then routinely stored at -20° C at this stage.

The enzyme solution was dialyzed for 6 hours against frequent changes of cold 0.05 M phosphate buffer, pH 6.5 containing 10^{-4} M EDTA and 10^{-4} M dithiothreitol. The enzyme was relatively unstable at this stage and with prolonged dialysis the activity was considerably reduced. The dialyzed enzyme was then subjected to column chromatography on DEAE-cellulose (diethylaminoethyl-cellulose). The column was prepared by a procedure similar to that reported by Sober et al. (1956). DEAE-cellulose (obtained from Sigma Chemical Co.) was suspended in 1.0 N sodium hydroxide and decanted after 12 hours to remove the fine particles. The cellulose was suspended and decanted alternately with 0.05 M phosphate buffer, pH 6.5, until the hydrogen concentration was equal to

that of the buffer (pH 6.5). The cellulose was transferred to a chromatographic column (Pharmacia, Uppsala, Sweden) of dimensions 2.5 x 45 cm, packed to a height of 40 cm and equilibrated with 0.05 M phosphate buffer, pH 6.5, containing 10^{-4} M EDTA and 10^{-4} M dithiothreitol. The enzyme was eluted by applying a linear gradient of EDTA. The mixing chamber contained 0.05 M phosphate buffer, pH 6.5 and 0.0001 M EDTA, pH 6.5 and the reservoir 0.07 M EDTA, pH 6.5. Successive 5.0 ml fractions were collected at 4° C with the aid of a Research Specialties Fraction Collector fitted with a drop counter. Enzyme elution pattern was determined by the spectrophotometric assay (Fig. 7). Fractions containing highest enzyme activity were pooled and the enzyme was precipitated by the addition of solid ammonium sulfate to 80% saturation. After allowing to stand for 1 hour, the enzyme was recovered by centrifugation and dissolved in a small amount of 0.02 M phosphate buffer, pH 6.5, containing 10^{-3} M EDTA. The enzyme could be routinely stored at this stage for at least 3-4 months at -20° C with little loss of activity. This enzyme preparation, following dialysis, was routinely used for all kinetic determinations.

Further purification was achieved by calcium phosphate gel fractionation. Calcium phosphate gel, suspended in

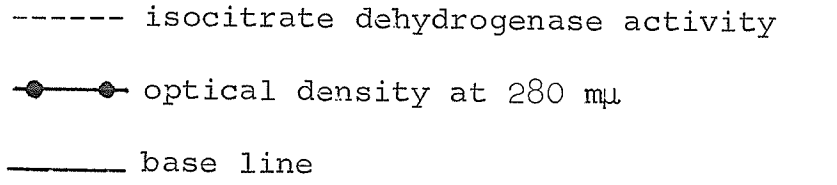

Fig. 7. Gradient elution of NAD-specific isocitrate dehydrogenase from a DEAE-cellulose column.

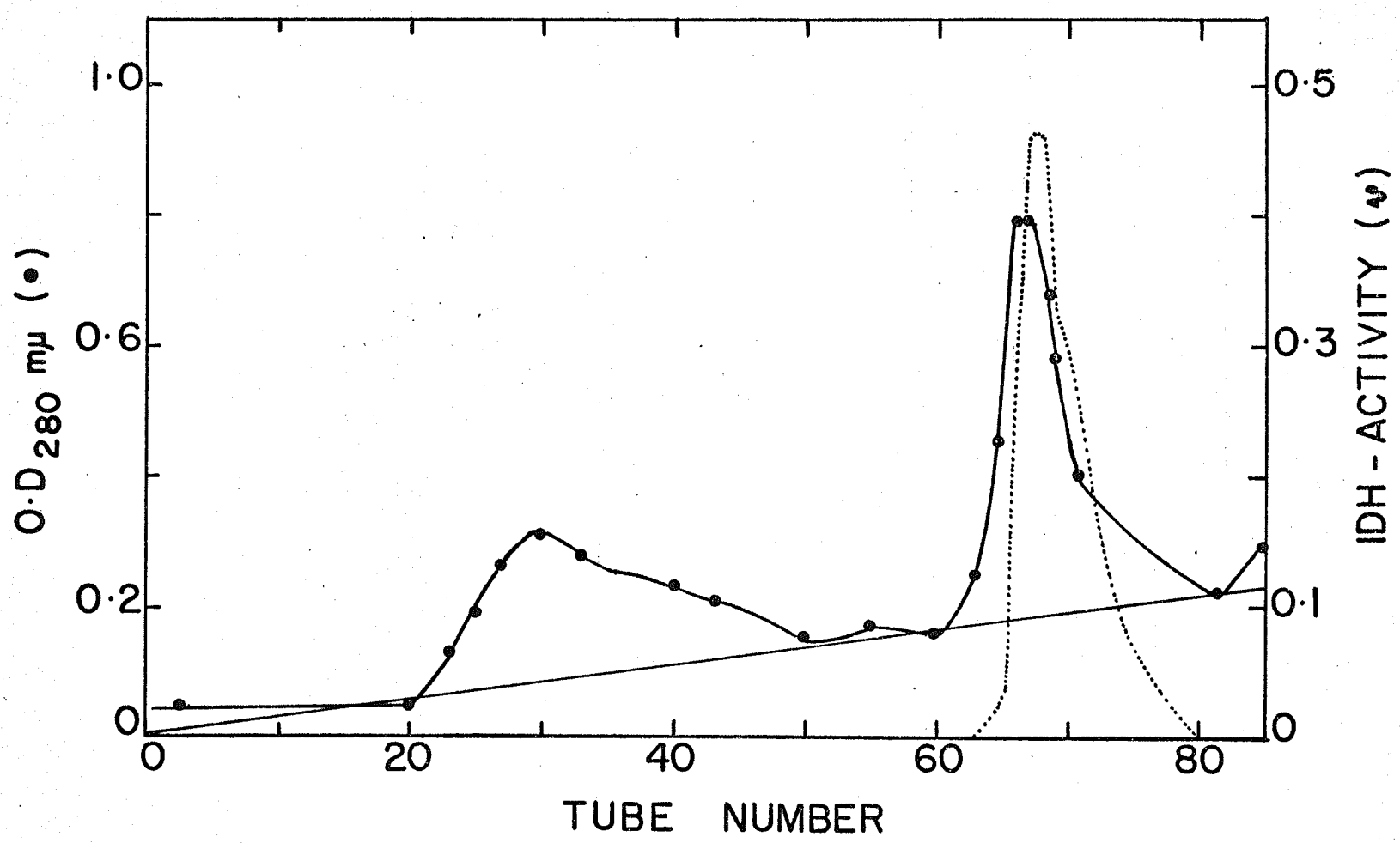
1·0
0·6
0·2
0
O·D 280 mμ (●)
0·5
0·3
0·1
0
IDH - ACTIVITY (▲)
0
20
40
60
80
TUBE NUMBER

distilled water, was added at a concentration of 1 mg gel/mg or protein, and the suspension was gently stirred for 10 minutes. The gel was removed by centrifugation. Calcium phosphate gel was then added at a concentration of 1.4 mg gel/mg of protein and stirred for 10 minutes. The gel was recovered and was suspended in 0.2 M potassium phosphate buffer, pH 6.5 containing .035 M EDTA, in a volume equal to the original volume of enzyme. The suspension was gently stirred for 10 minutes at which time the gel itself was solubilized. The enzyme was removed by the addition of solid ammonium sulfate to 80% saturation. Gel adsorption and solubilization was repeated four times and the eluates were pooled. The enzyme was recovered by centrifugation and was dissolved in 0.02 M potassium phosphate buffer, pH 6.5, containing 10^{-3} M EDTA. This procedure yielded an enzyme preparation approximately 450-fold purified compared to the crude extract and a specific activity of 40,000-50,000. The total recovery of the enzyme varied from 36-48% of the enzyme in crude extracts. Summary of a typical purification procedure for NAD-specific isocitrate dehydrogenase from Neurospora crassa is presented in Table 3.

Table 3. Summary of purification procedure for NAD-specific isocitrate dehydrogenase from 10 gms lyophilized *Neurospora crassa*.

Step	Protein (mg)	Total units	Specific activity units/mg	Recovery (%)
1. Extraction-crude extract.	1470	102,000	69.5	100
After pH 5 pption.	915	99,000	108	97
2. Ethanol fractionation				
9% EtoH supernatant	717	108,000	150	102
9-20% Fraction	161	90,000	560	88
3. Refractionation.				
After pH 5 pption	108	90,000	834	88
9% EtoH supernatant	88.5	81,000	915	80
9-15% fraction	36.4	62,000	1700	61
4. Ultracentrifugation	34.0	66,000	1940	64
5. DEAE-chromatography	3.2	49,500	15400	48
6. Pooled calcium phosphate eluates	1.0	44,000	44000	42

Storage of Enzyme

Experiments indicated that the stability of the enzyme was dependent upon protein concentration. The enzyme lost approximately 90% of its activity in 12 hours at -20° C when stored at a protein concentration of less than 1 mg/ml. However, the purified enzyme suspended at 2-3 mg/ml in buffer containing EDTA could be stored frozen at -20° C for at least 3 months without significant loss of enzyme activity. Small amounts of ammonium sulfate also appeared to stabilize the enzyme and as a result the enzyme was routinely stored without prior dialysis.

Homogeneity of the purified enzyme

The purity of the enzyme was determined by disc electrophoresis as previously described. The sample gel usually contained 0.2 mg of protein. The purified preparation exhibits one major protein band and two additional faint protein bands (Fig. 8). These results suggest that the enzyme preparation was approximately 80-90% pure.

In the analytical ultracentrifuge, two peaks were present; the major peak corresponded to an $S_{20,w}$ value of 5.8

Fig. 8 Polyacrylamide electrophoresis of purified NAD-specific isocitrate dehydrogenase from Neurospora. 200 μg of protein was applied on the gel.

while the minor fast moving peak exhibited an $S_{20,w}$ value of 20.2. Calculation of the area under the two peaks showed that the slowly sedimenting peak was present approximately to the extent of about 80% of the total protein.

KINETIC ANALYSIS

1. Initial Velocity Analysis at pH 6.5

a) In the presence of AMP.

NAD-specific isocitrate dehydrogenase had been previously demonstrated to obey classical Michaelis-Menten kinetics at a pH of 6.5 (Sanwal et al., 1964). It was considered essential to investigate the nature of the enzymic reaction mechanism at this pH where apparently no allosteric effects were present. In order to obtain maximal activity all experiments were conducted in the presence of saturating but non-inhibitory concentrations of AMP, i.e., 0.533 mM, approximately 20 x K_m value. Threo-D_sL_s-isocitrate was used throughout these experiments. All reaction mixtures contained 3.3 mM $MgSO_4$, a saturating value determined from Fig. 9.

When NAD was varied against isocitrate as the fixed changing substrate, both the double reciprocal plots (Fig. 10) and the replots of slopes and intercepts (Fig. 11) were linear. With isocitrate as the variable and NAD as the changing fixed substrate, the double reciprocal plots as well as replots of slopes and intercepts were also linear. These data fit the

Fig. 9 Double reciprocal plot of 1/velocity versus $1/Mg^{++}$ at several fixed concentrations of isocitrate.

All experiments were performed in phosphate buffer, 0.1 M, pH 6.5 in the presence of saturating concentrations of AMP (.66 mM) and NAD (.5 mM). The lines have been fitted by eye.

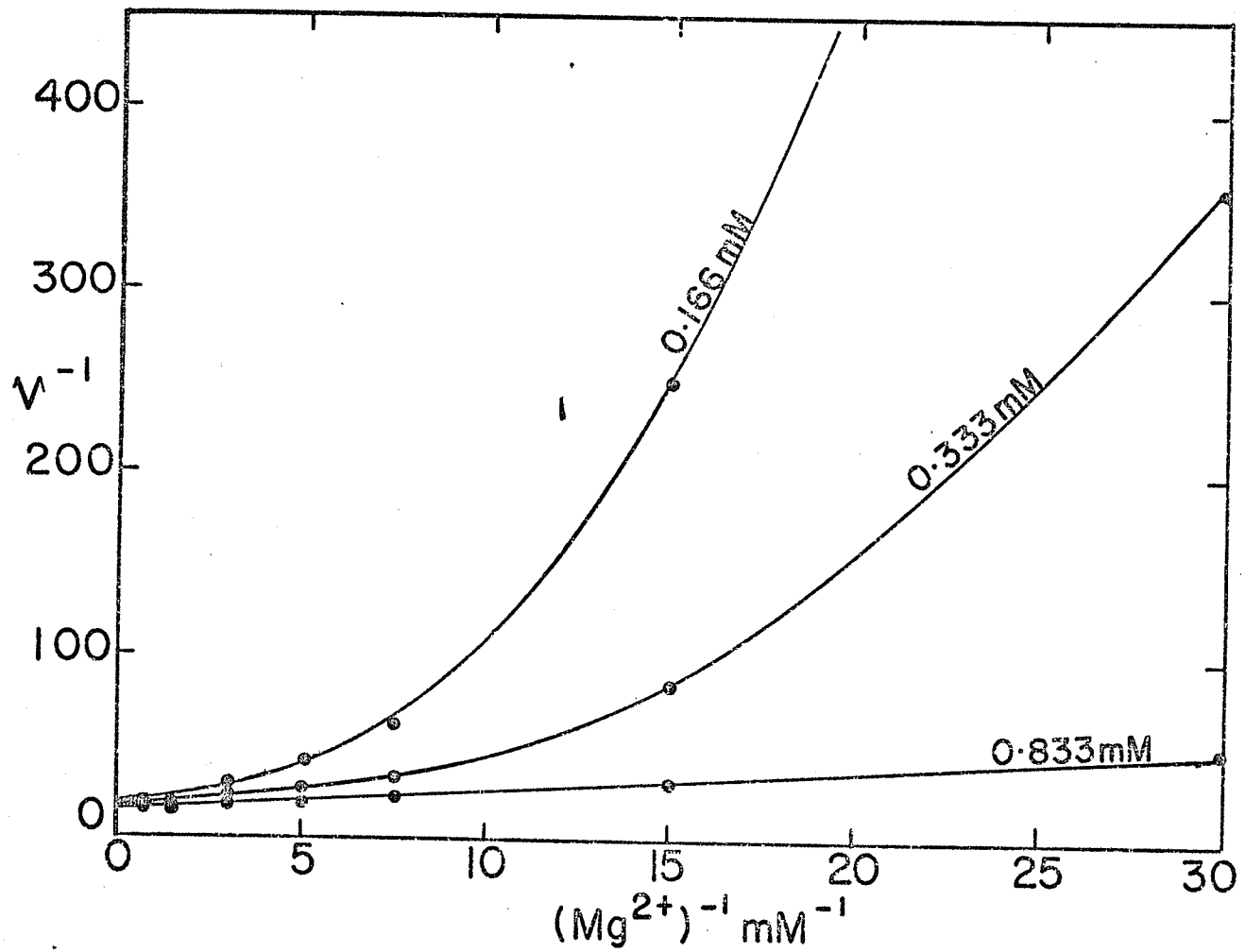
400
300
200
100
0
v^{-1}
0·166 mM
0·333 mM
0·833 mM
0
5
10
15
20
25
30
$(Mg^{2+})^{-1}$ mM^{-1}

Fig. 10. Double-reciprocal plots of 1/velocity versus 1/NAD at several fixed concentrations of isocitrate.

Enzyme concentration was 100 units per cuvet. Experiments were performed in 0.2 M phosphate buffer, pH 6.5. Lines have been drawn from fits to equation (23).

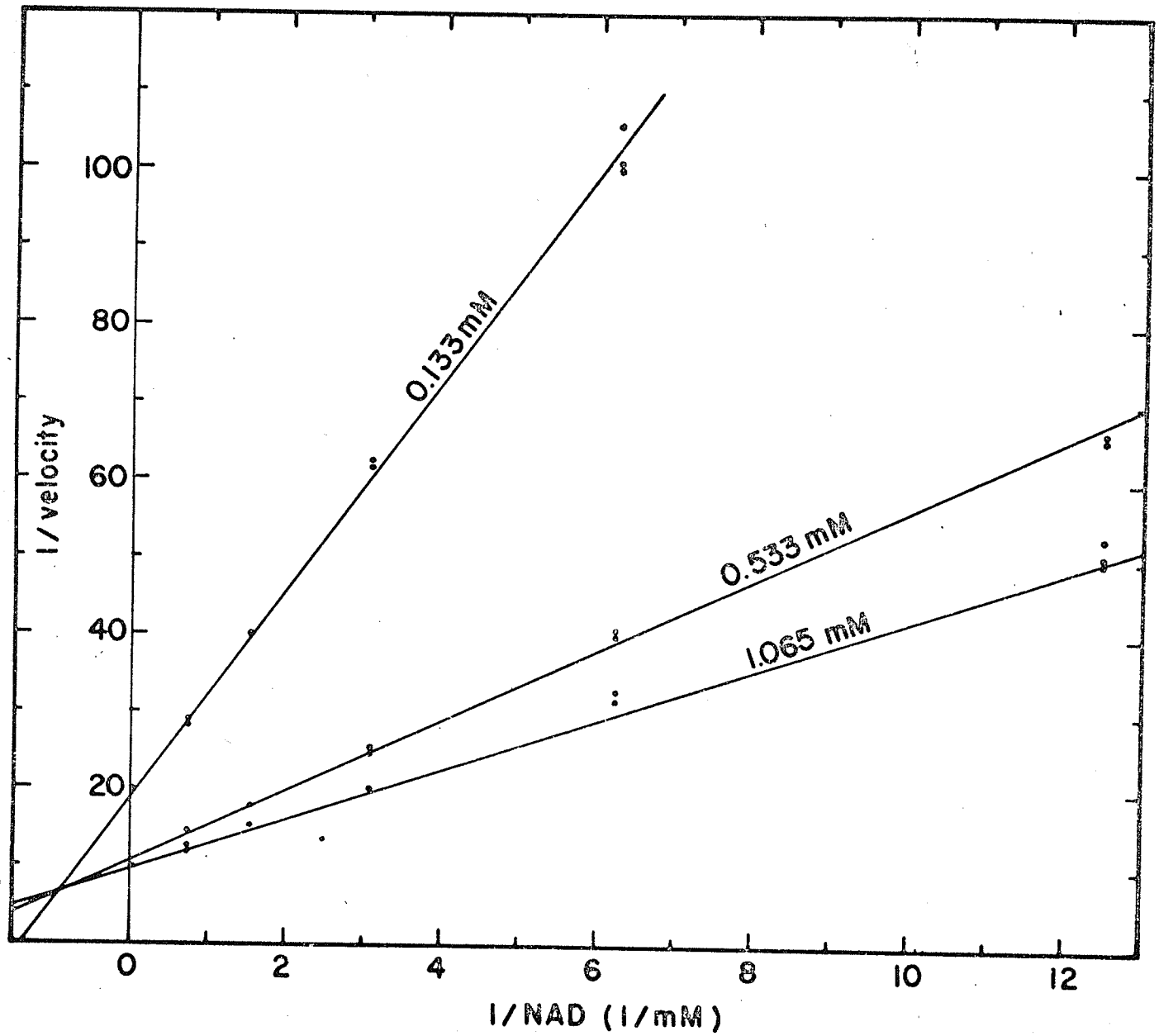
100
80
60
40
20
1/velocity
0.133mM
0.533 mM
1.065 mM
0
2
4
6
8
10
12
1/NAD (1/mM)

Fig. 11. Replots of slopes and intercepts from Fig. 10 versus reciprocal of isocitrate concentrations.

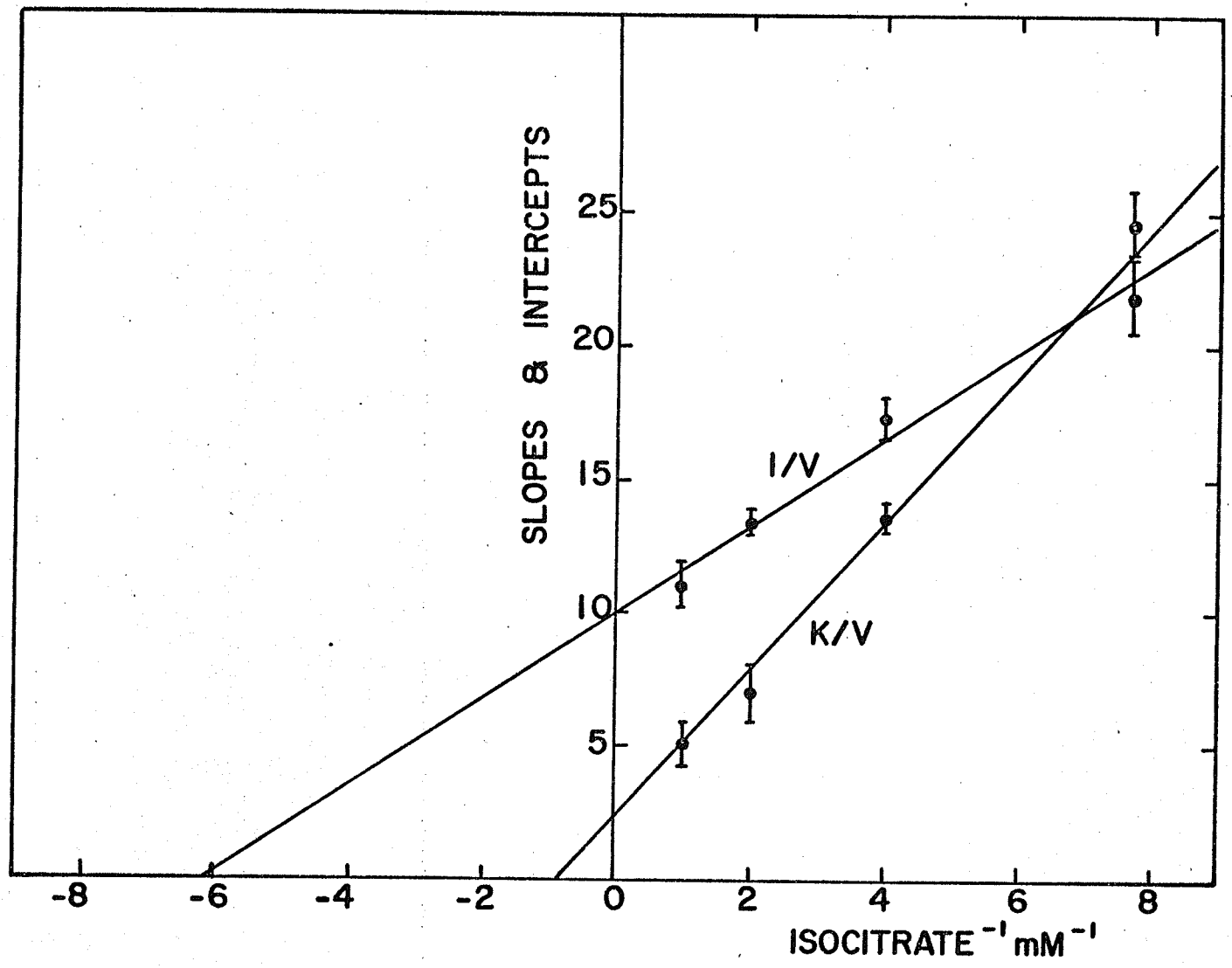
SLOPES & INTERCEPTS
25
20
15
10
5
I/V
K/V
-8
-6
-4
-2
0
2
4
6
8
ISOCITRATE $^{-1}$ mM $^{-1}$

following initial velocity equation

$$\frac{1}{v} = \left(\frac{K_{ia}K_b}{AB} + \frac{K_a}{A} + \frac{K_b}{B} + 1\right)\left(\frac{1}{V}\right) \qquad \ldots\ldots\ldots (33)$$

(where A and B are substrate concentrations, K_a and K_b are Michaelis constants of A and B respectively, and K_{ia} is the dissociation constant of A).

As had already been shown by Cleland (1963a), this equation is obeyed by several sequential mechanisms (such as Rapid Equilibrium Random or Ordered mechanisms) and it is impossible to tell A and B apart from the initial velocity analysis alone.

Product Inhibition Studies at pH 6.5 in the Presence of AMP

To distinguish between various possible sequential mechanisms and to determine the order of binding of the substrates and release of products, inhibition studies were attempted using the various products as inhibitors.

With NAD as the varied substrate, NADH produced competitive inhibition (Fig. 12). Slopes of these plots were found to be a linear function of the concentration of NADH (Fig. 13). When isocitrate was used as the variable substrate

Fig. 12. Product inhibition of isocitrate dehydrogenase by NADH with NAD as the variable substrate and a constant high concentration of isocitrate (6.6 mM).

Lines have been drawn from fits to equation (23). Phosphate buffer, 0.2 M, pH 6.5, was used in all experiments. Concentration of enzyme in each cuvet was 50 units.

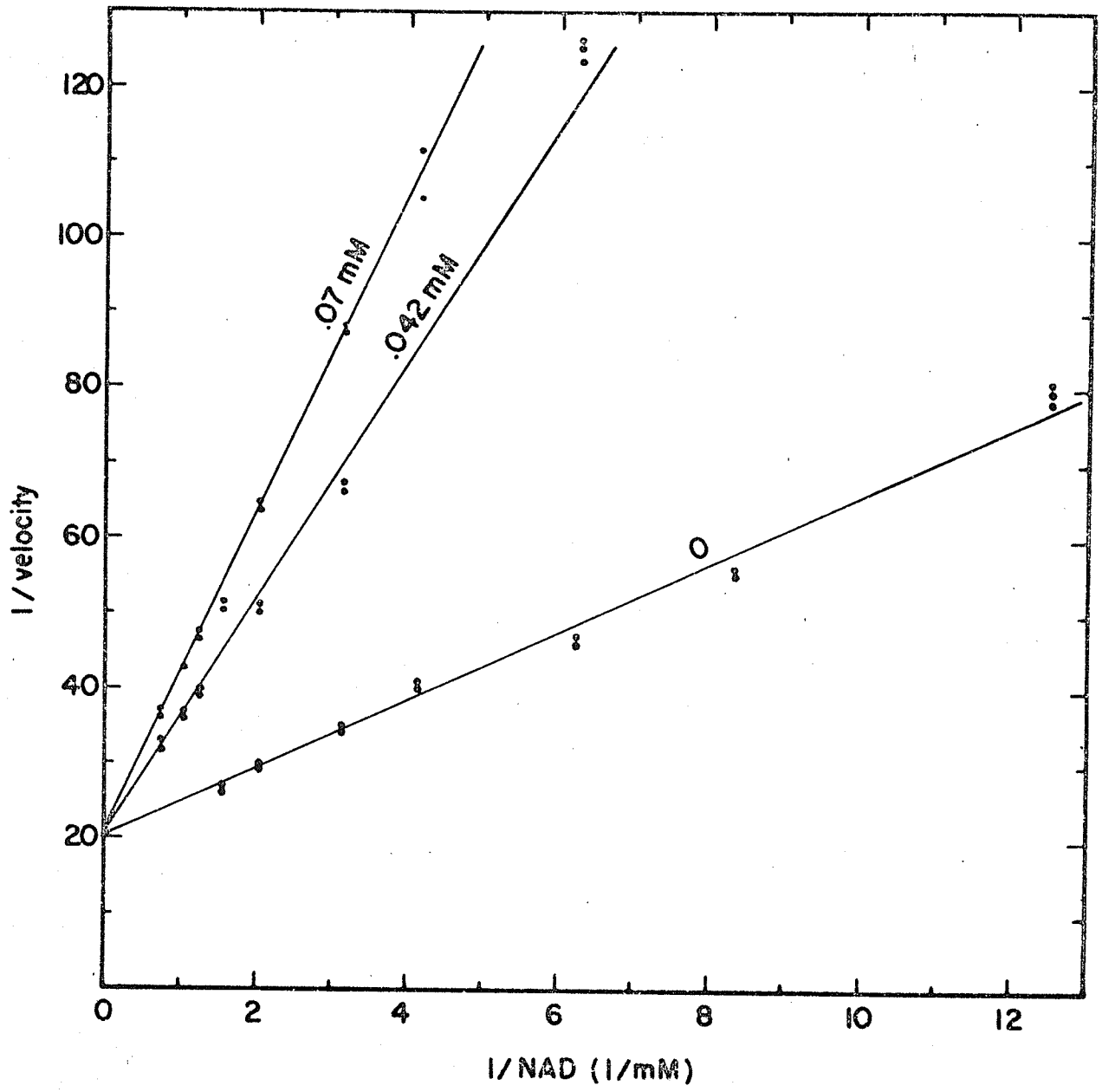
120
100
80
60
40
20
0
2
4
6
8
10
12
1/velocity
1/NAD (1/mM)
.07 mM
.042 mM
0

Fig. 13. Replot of slopes from Fig. 12 versus NADH concentration.

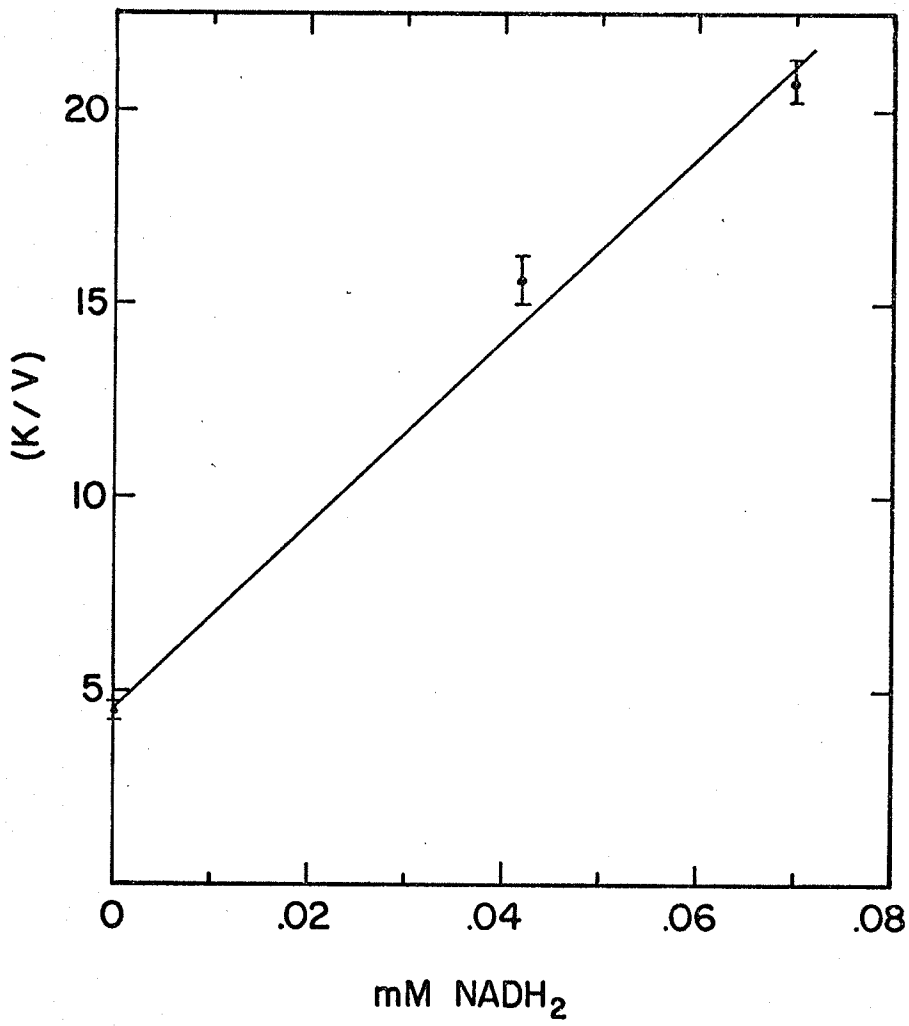
20
15
10
5
(K/V)
0
.02
.04
.06
.08
mM NADH2

and NADH as inhibitor, linear double-reciprocal plots showing noncompetitive inhibition were obtained (Fig. 14). The inhibition was nearly abolished by using saturating levels of NAD in the reaction mixtures. A replot of intercepts was linear but slopes appeared to be parabolic (Fig. 15).

Using α-ketoglutarate (α-kg) as product inhibitor and NAD as the variable substrate in the presence of high concentrations of isocitrate (20 x K_m), inhibition was found to be uncompetitive (Fig. 16). A replot of intercepts versus inhibitor concentrations was linear. When isocitrate was the variable substrate, the inhibition was found to be noncompetitive (Fig. 17). A replot of intercepts was linear but slopes appeared to be parabolic (Fig. 18). Therefore the inhibition by α-ketoglutarate when isocitrate was varied is actually S-parabolic I-linear noncompetitive and the data corresponds to equation (20). This suggests that α-ketoglutarate may combine with the enzyme-NAD complex in a dead-end manner as well as combining as a product inhibitor.

When $KHCO_3$ was used as inhibitor and NAD was varied in the presence of nonsaturating concentrations of isocitrate, the inhibition was found to be noncompetitive (Fig. 19). Replot of slopes and intercepts against inhibitor concentrations (Fig.

Fig. 14. Product inhibition of isocitrate dehydrogenase by NADH with isocitrate as the variable substrate at a constant unsaturating concentration of NAD (0.2 mM).

Lines have been drawn from fits to equation (23).

Enzyme concentration was 125 units per cuvet.

Phosphate buffer, 0.2 M, pH 6.5, was used for all experiments.

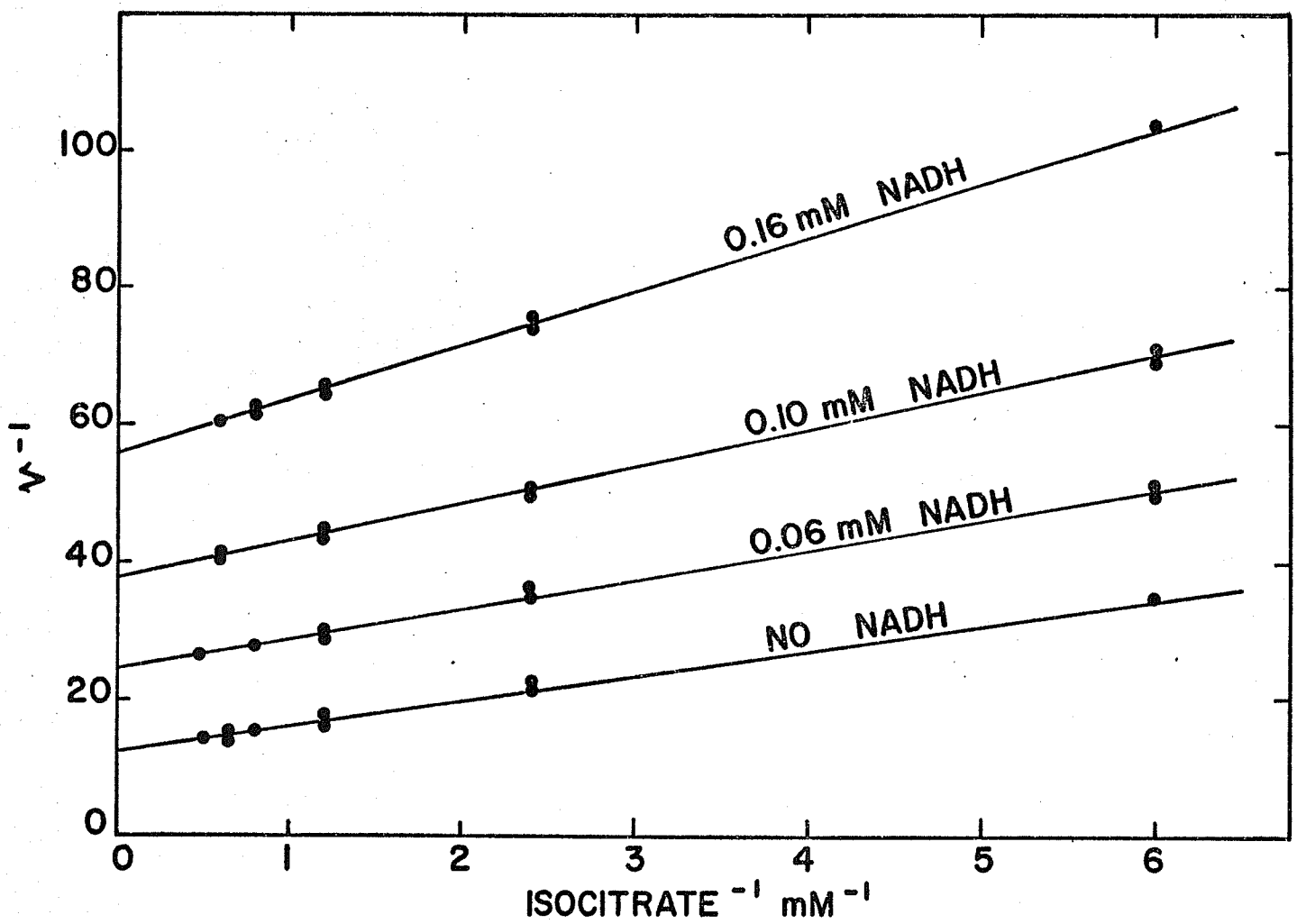
100
80
60
40
20
0
v^{-1}
0.16 mM NADH
0.10 mM NADH
0.06 mM NADH
NO NADH
0
1
2
3
4
5
6
ISOCITRATE $^{-1}$ mM $^{-1}$

Fig. 15. Replots of slopes and intercepts from Fig. 14 versus NADH concentrations.

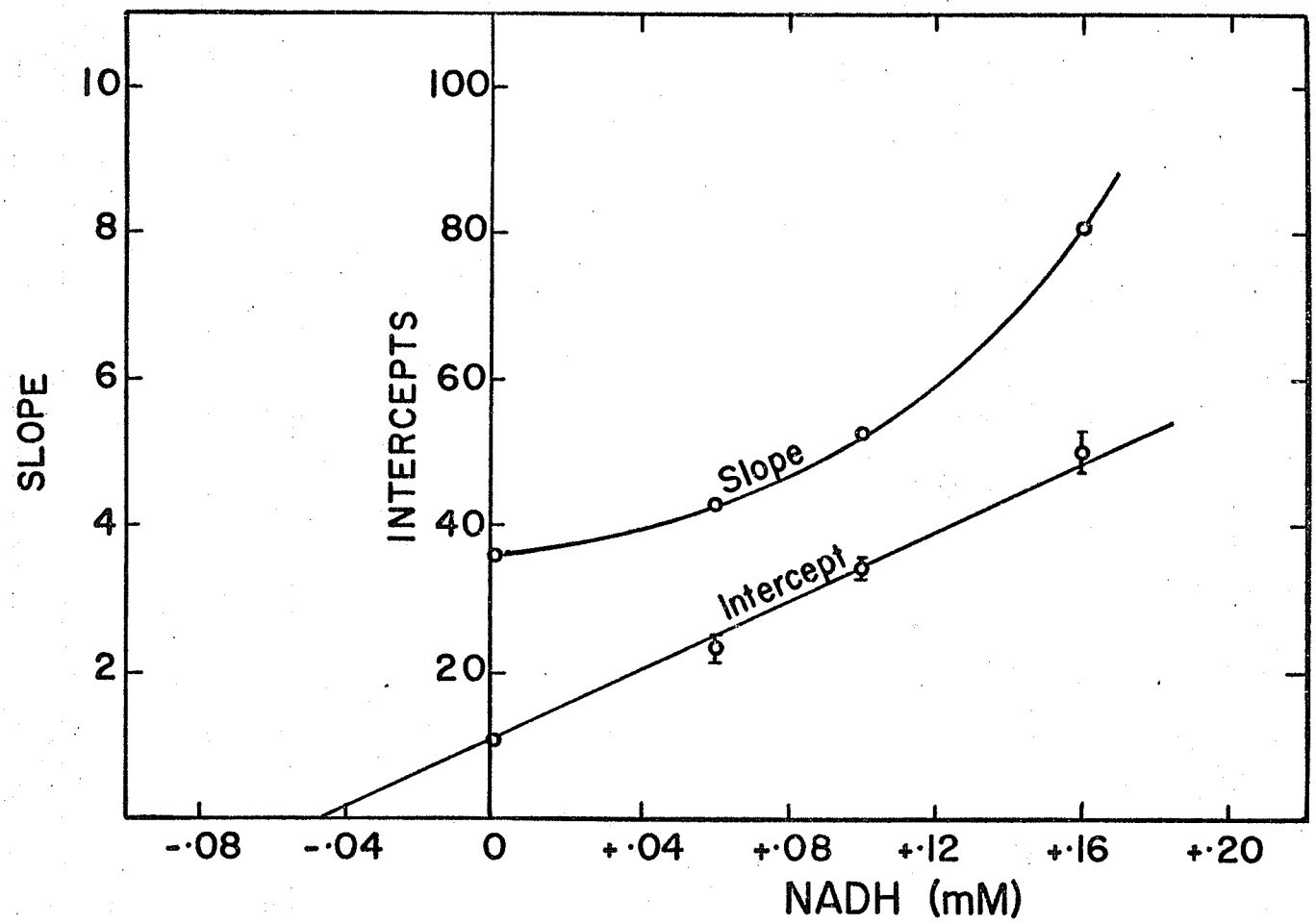
SLOPE
INTERCEPTS
Slope
Intercept
NADH (mM)
10
8
6
4
2
100
80
60
40
20
-·08
-·04
0
+·04
+·08
+·12
+·16
+·20

Fig. 16. Product inhibition of isocitrate dehydrogenase by α-ketoglutarate with NAD as the variable substrate and a fixed concentration of isocitrate (4.056 mM).

Lines have been drawn from an overall fit to equation (28). Enzyme concentration was 125 units per cuvet. Experiments performed with 0.2 M phosphate buffer, pH 6.5.

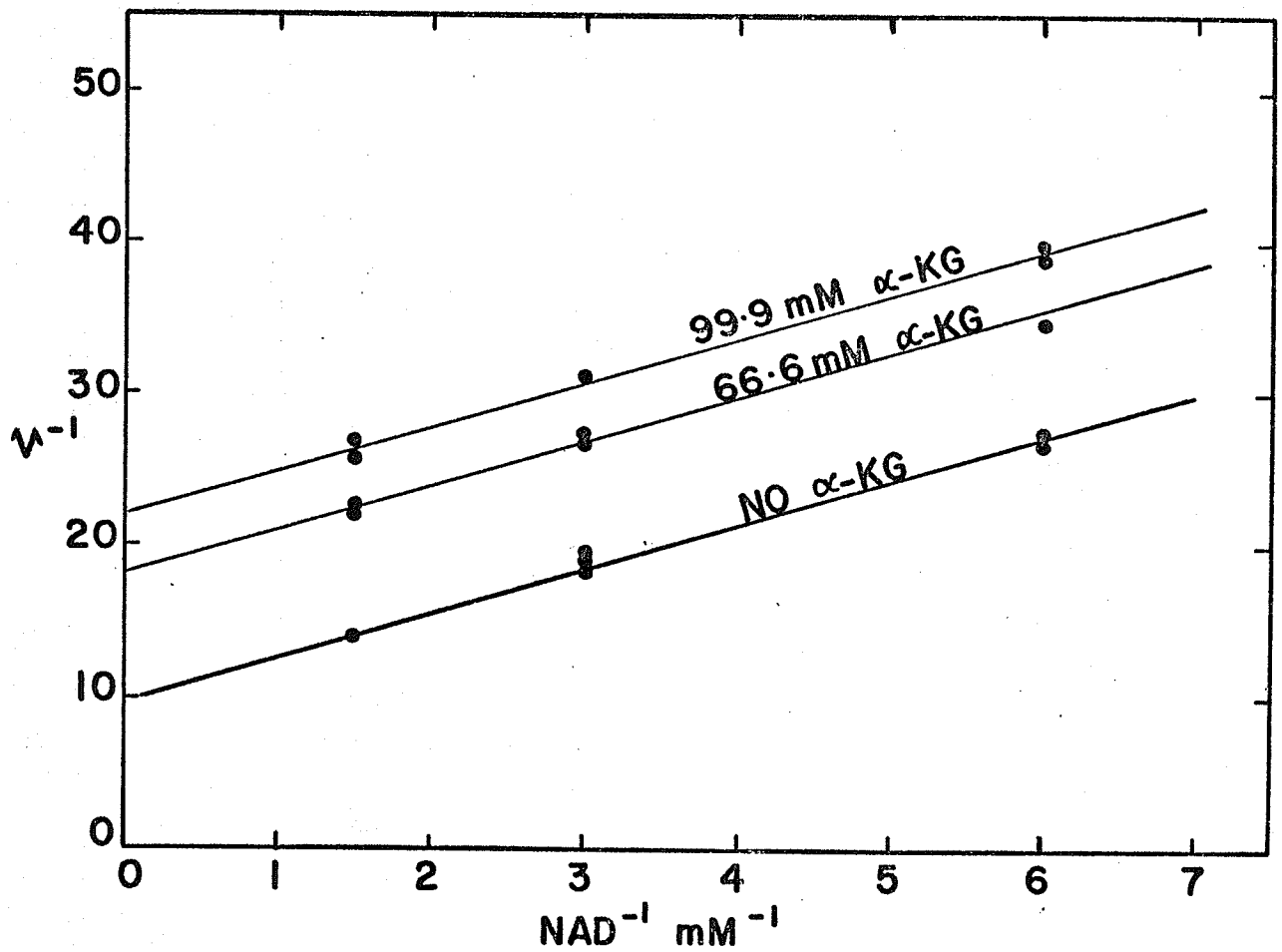
50
40
30
20
10
0
v⁻¹
99·9 mM α-KG
66·6 mM α-KG
NO α-KG
0
1
2
3
4
5
6
7
NAD⁻¹ mM⁻¹

Fig. 17. Product inhibition of isocitrate dehydrogenase by α-ketoglutarate with isocitrate as the variable substrate and a constant concentration of NAD (0.8 mM).

Lines have been drawn from an overall fit to equation (27). Enzyme concentration in each cuvet was 125 units. Phosphate buffer, 0.2 M, pH 6.5, was used in all experiments.

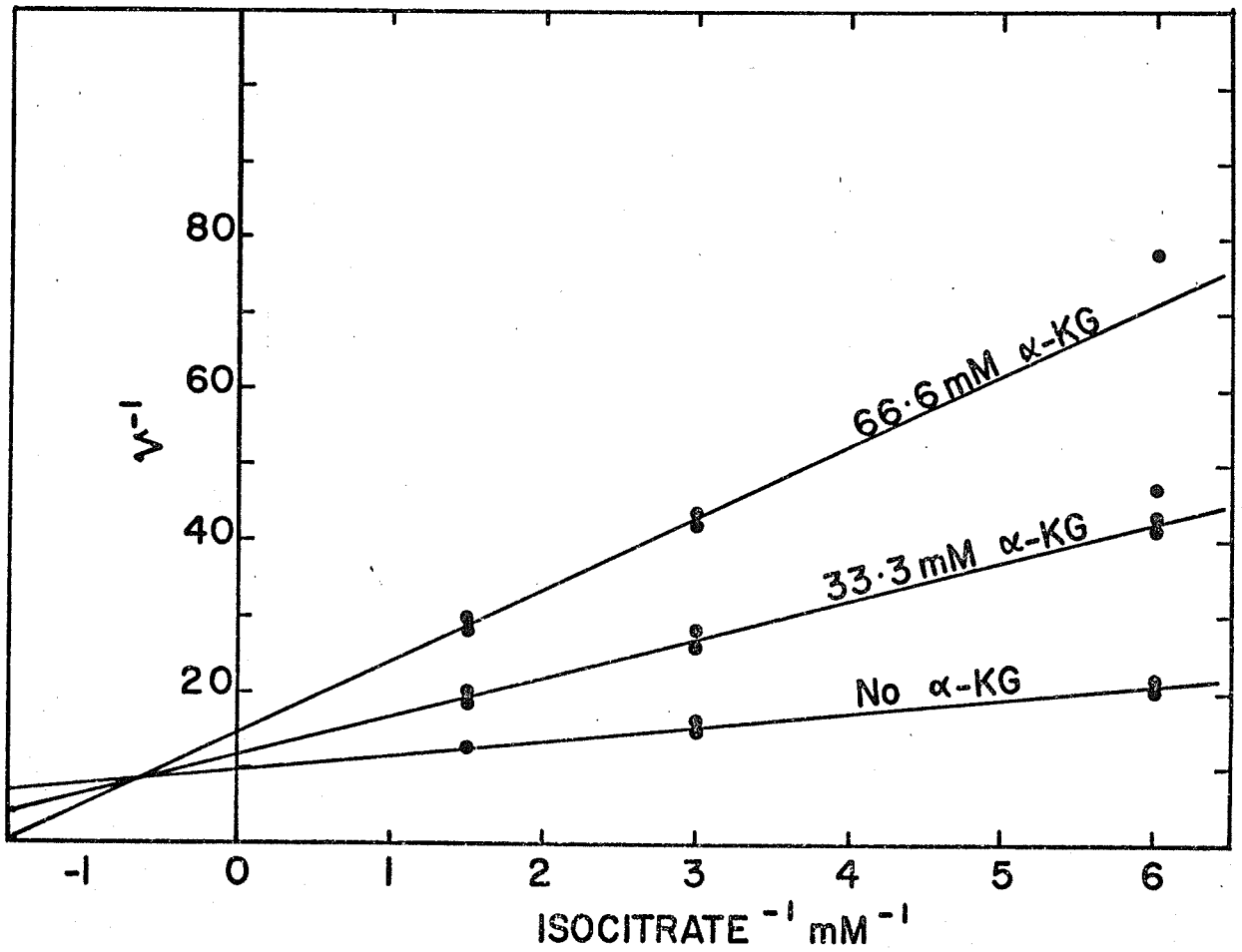
80
60
40
20
v^{-1}
66·6 mM α-KG
33·3 mM α-KG
No α-KG
-1
0
1
2
3
4
5
6
ISOCITRATE $^{-1}$ mM $^{-1}$

Fig. 18. Replots of slopes and intercepts from Fig. 17 versus concentrations of α-ketoglutarate.

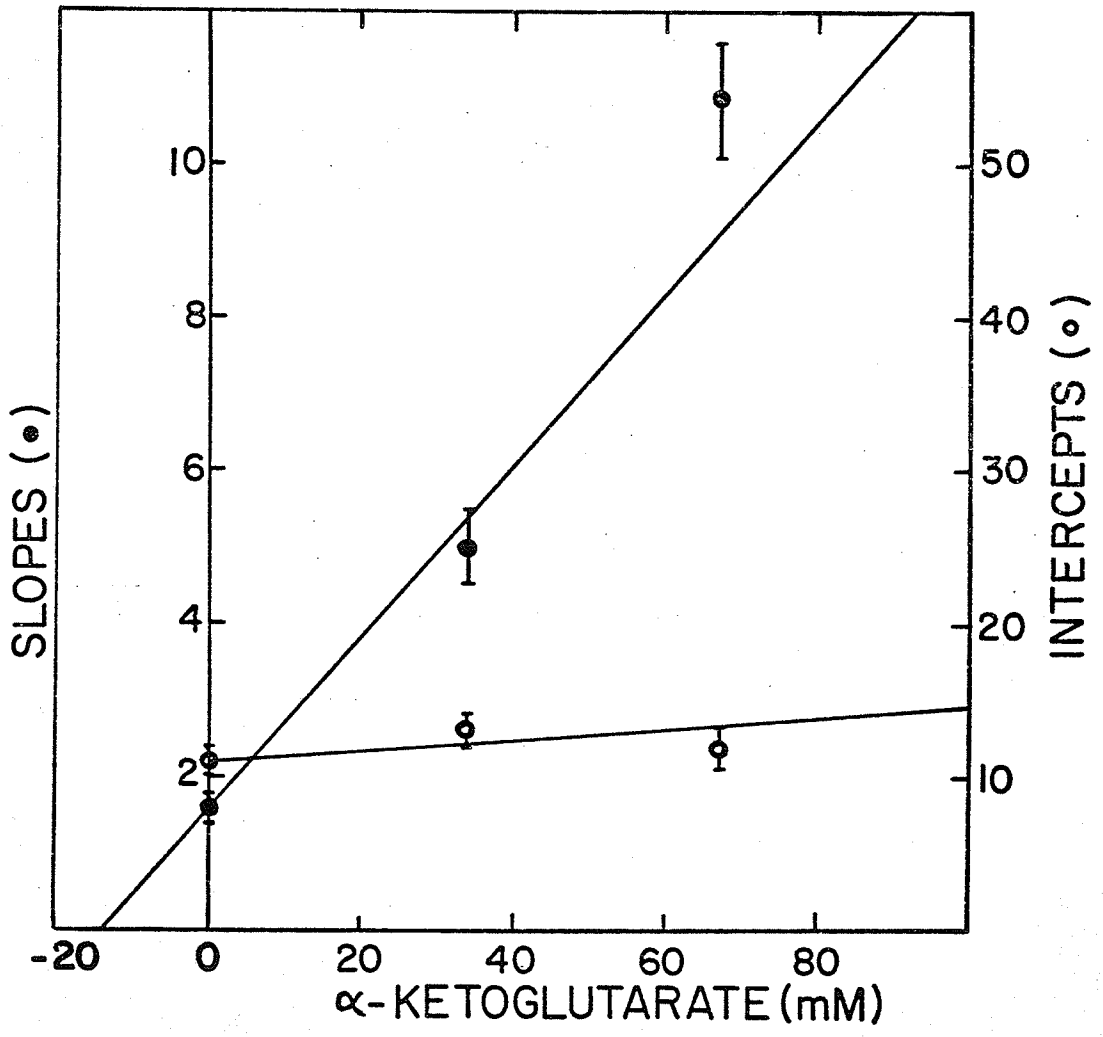
SLOPES (•)
INTERCEPTS (○)
α-KETOGLUTARATE (mM)
10
8
6
4
2
50
40
30
20
10
-20
0
20
40
60
80

Fig. 19. Product inhibition of isocitrate dehydrogenase at pH 6.5 by HCO_3^- with NAD as the variable substrate and a constant concentration of isocitrate (0.4878 mM), unsaturating.

Lines are drawn from an overall fit to equation (27). Enzyme concentration was 170 units per cuvet. Phosphate buffer, 0.2 M, pH 6.5 was used.

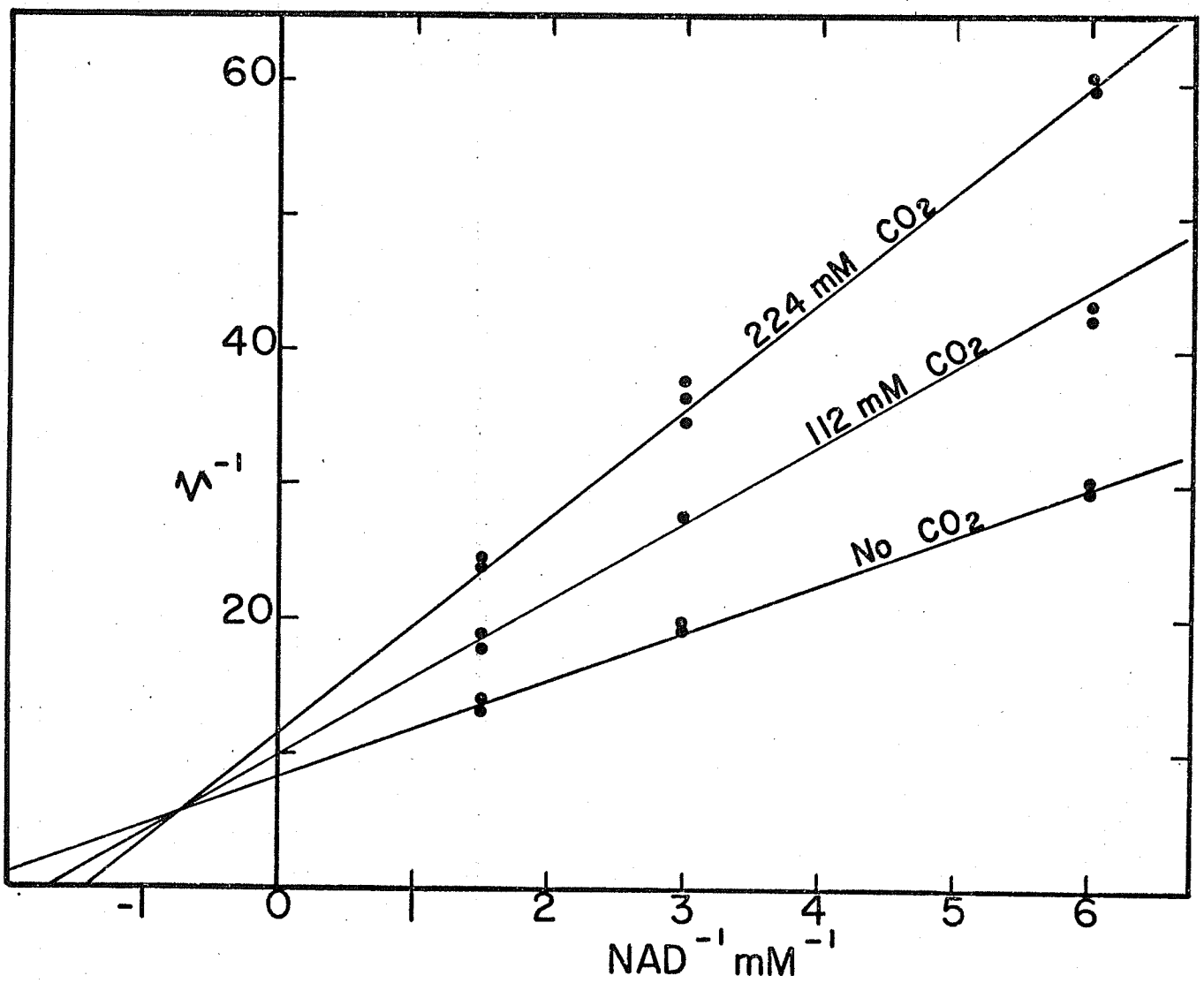
60
40
20
v⁻¹
224 mM CO2
112 mM CO2
No CO2
-1
0
1
2
3
4
5
6
NAD⁻¹ mM⁻¹

Fig. 20. Replots of slopes and intercepts from Fig. 19 versus concentrations of HCO_3^-.

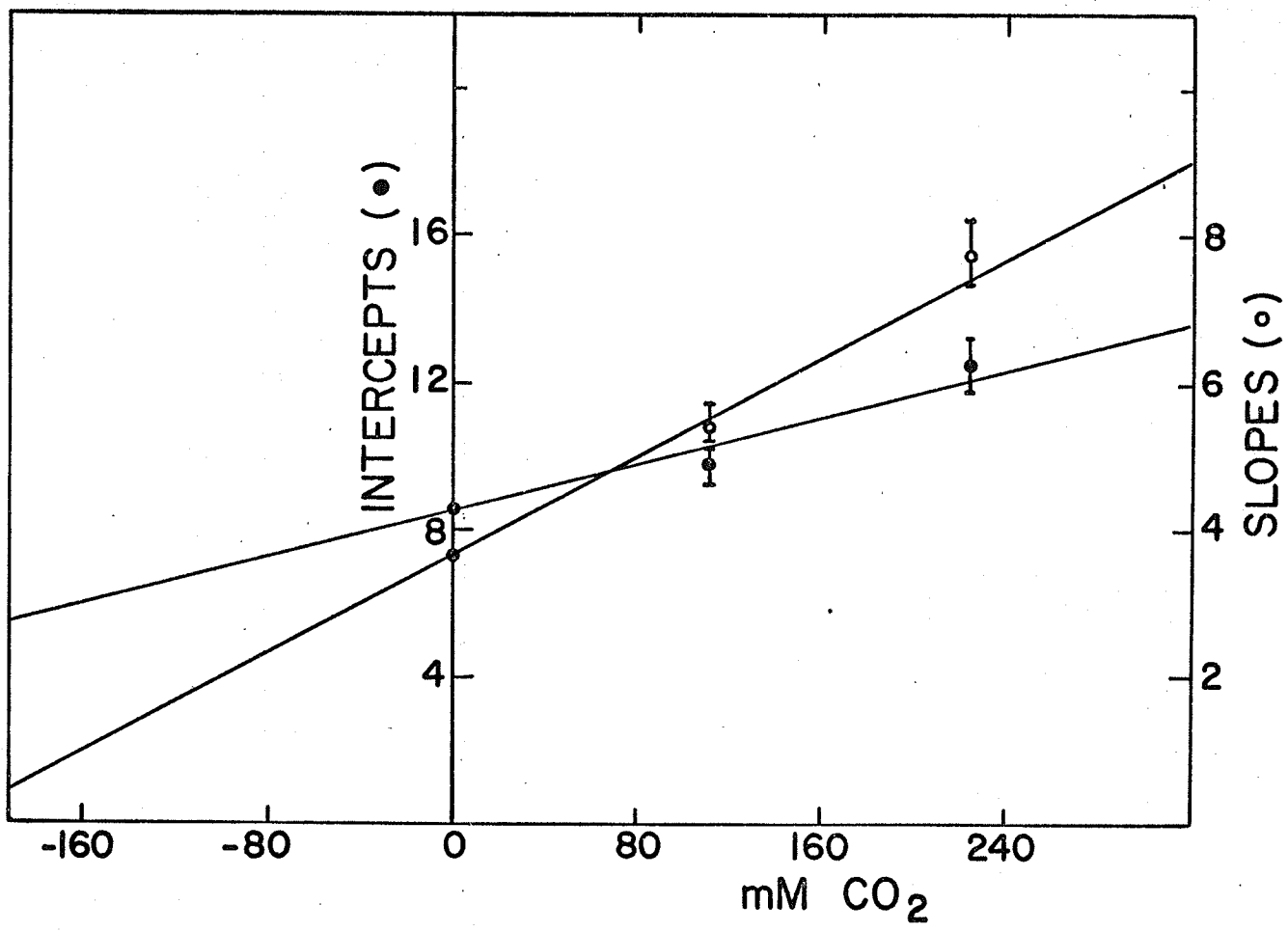
INTERCEPTS (•)
SLOPES (○)
16
12
8
4
8
6
4
2
-160
-80
0
80
160
240
mM CO_2

20) were also linear. When $KHCO_3$ was used as inhibitor and isocitrate was the varied substrate (Fig. 21), the inhibition was again found to be noncompetitive. Replots of slopes and intercepts (Fig. 22) appeared linear although parabolic slopes could not be ruled out due to large standard errors in fits to equation (23). As with α-ketoglutarate, it appeared that $KHCO_3$ combined as a dead-end inhibitor with the enzyme-NAD complex as well as a product inhibitor.

Initial Velocity and Product Inhibition Analysis at pH 7.6, in the Presence of AMP.

a) In the absence of the allosteric effector, citrate.

As previously described (Sanwal et al., 1965) NAD-specific isocitrate dehydrogenase exhibits allosteric effects at its pH optimum of 7.6. When isocitrate was varied against several fixed concentrations of NAD, the double reciprocal plots were curved (Fig. 23). These curves were fitted to equation (24) and significant fits were obtained, but produced a negative b coefficient, which would be impossible if these curves were parabolas.

When NAD was varied against several fixed concentrations of isocitrate, the double reciprocal plots were linear (Fig.

Fig. 21. Product inhibition of isocitrate dehydrogenase by HCO_3^- with isocitrate as the variable substrate and a fixed concentration of NAD (0.8 mM).

Individual lines are drawn from fits to equation (23). Enzyme concentration was 125 units per cuvet. Phosphate buffer, 0.2 M, pH 6.5, was used in all experiments.

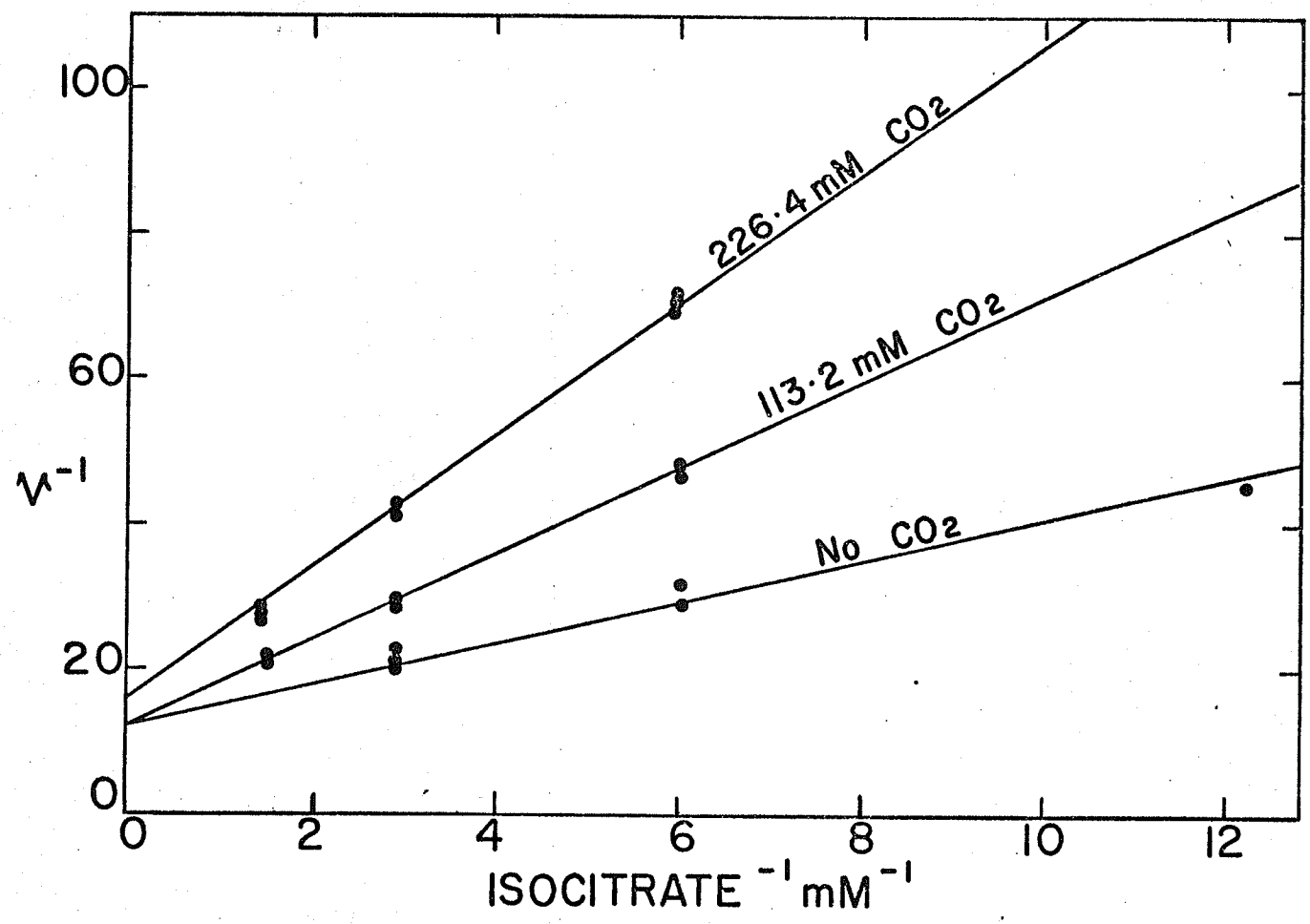
100
60
20
0
v^{-1}
226·4 mM CO_2
113·2 mM CO_2
No CO_2
0
2
4
6
8
10
12
ISOCITRATE $^{-1}$ mM $^{-1}$

Fig. 22. Replots of slopes and intercepts from Fig. 21 versus concentrations of HCO_3^-.

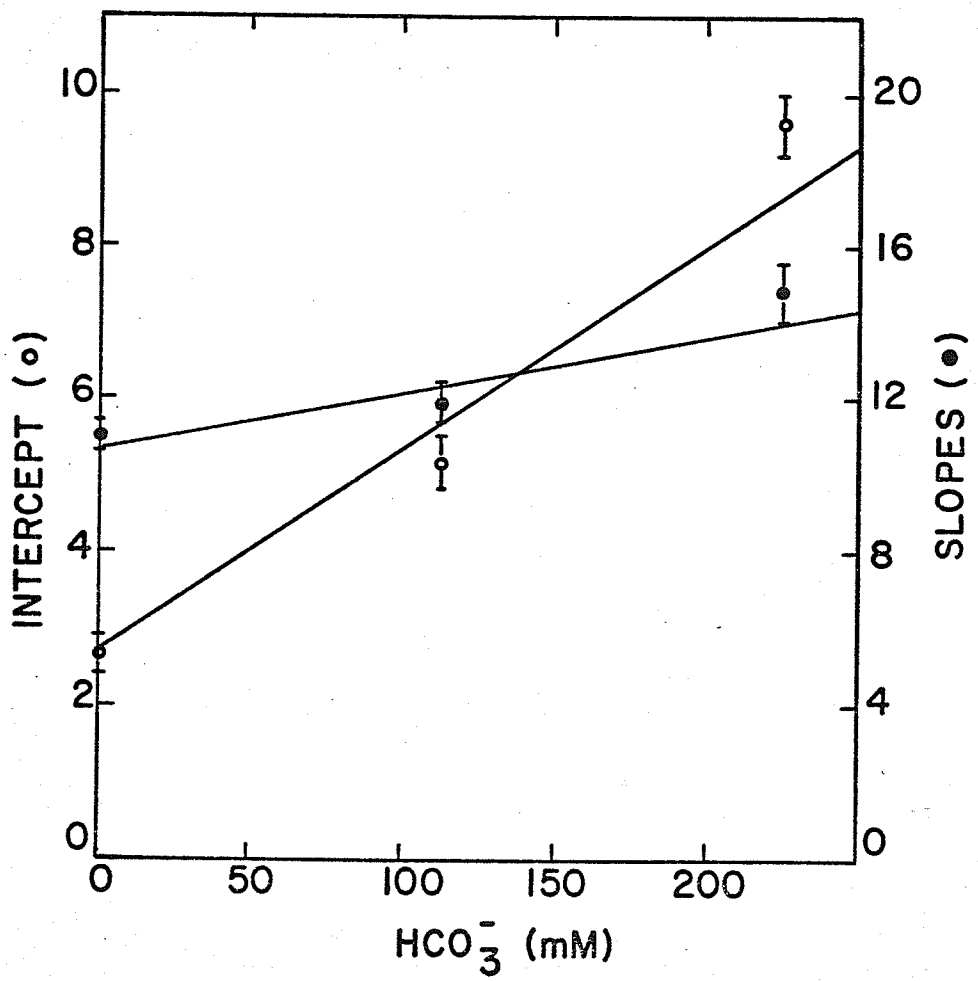
INTERCEPT (○)
SLOPES (●)
HCO_3^- (mM)
0
2
4
6
8
10
0
4
8
12
16
20
0
50
100
150
200

Fig. 23. Double-reciprocal plots of 1/velocity versus 1/isocitrate at several fixed concentrations of NAD.

Enzyme concentration was 100 units per cuvet. The lines have been drawn from fits to equation (24), dotted lines being the extrapolated parts of the curves. Tris-acetate buffer, 0.2 M, pH 7.6, was used in all the experiments.

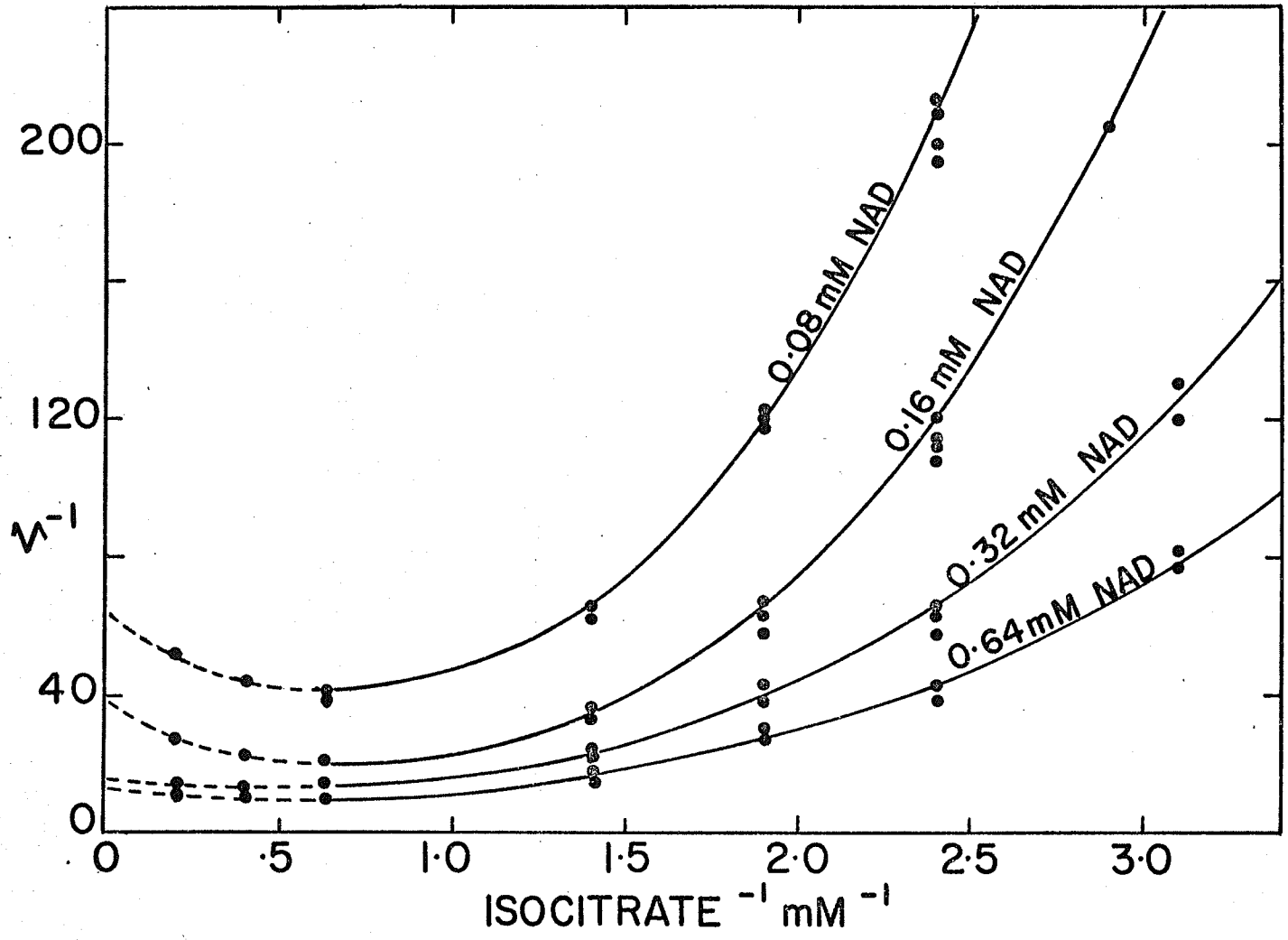
200
120
40
0
v⁻¹
0·08 mM NAD
0·16 mM NAD
0·32 mM NAD
0·64 mM NAD
0
·5
1·0
1·5
2·0
2·5
3·0
ISOCITRATE ⁻¹ mM ⁻¹

24). Replots of slopes and intercepts against isocitrate concentrations were curved (Fig. 25) and were not analyzed further.

b) In the presence of the allosteric modifier, citrate.

Isocitrate dehydrogenase was shown to be activated by citrate and erythro-L_s-isocitrate at pH 7.6, and to change the curved double reciprocal plots, i.e, Fig. 23, into linear plots. The effect of citrate on the velocity of the enzymic reaction at pH 7.6 was tested.

Citrate was varied against several fixed concentrations of isocitrate in the presence of a constant amount of NAD and the double reciprocal plots of $1/v-v^o$ vs 1/citrate were linear (Fig. 26). Attempts were made to fit the data from Fig. 26 to the following initial velocity equation:

$$\frac{1}{v-v^o} = \left(1 + \frac{B}{K_1}\right)\left(\frac{K_{ia}K_b}{AB} + \frac{K_b}{B} + \frac{K_a}{A} + 1\right) x \left(\frac{K_2}{V}\left(1 + \frac{B}{K_1}\right)\frac{1}{M} + \frac{1}{V}\right) \quad \ldots\ldots\ldots (34)$$

(where v is the velocity in the presence of modifier (M), v^o is the velocity in the absence of modifier, B is the substrate, A is coenzyme, and K_1 and K_2 are dissociation constants of B and M respectively, from the allosteric sites).

Fig. 24. Double-reciprocal plots of 1/velocity versus 1/NAD at several fixed concentrations of isocitrate.

Individual lines are drawn from fits to equation (23). Enzyme concentration was 100 units per cuvet. All experiments were performed in 0.2 M Tris-acetate buffer, pH 7.6.

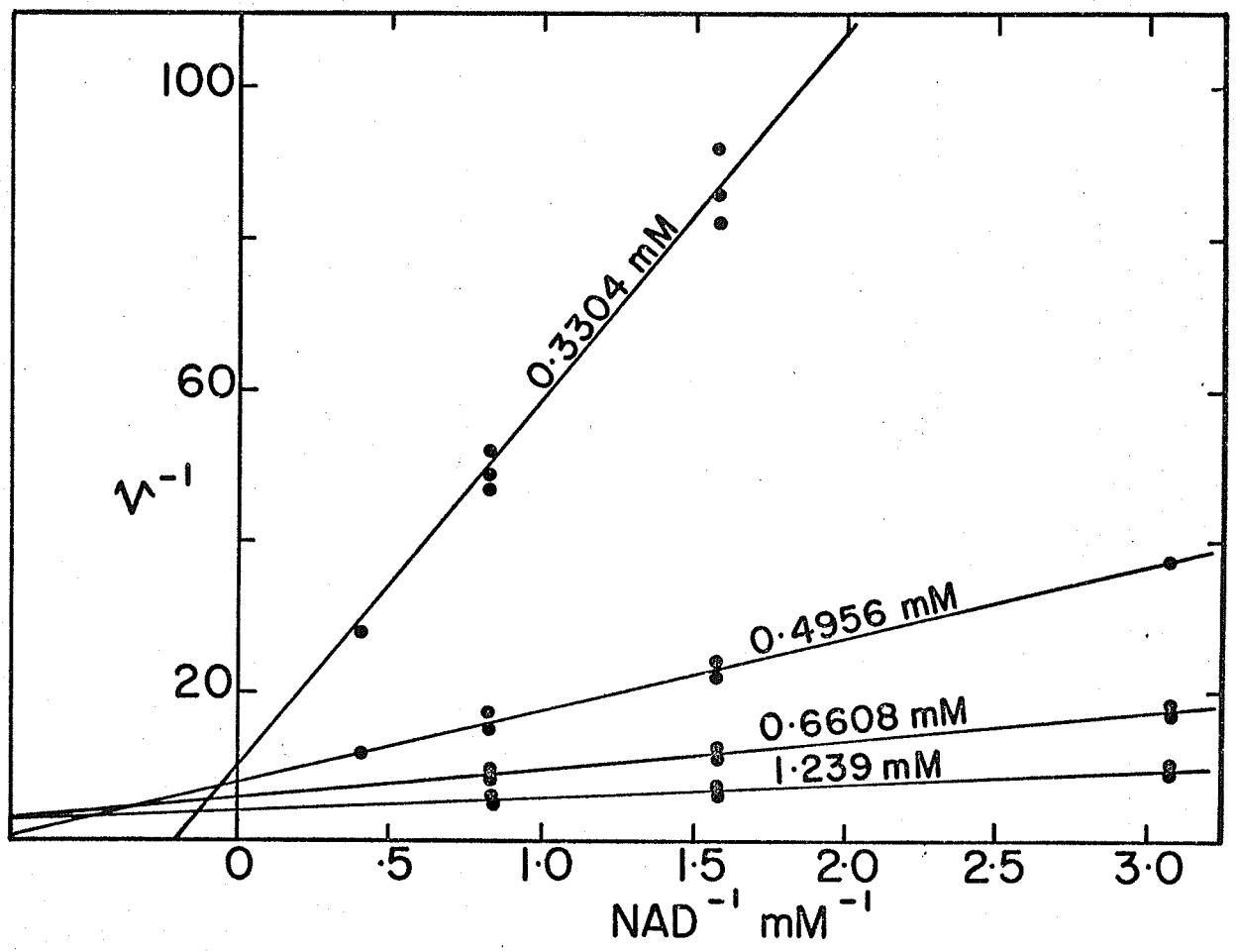
100
60
20
v⁻¹
0·3304 mM
0·4956 mM
0·6608 mM
1·239 mM
0
·5
1·0
1·5
2·0
2·5
3·0
NAD⁻¹ mM⁻¹

Fig. 25. Replots of slopes, intercepts and apparent Michaelis constants (K_{app}) from Fig. 24 versus concentrations of isocitrate.

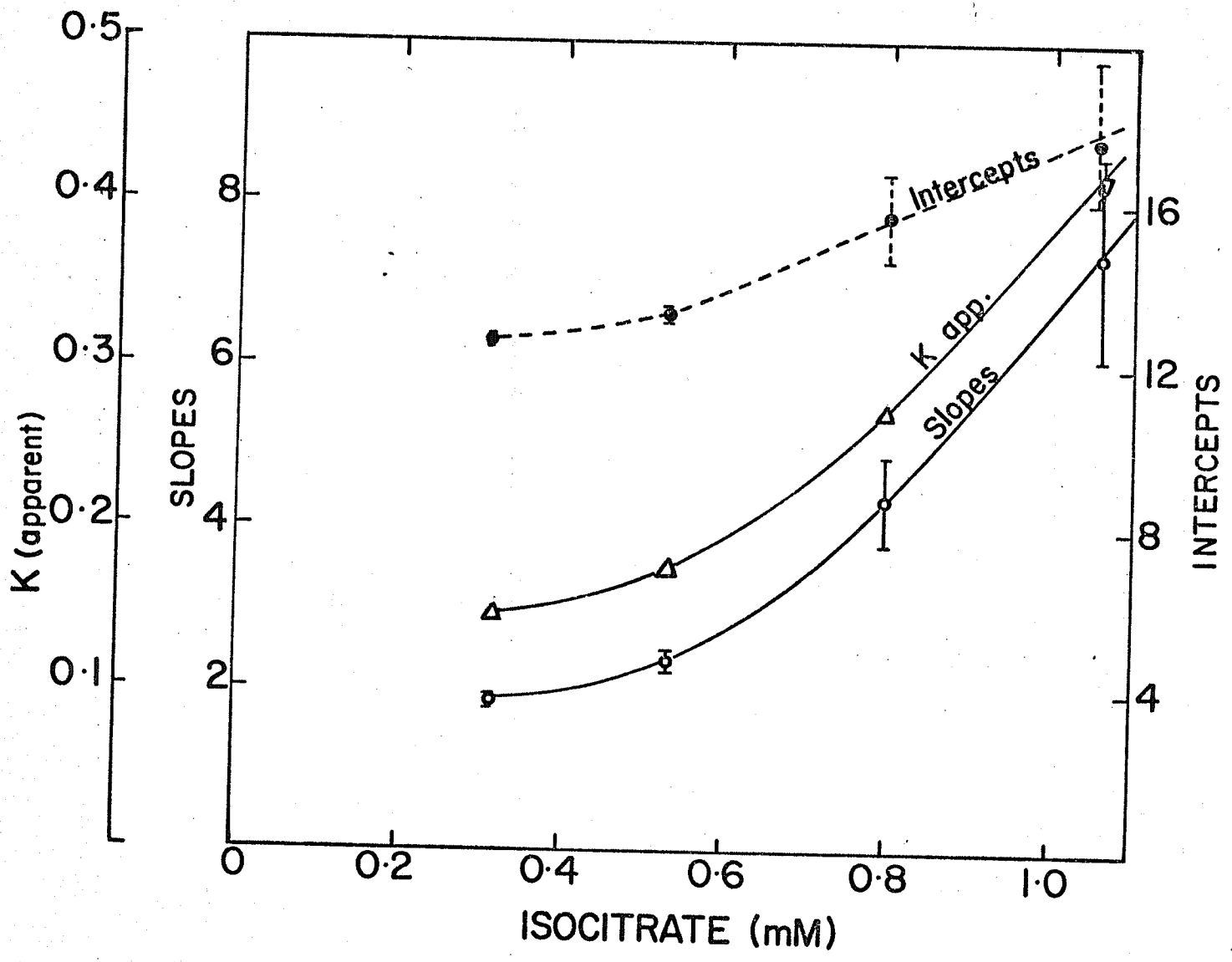
0·5
0·4
0·3
0·2
0·1
K (apparent)
8
6
4
2
SLOPES
16
12
8
4
INTERCEPTS
Intercepts
K app.
Slopes
0
0·2
0·4
0·6
0·8
1·0
ISOCITRATE (mM)

Fig. 26. The effect of citrate on the velocity of enzymic reaction at pH 7.6. Here v = velocity in the presence of citrate and v^o = velocity in the absence of citrate.

Lines shown are fitted to equation (23).

Figures above the lines refer to the concentration of isocitrate. All reaction mixtures contained 0.8 mM NAD. Enzyme concentration was about 250 units per cuvet. Tris-acetate buffer (0.2 M) was used throughout.

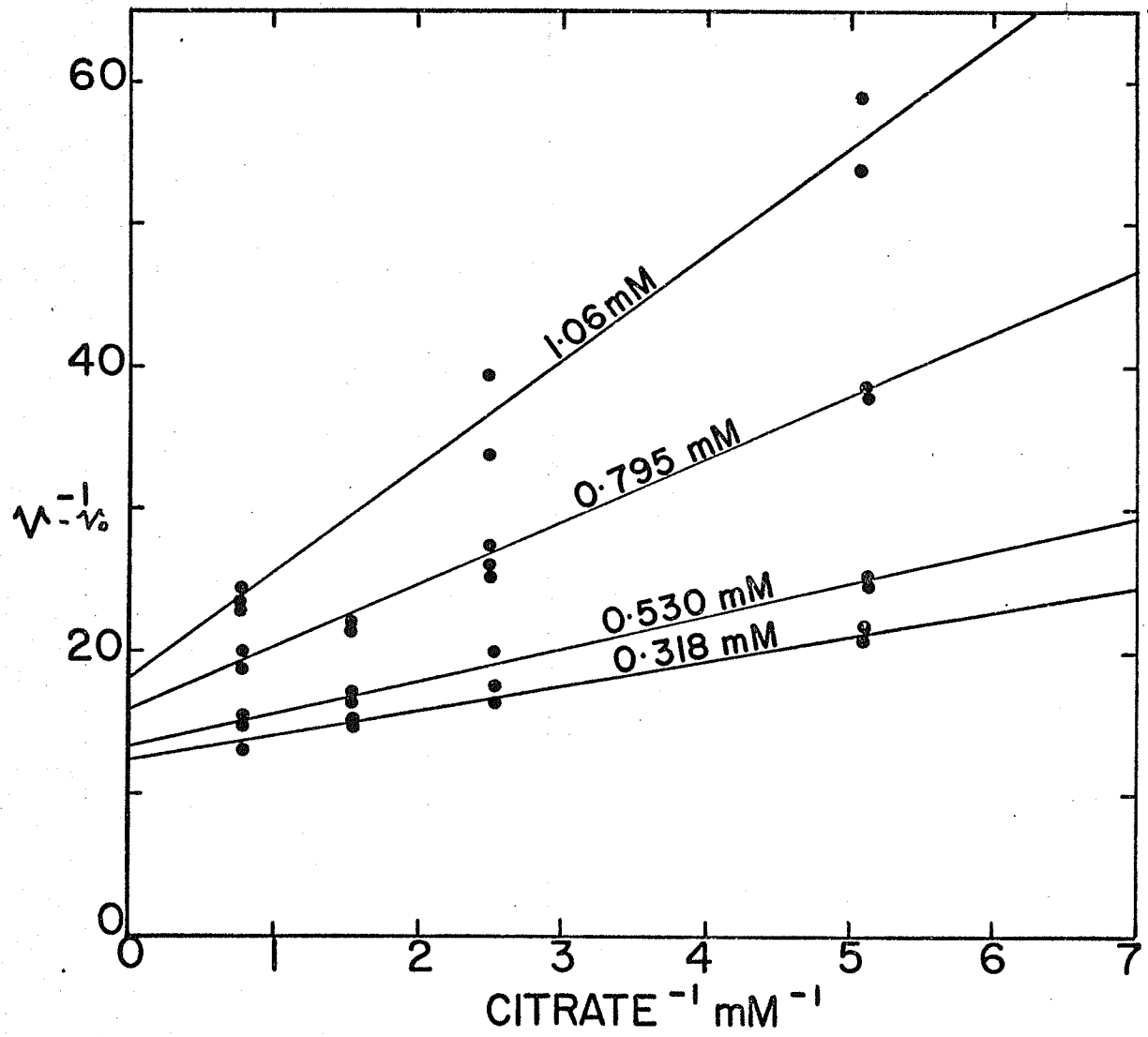
60
40
20
0
v^{-1} - v_0
1·06mM
0·795 mM
0·530 mM
0·318 mM
0
1
2
3
4
5
6
7
CITRATE $^{-1}$ mM $^{-1}$

This is the equation for an enzyme demonstrating a total allosteric mechanism (no activity without substrate or modifier binding at the allosteric site). The equation predicts that double reciprocal plots of $1/v-v^o$ versus $1/M$ will be linear and the apparent Michaelis constant (slope /intercept) will be a linear function of B. The results of Fig. 26 obey this prediction. However on replotting K_{app} versus isocitrate concentration (Fig. 25) curved lines were obtained indicating a dependence of the citrate dissociation constant on isocitrate concentration.

The effect of saturating citrate concentrations (2 mM) on the initial velocity pattern at pH 7.6 was tested. When NAD was used as the variable substrate and isocitrate as the changing fixed substrate (Fig. 27), the double reciprocal plots were linear. Replots of slopes and intercepts against the reciprocal of isocitrate concentration (Fig. 28) were linear. When NAD was varied against several fixed concentrations of NADH as product inhibitor (Fig. 29), competitive inhibition was obtained. The replot of slopes against NADH was also linear.

Fig. 27. Double-reciprocal plots of 1/velocity versus 1/NAD at several fixed concentrations of isocitrate in the presence of a constant high concentration of citrate (2.2 mM).

Each cuvet contained about 400 units of enzyme. The lines have been drawn from an overall fit to equation (33). All experiments performed in Tris-acetate buffer, 0.2 M, pH 7.6.

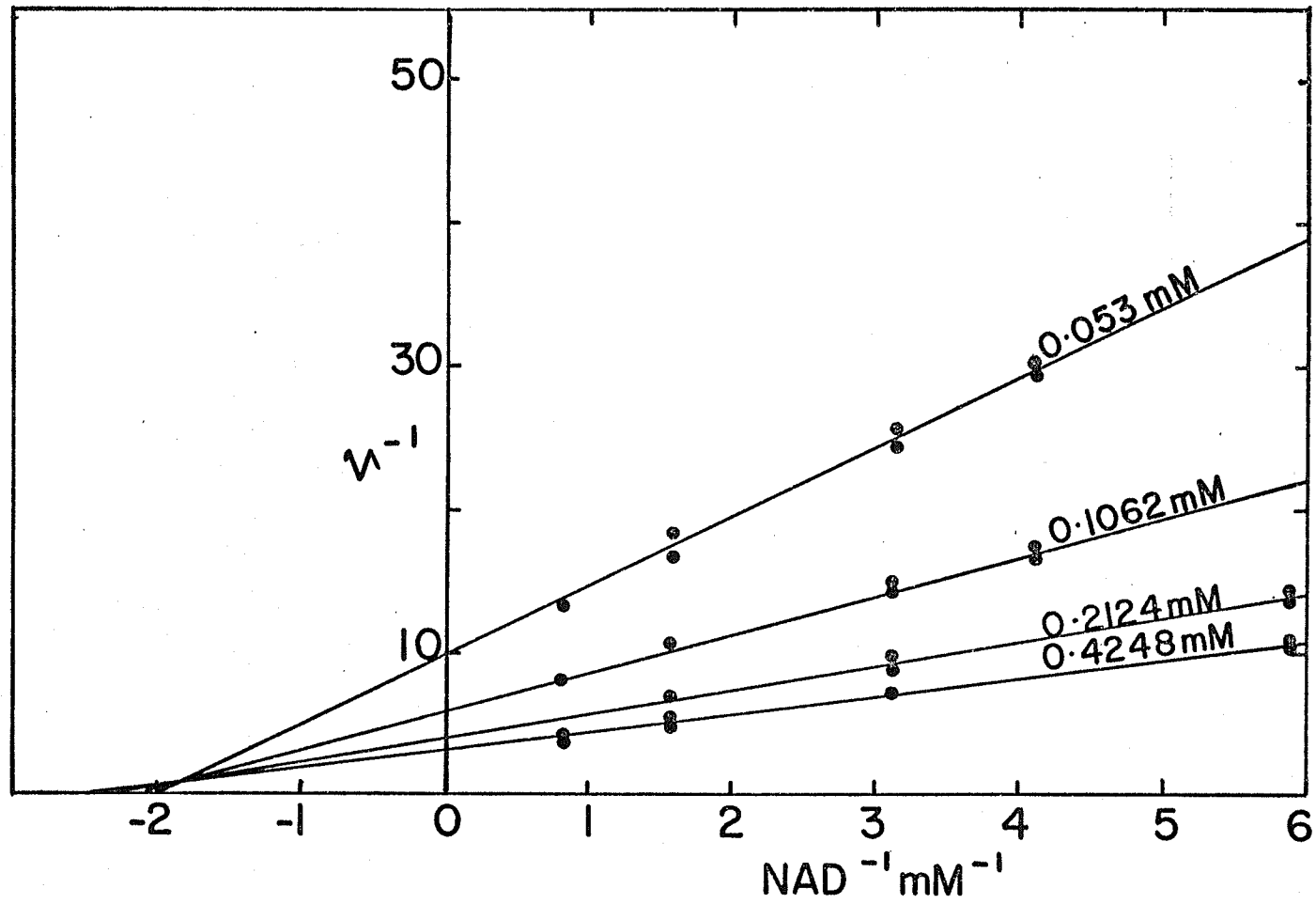
50
30
10
v^{-1}
0·053 mM
0·1062 mM
0·2124 mM
0·4248 mM
-2
-1
0
1
2
3
4
5
6
NAD $^{-1}$ mM $^{-1}$

Fig. 28. Replots of intercepts and slopes from Fig. 27 versus the reciprocals of isocitrate concentrations.

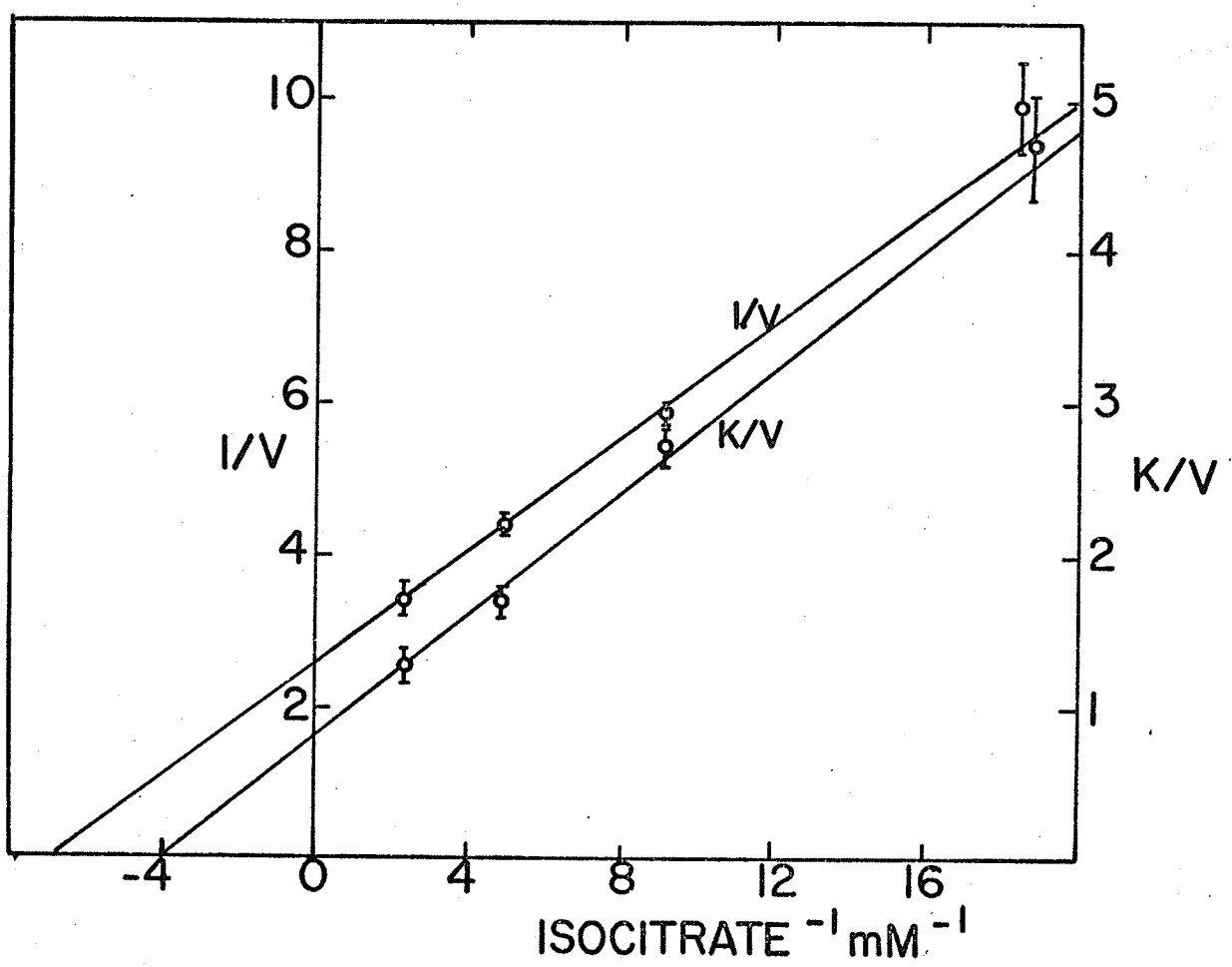
10
8
6
4
2
I/V
I/V
K/V
5
4
3
2
1
K/V
-4
0
4
8
12
16
ISOCITRATE $^{-1}$ mM $^{-1}$

Fig. 29. Product inhibition of isocitrate dehydrogenase by NADH at pH 7.6 in the presence of a constant high concentration of citrate (2.2 mM). NAD was used as the variable substrate and isocitrate was kept constant (2 mM).

Lines are drawn from an overall fit to equation (26). Enzyme (60 units) was used in each cuvet. Tris-acetate, 0.2 M, was used in all experiments.

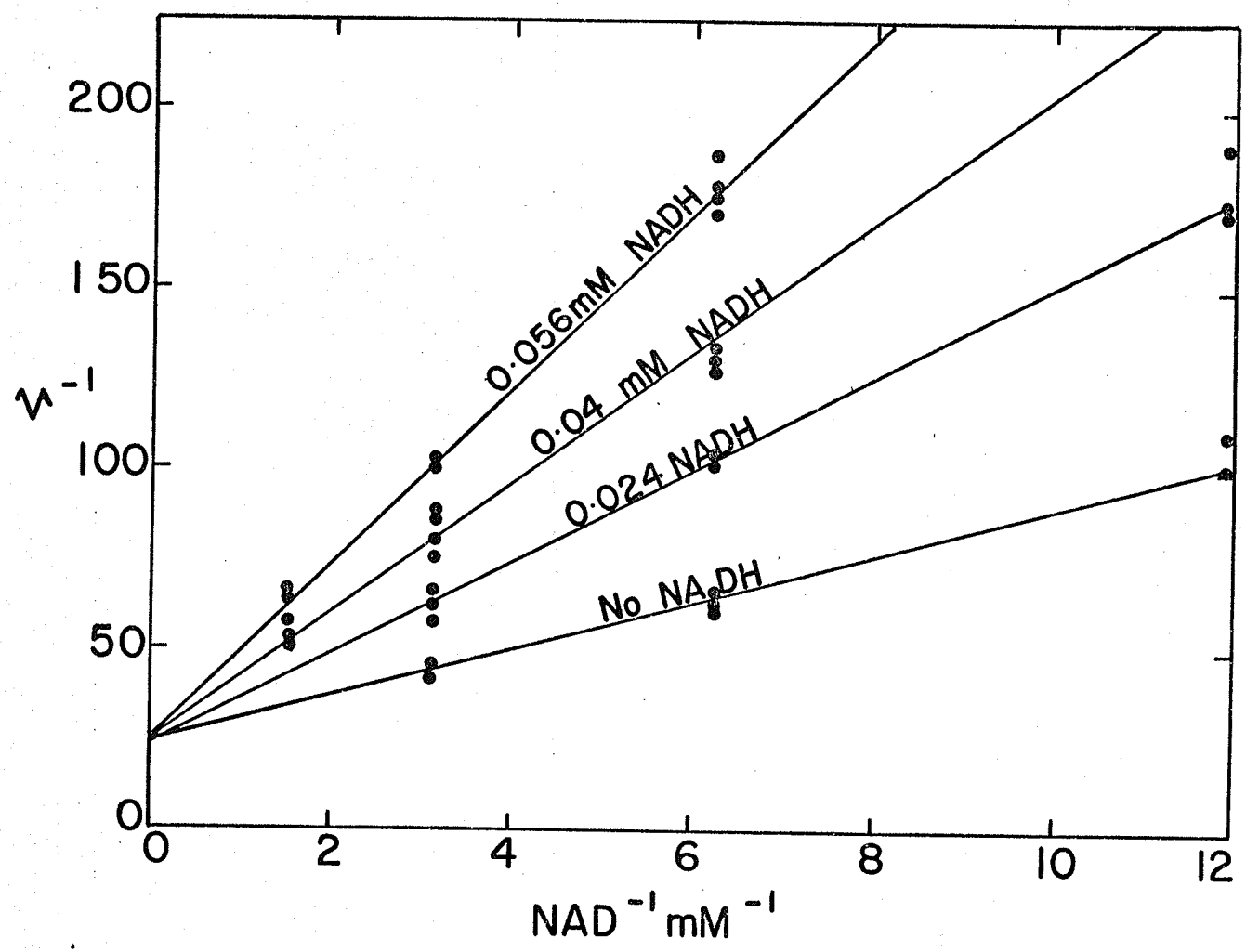
200
150
100
50
0
v^{-1}
0·056mM NADH
0·04 mM NADH
0·024 NADH
No NADH
0
2
4
6
8
10
12
$NAD^{-1}\,mM^{-1}$

Initial Velocity Analysis in the Absence of AMP.

AMP had been shown previously (Sanwal et al., 1964) to activate the enzymic reaction. However there appeared to be no absolute requirement for AMP since the V_{max} of the reaction was unaffected in the absence or presence of this modifier. The mechanism of activation of isocitrate dehydrogenase was then analyzed at pH 6.5 by initial velocity and product inhibition studies.

When NAD was varied at several fixed concentrations of isocitrate in the absence of AMP, the double reciprocal plots were markedly curved at low isocitrate concentration but become linear at high concentrations of isocitrate (Fig. 30). The data from Fig. 30 were fitted to the Hill equation (22):

$$\log \frac{v}{V - v} = n \log S - \log K \qquad \ldots\ldots (22)$$

(where v is initial velocity, V is maximum velocity, S is substrate concentration, K is a complex dissociation constant and n is equal to the Sigmoid coefficient).

Plotting log (v/V - v) versus log S straight lines were obtained (Fig. 31) of slope = n. At low isocitrate concentrations the value of n was 2.5 which changed to a value

Fig. 30. Double-reciprocal plots of 1/velocity versus 1/NAD at several fixed concentrations of isocitrate in the absence of AMP.

Phosphate buffer, 0.2 M, pH 6.5, was used in all experiments. The solid line has been drawn from fit to equation (23). The dashed lines are fitted by eye.

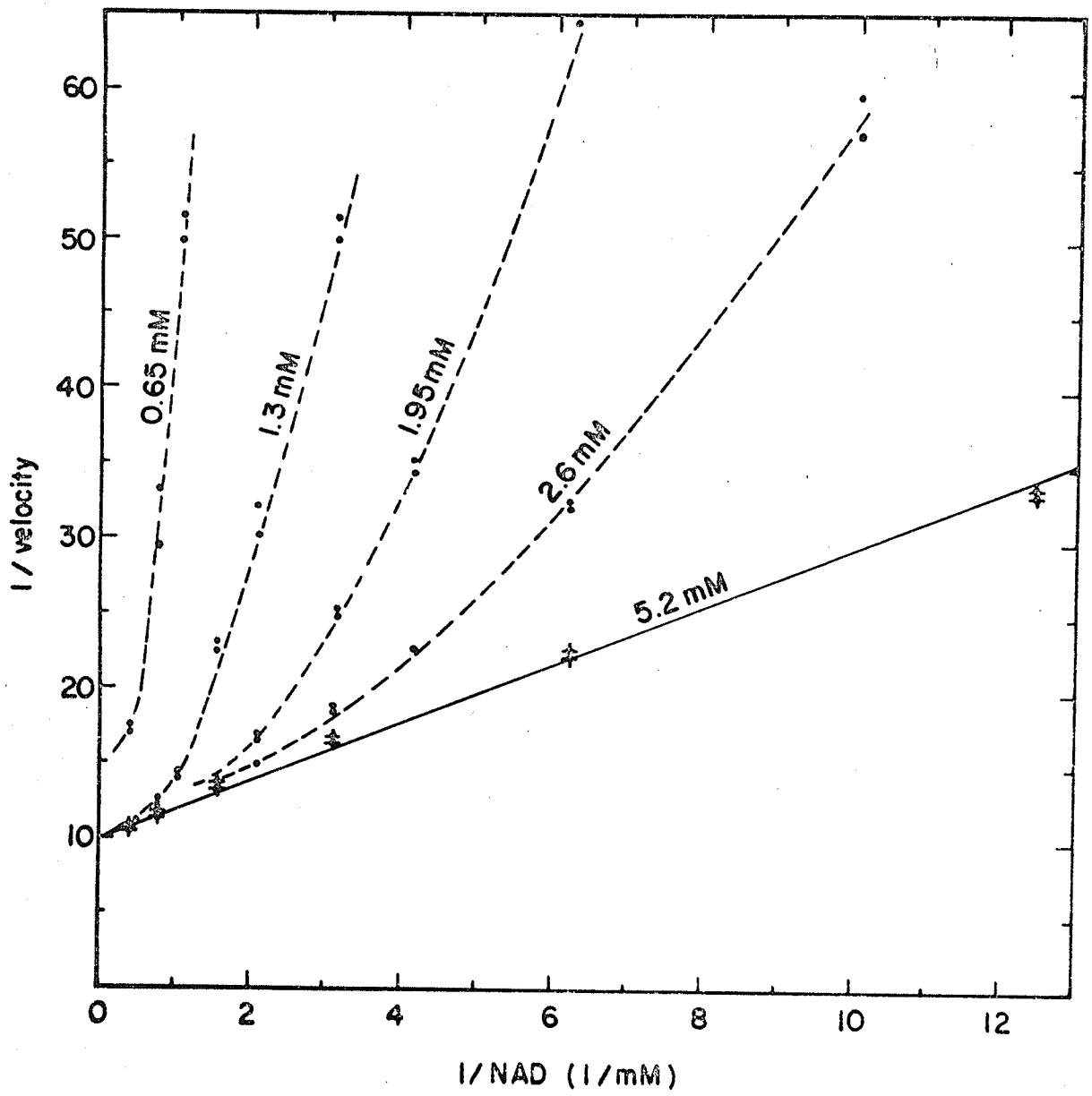
60
50
40
30
20
10
0
2
4
6
8
10
12
1/ velocity
1/NAD (1/mM)
0.65 mM
1.3 mM
1.95mM
2.6mM
5.2 mM

Fig. 31. Data from Fig. 30 drawn in the form of log-log plots (equation 22).

The lines have been fitted by eye.

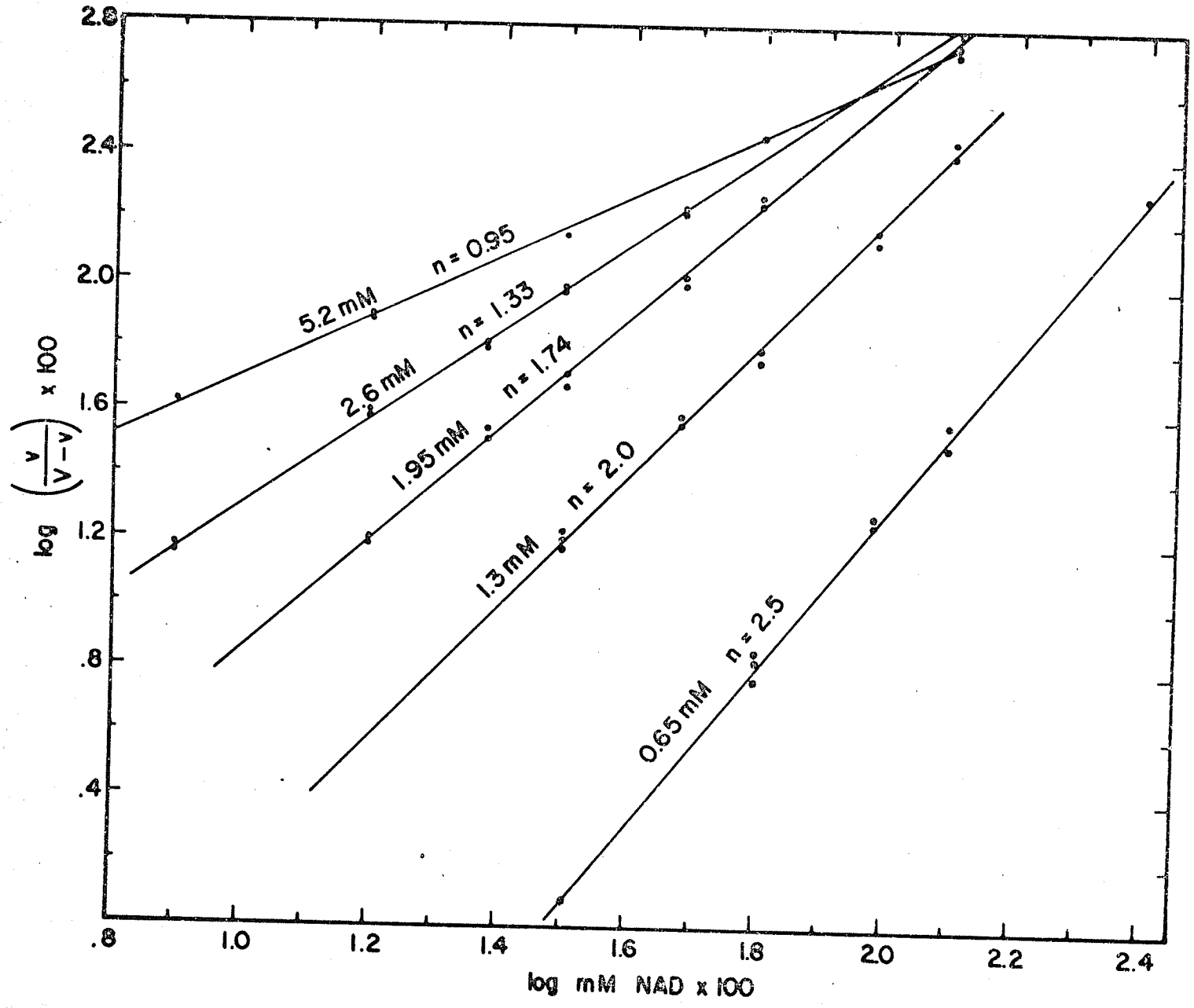
2.8
2.4
2.0
1.6
1.2
.8
.4
.8
1.0
1.2
1.4
1.6
1.8
2.0
2.2
2.4
log $\left(\frac{v}{V-v}\right)$ x 100
log mM NAD x 100
5.2 mM n = 0.95
2.6 mM n = 1.33
1.95 mM n = 1.74
1.3 mM n = 2.0
0.65 mM n = 2.5

of 1 when isocitrate concentration was increased.

When isocitrate concentration was varied against several fixed changing concentrations of NAD, the double reciprocal plots were nonlinear (Fig. 32). In contrast to Fig. 30 the lines did not become linear at high levels of NAD. When the data of Fig. 32 were plotted by means of equation (22), the value of n was approximately 3.7 at low levels of NAD but approached 2.8 with near saturation levels of NAD (Fig. 33).

The effect of citrate was then tested on the reaction in the absence and presence of AMP. Varying isocitrate concentrations at a fixed unsaturating concentration of NAD (0.8 mM), citrate was shown to activate the reaction in the absence of AMP (Fig. 34). It was also demonstrated that activation by citrate did not occur in the presence of AMP at pH 6.5.

When NAD was used as the variable substrate and isocitrate was the changing fixed substrate in the presence of nearly saturating concentrations of citrate (6.6 mM), the double reciprocal plot was concave up near the y axis at 0.166 mM isocitrate, but linear at high isocitrate concentrations (Fig. 35). The data obtained using the lowest isocitrate

Fig. 32. Double-reciprocal plots of 1/velocity versus 1/isocitrate at two fixed levels of NAD in the absence of AMP.

The buffer was 0.2 M phosphate, pH 6.5. The solid line (lower) has been drawn from fits to equation (24), dotted part being extrapolated parts of the curve. The dashed line is fitted by eye.

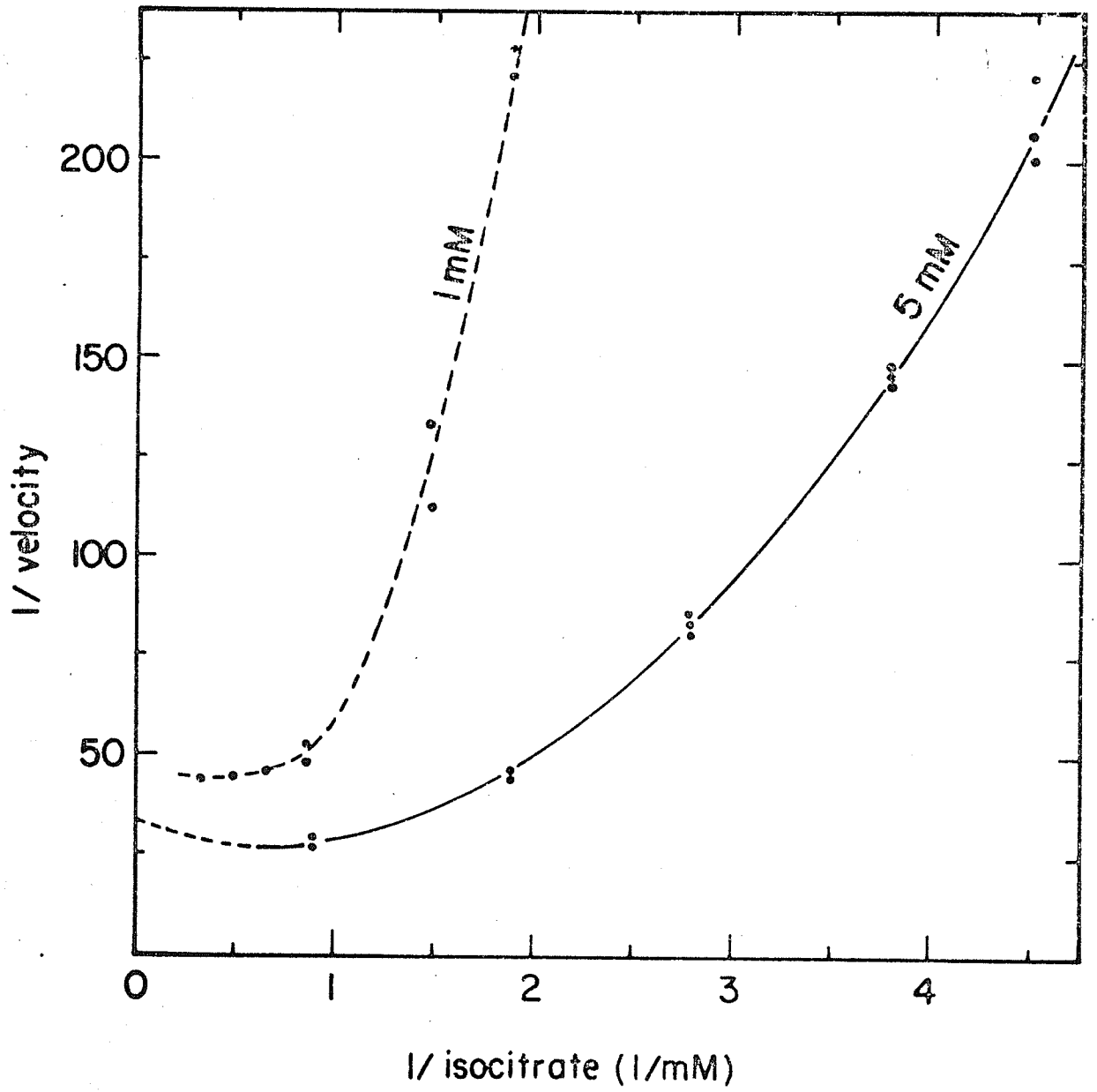
200
150
100
50
1/ velocity
1mM
5mM
0
1
2
3
4
1/ isocitrate (1/mM)

Fig. 33. Data from Fig. 32 drawn in the form of log-log plots (equation 22).

The lines have been fitted by eye.

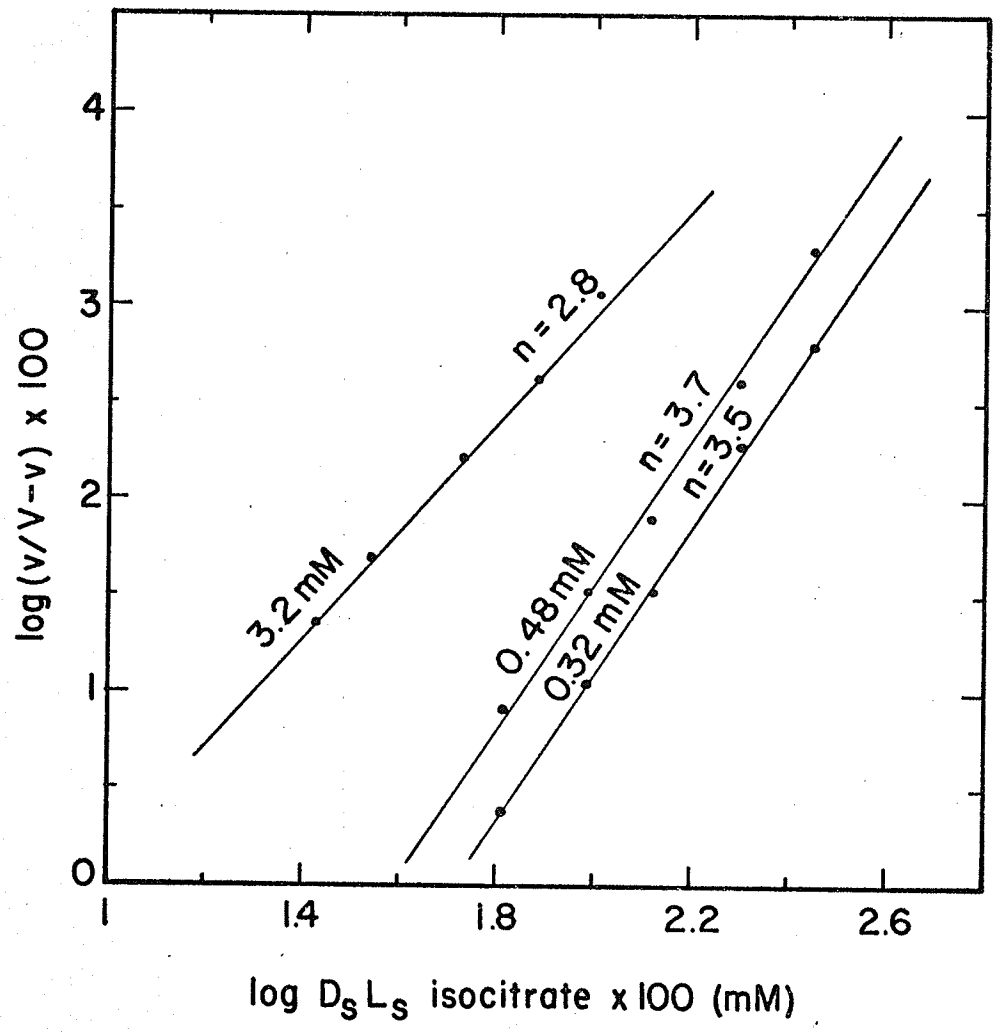
log (v/V-v) x 100
log $D_S L_S$ isocitrate x 100 (mM)
0
1
2
3
4
1
1.4
1.8
2.2
2.6
3.2 mM
n=2.8
0.48 mM
n=3.7
0.32 mM
n=3.5

Fig. 34. The activation of isocitrate dehydrogenase by citrate in the presence and absence of AMP at pH 6.5.

When used, AMP concentration was 0.533 mM and citrate concentration was 1.5 mM. The NAD concentration was kept constant (0.8 mM unsaturating). (A) refers to assay in the presence of AMP.

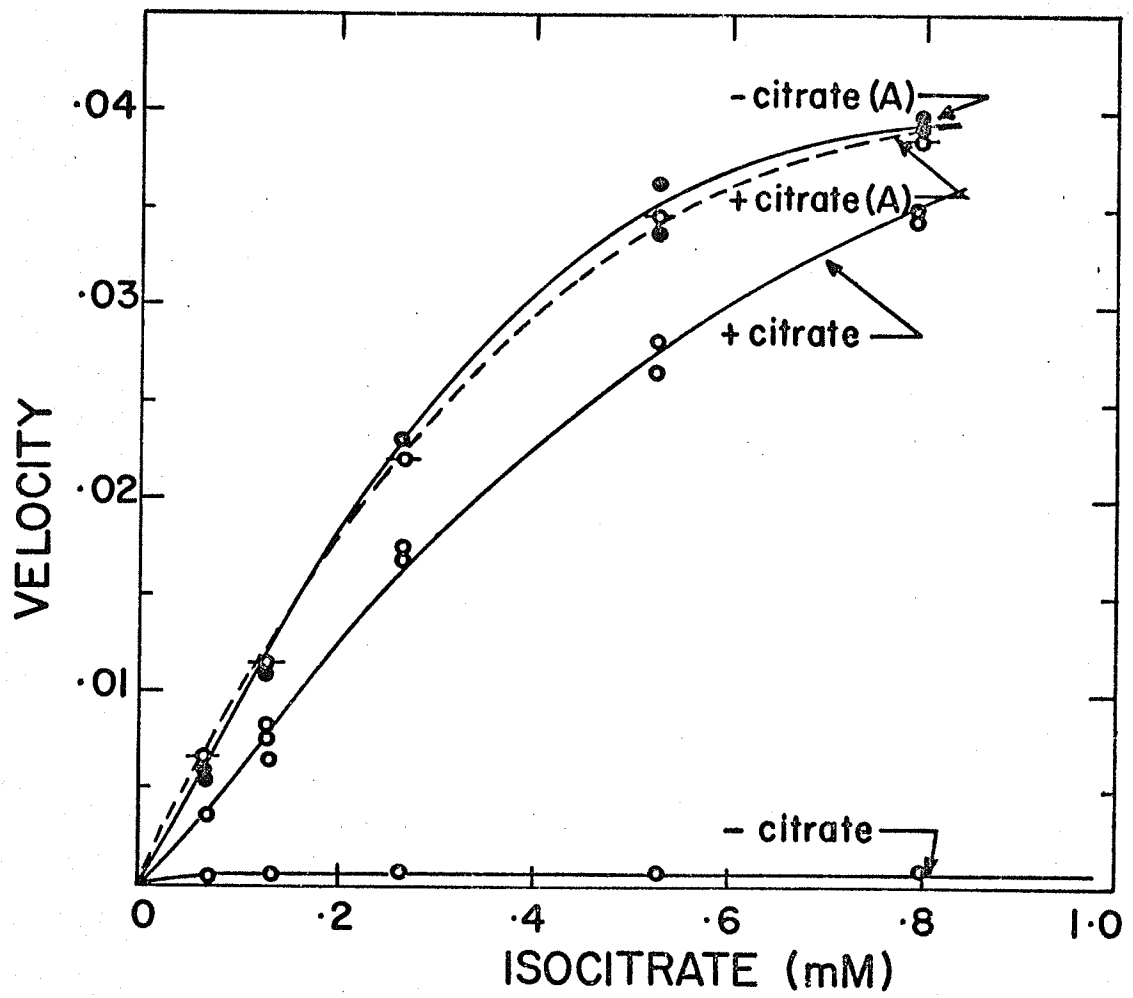
·04
·03
·02
·01
VELOCITY
- citrate (A)
+ citrate (A)
+ citrate
- citrate
0
·2
·4
·6
·8
1·0
ISOCITRATE (mM)

Fig. 35. Double-reciprocal plots of 1/velocity versus 1/NAD at several fixed levels of isocitrate in the absence of AMP.

All cuvets contained 6.6 mM citrate and 0.2 M phosphate buffer, pH 6.5. The uppermost line (0.166 mM isocitrate) has been drawn from fits to equation (35) and the lower two lines from fits to equation (23).

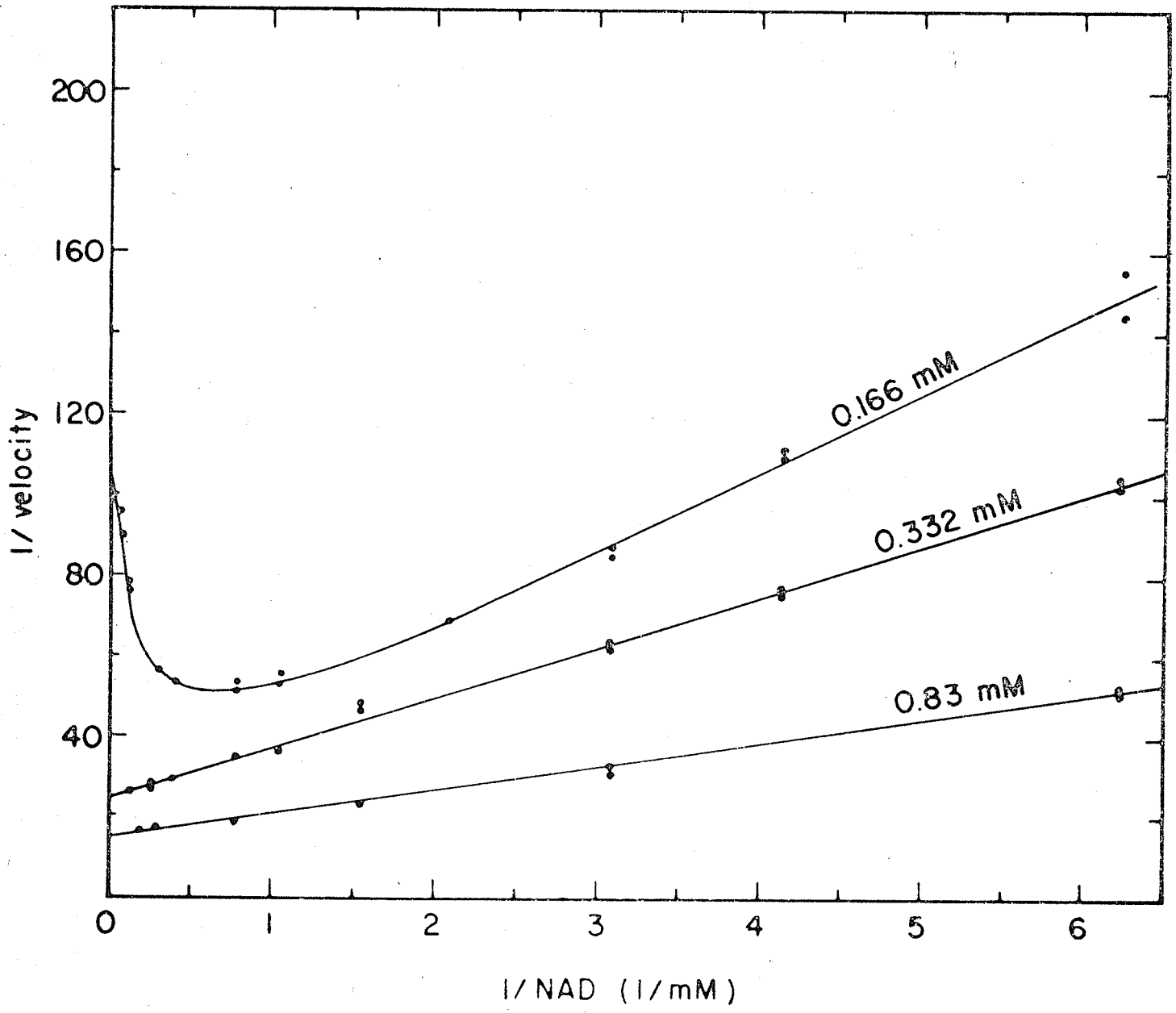
200
160
120
80
40
1/ velocity
0.166 mM
0.332 mM
0.83 mM
0
1
2
3
4
5
6
1/ NAD (1/mM)

concentration gave a significant fit to equation (35), a 2/1 function:

$$v = \frac{V\,(S^2 + cS)}{a + bS + S^2} \qquad \ldots\ (35)$$

When isocitrate was used as the variable substrate and NAD as the fixed changing substrate in the presence of constant high levels of citrate (6.6 mM), similar double reciprocal plots were obtained (Fig. 36). At low levels of NAD (0.16 mM), the results gave a significant fit to equation (35), but insignificant fits to equation (23) or (24). Again, at higher concentrations of NAD, the double reciprocal plots became linear.

Product Inhibition in the Absence of AMP.

Using NADH as a product inhibitor at pH 6.5 under conditions where the enzyme was saturated with isocitrate, and NAD was the variable substrate, the double reciprocal plots showed noncompetitive inhibition (Fig. 37). This result may be contrasted with that obtained in the presence of AMP (Fig. 12). The replot of intercepts appeared hyperbolic, although the fitted constants gave large errors.

Fig. 36. Double-reciprocal plots of 1/velocity versus 1/isocitrate at several fixed levels of NAD in the absence of AMP.

All assay mixtures, pH 6.5, contained 6.6 mM citrate. The uppermost line has been drawn from fits to equation (35) and the lower two lines from fits to equation (23).

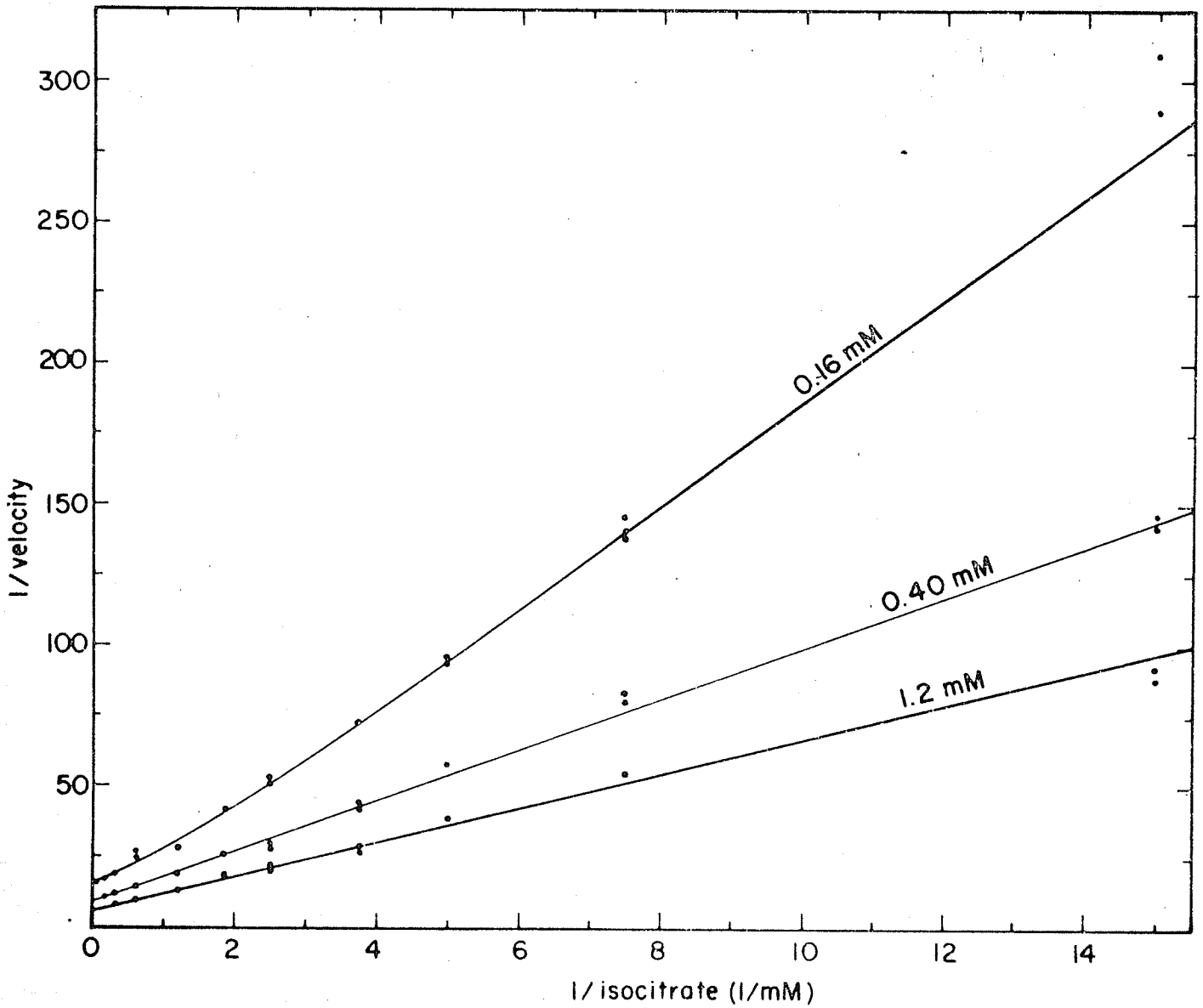
300
250
200
150
100
50
1/ velocity
0.16 mM
0.40 mM
1.2 mM
0
2
4
6
8
10
12
14
1/ isocitrate (1/mM)

Fig. 37. Product inhibition of isocitrate dehydrogenase at pH 6.5 by NADH (in the absence of AMP) with NAD as the variable substrate and a constant high concentration of isocitrate (13.2 mM).

Lines have been drawn from fits to equation (23).

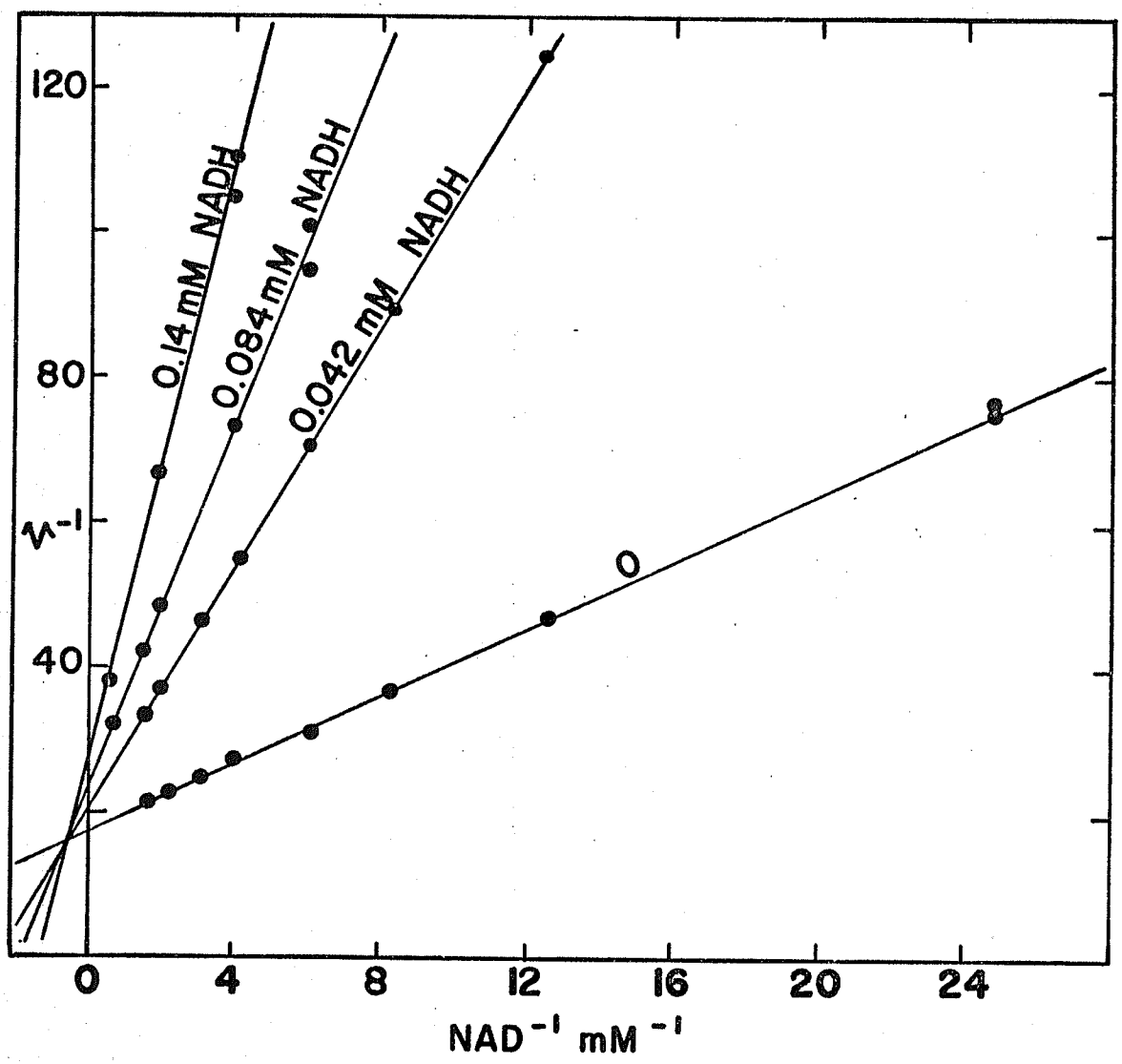
120
80
40
v-1
0.14 mM NADH
0.084 mM NADH
0.042 mM NADH
0
0
4
8
12
16
20
24
NAD-1 mM-1

The nature of the activation of isocitrate dehydrogenase by AMP was then tested. When AMP concentration was varied against several changing concentrations of isocitrate, in the presence of saturating NAD (2 mM), the double reciprocal plots were markedly nonlinear at low isocitrate, but become linear at high isocitrate concentrations (Fig. 38). When these curves were plotted according to equation (22), the value of n at low isocitrate (0.1333 mM) was 2.1, but changed to approximately 1 at higher concentrations. Similar results were obtained at pH 7.6.

Kinetic Constants

The Michaelis constants are defined here as the concentration of substrate giving 1/2 the value of the maximum velocity in initial velocity studies, when the enzyme is saturated with the other reactants. The K_m for the fixed changing substrate was routinely obtained from the intersection point on the horizontal axis of a replot of intercepts against reciprocals of fixed changing substrate. The K_m of the varied substrate was obtained from the ratio of the intersection points on the vertical axis of the 1/V and K/V replot. V_{max} was obtained from the intersection point on the vertical axis

Fig. 38. Double-reciprocal plots of 1/velocity versus 1/AMP at pH 6.5 at several fixed concentrations of isocitrate. The NAD concentration throughout was 2 mM.

The lowermost line has been drawn from fits to equation (23). The dashed lines are fitted by eye.

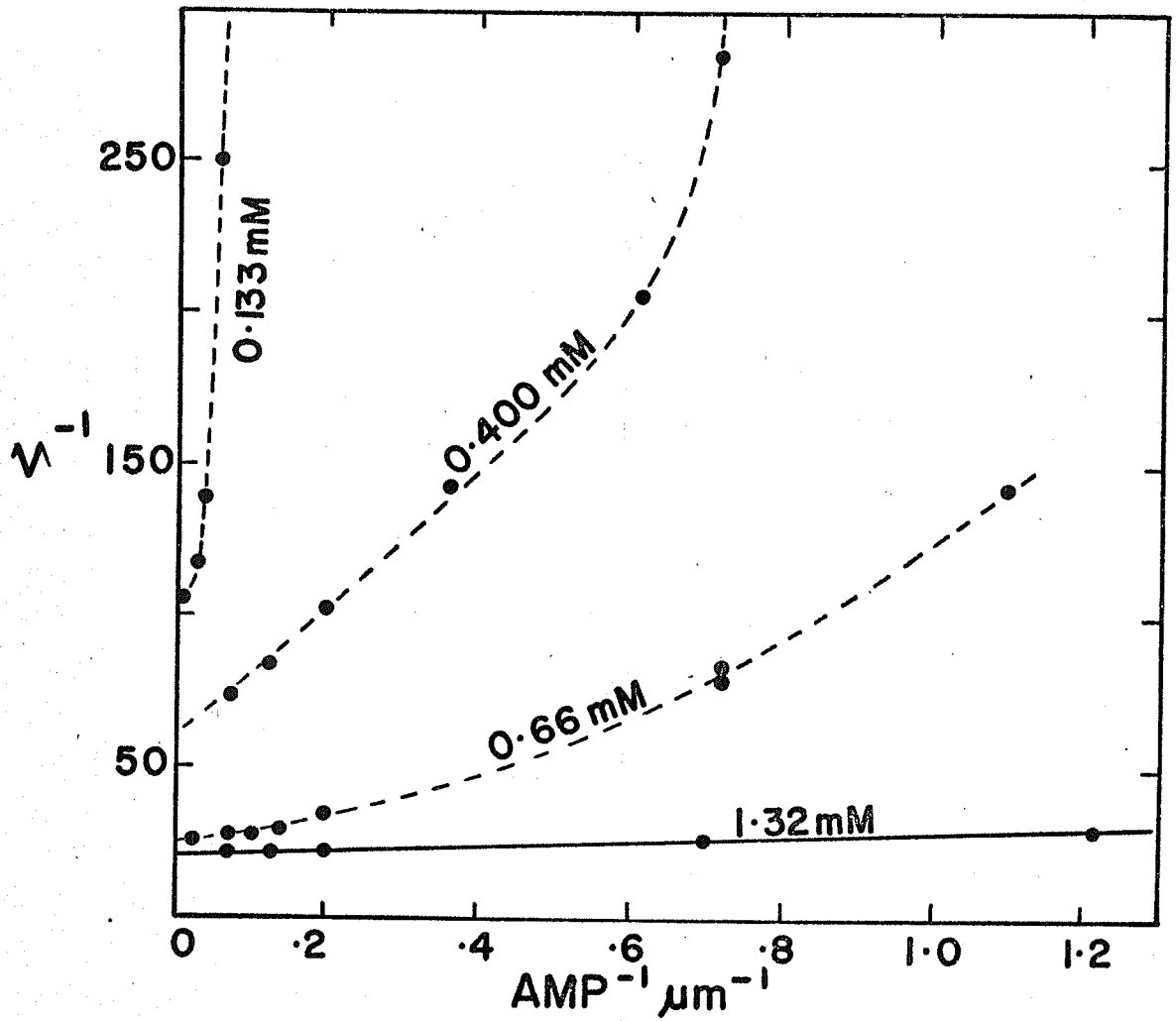
250
150
50
v^{-1}
0·133 mM
0·400 mM
0·66 mM
1·32 mM
0
·2
·4
·6
·8
1·0
1·2
$AMP^{-1}\ \mu m^{-1}$

of the intercept replot. This point represents the maximum velocity at infinite concentration of both reactants.

Inhibition Constants

The inhibition constant for the first substrate (A) to combine with the enzyme, K_{ia} (also the dissociation constant of A) was determined from the common intersection point of the reciprocal plots (above, on, or below the horizontal axis) when A was the variable substrate (Frieden, 1957a). K_{ia} could also be obtained from the slope of the replot of K/V.

Product inhibition constants were determined in the case of competitive inhibition from the intersection point on the horizontal axis of a slope versus inhibitor replot. In the case of noncompetitive inhibition, replot of slopes versus inhibitor gave a horizontal intersection point of:

$$- K_i \ (1 + P/K_{ip})$$

and a replot of 1/V gave

$$- K_i \ (1 + P/K_p)$$

(where P was the concentration of non-varied substrate K_{ip} and K_p were the inhibition and Michaelis constant of P, and K_i was

the inhibition constant of product). In the case of uncompetitive inhibition, the inhibition constant was obtained from the horizontal intercept of a 1/V versus inhibitor plot.

All constants were evaluated from initial velocity data which yielded linear replots. This was the case only in initial velocities at pH 6.5 in the presence of AMP or one saturating substrate and in initial velocity studies at pH 7.6 in the presence of saturating citrate. All constants which could be evaluated from the data presented are given in Table 4.

Table 4. Some kinetic constants of isocitrate dehydrogenase.

Constant	pH 6.5 (mM)	pH 7.6* (mM)
K_{NAD} (K_a)	0.265 ± .068	0.327 ± 0.073
$K_{isocitrate}$ (K_b)	0.16 ± .04	0.154 ± 0.03
K_{ia}	0.712 ± 0.15	0.552 ± 0.159
K_{ip}	370 ± 130	
K_{iq}	80 ± 5	
K_{ir}	0.017 ± 0.003	0.02 ± 0.001

K_{ia}, K_{ip}, K_{iq}, and K_{ir} are the inhibition constants for NAD, CO_2, α-ketoglutarate and NADH respectively. *In the presence of 2.2 mM citrate. The validity of K_{ip} and K_{iq} are in doubt owing to the problems discussed in the text.

INTERPRETATION OF THE KINETIC DATA

The nature of most kinetic deductions is such that they are only suggestive of a mechanism, but are not proof for it. Ideally, before a kinetic model is considered valid, all other likely models should also be examined and excluded as far as possible. For ease of discussion, a steady-state kinetic model for isocitrate dehydrogenase is first presented and inconsistencies with various other models based exclusively on equilibrium conditions (Monod et al., 1965; Atkinson et al., 1965) are pointed out in the discussion. The conclusion is reached that the reaction mechanism is Random in the absence of AMP and it changes to either Rapid Equilibrium Random or Ordered in its presence.

1) Reaction Sequence in the Presence of AMP at pH 6.5.

Initial velocity studies at pH 6.5 (Figs. 10, 11) show that the reaction obeys the equation:

$$v = \frac{VAB}{K_{ia}K_b + K_bA + K_aB + AB}$$

which indicates that both NAD and isocitrate must bind to the enzyme before products are released. This rules out a Ping-Pong

type of mechanism because as has been shown by Cleland (1963a,b), in such a mechanism the $K_{ia}K_b$ term is missing from the denominator of the rate equation. Product inhibition data indicate that the simplest mechanism compatible with it is an ordered addition of substrates and liberation of products (ordered Bi Ter) or a Rapid Equilibrium Random Mechanism:

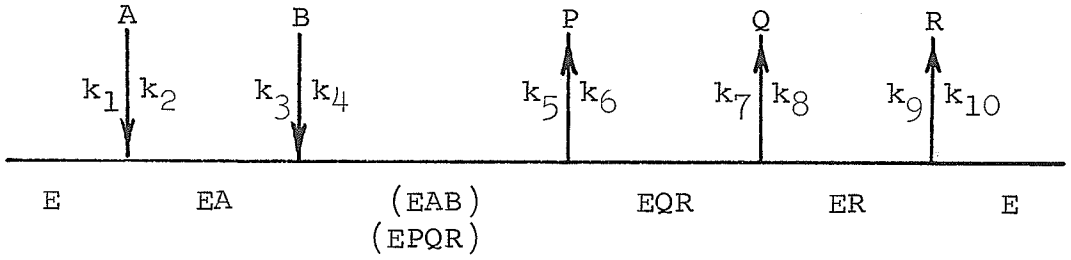

(where A is NAD, B is isocitrate, P is CO_2, Q is α-ketoglutarate and R is NADH).

or,

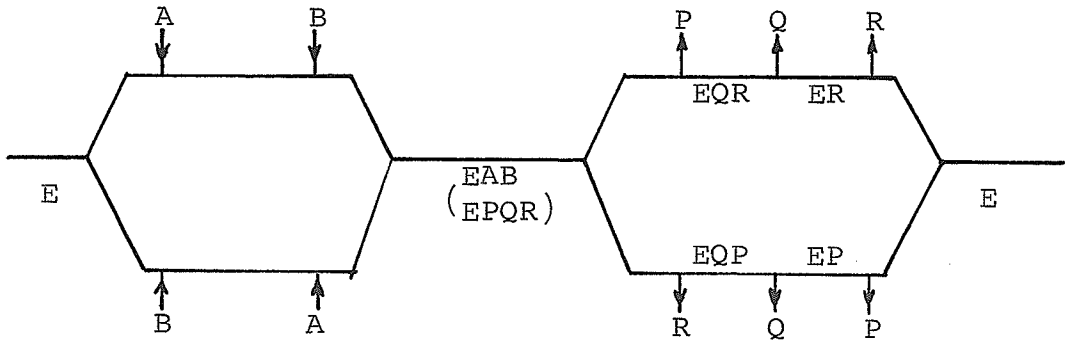

The rate equation, derived by King and Altman's method (1956), for the ordered mechanism is (equation 36):

$$v = \frac{V_1 \left(AB - \frac{PQR}{K_{eq}}\right)}{K_{ia}K_b + K_bA + K_aB + AB + \frac{K_{ia}K_bK_qP}{K_pK_{iq}} + \frac{K_{ia}K_bR}{K_{ir}} + \frac{K_bAP}{K_{ip}}}$$

$$+ \frac{K_{ia}K_bK_rPQ}{K_pK_{iq}K_{ir}} + \frac{K_aBR}{K_{ir}} + \frac{K_{ia}K_bQR}{K_{iq}K_{ir}} + \frac{K_{ia}K_bK_qPR}{K_pK_{iq}K_{ir}} + \frac{ABP}{K_{ip}}$$

$$+ \frac{K_{ia}K_bPQR}{K_pK_{iq}K_{ir}} + \frac{K_rK_bAPQ}{K_pK_{iq}K_{ir}} + \frac{ABQ}{K_{iq}} + \frac{K_{ia}K_bBQR}{K_{ib}K_{iq}K_{ir}} + \frac{ABPQ}{K_{ip}K_{iq}} + \frac{K_{ia}K_bBPQR}{K_p\ K_{ib}K_{iq}K_{ir}}$$

..... (36)

(where K_a, K_b, K_p, K_q and K_r are Michaelis constants of A, B, P, Q, R and K_{ia}, K_{ib}, K_{ip}, K_{iq}, and K_{ir} are inhibition constants).

A Rapid Equilibrium Random mechanism where A and B can both bind the free enzyme, but the rate limiting step is the interconversion of the central complex with some dead-end complexes (of the kind enzyme-NAD-α-ketoglutarate or enzyme-NAD-CO_2, for example) gives an identical rate equation and it is extremely difficult to distinguish between these two mechanisms from kinetic data alone.

The mechanism given by equation (36) predicts that NADH and NAD combine with the free enzyme form resulting in linear

competitive inhibition, which is indeed the case in Fig. 12. Also, using CO_2 as inhibitor and NAD as the varying substrate, linear noncompetitive inhibition should result and the data from Fig. 19 and Fig. 20 support this prediction. With α-ketoglutarate as inhibitor, linear uncompetitive inhibition with NAD as varying substrate (Fig. 16), and linear noncompetitive inhibition with isocitrate (Fig. 17) as varying substrate is predicted by equation (36) and this is the experimental result. The data, therefore, indicates that either an ordered sequential or dead-end Rapid Equilibrium Random mechanism is valid.

The rate equation (36) is useful also not only because it can be used to predict product inhibition patterns but may be used to distinguish the Ordered (or dead-end Rapid Equilibrium Random) mechanism from Theorell-Chance type and a Rapid Equilibrium Random mechanism without dead-end complexes. The presence of ABPQ and BPQR terms in the denominator of equation (36) combined with the fact that mechanisms without central complexes are unlikely (Wratten and Cleland, 1963) rules out a Theorell-Chance type of mechanism. Similarly, the Rapid Equilibrium Random mechanism (without dead-end complexes) lacks APQ, BQR, ABPQ, and BPQR terms in the denominator of equation

(36). Further, a Random mechanism where binding of A and B is rate limiting, also can be ruled out on the basis of product inhibition data which shows that slopes and intercepts of double reciprocal plots are in general linear functions of inhibitor concentrations and when they are not they can be explained easily on the basis that the inhibitors act both as product and as dead-end inhibitors.

In initial velocity studies, when product concentration is zero, the rate equation (36) simplifies to:

$$v = \frac{VAB}{K_{ia}K_b + K_bA + K_aB + AB}$$

and as seen before does fit the data (Fig. 10 and Fig. 11).

When NADH (R) is present, the general rate equation reduces to:

$$\frac{1}{v} = \frac{K_a}{V}\left(1 + \frac{K_{ia}K_b}{K_aB}\right)\left(1 + \frac{R}{K_{ir}}\right)\frac{1}{A} + \frac{1}{V}\left(1 + \frac{K_b}{B}\right)$$

This equation predicts the linear competitive inhibition obtained by NADH when NAD is varied (Fig. 12).

When bicarbonate (P) is present the general rate equation reduces to:

$$\frac{1}{v} = \frac{K_a}{V}\left(1 + \frac{K_{ia}K_b}{B}\right)\left(1 + \frac{K_qP}{K_{iq}P}\right)\frac{1}{A} + \frac{1}{V}\left(1 + \frac{K_b}{B}\right)\left(1 + \frac{P}{K_{ip}}\right)$$

which predicts linear noncompetitive inhibition by bicarbonate when NAD is varied (Figs. 19, 20). Similarly, noncompetitive inhibition is predicted and obtained by bicarbonate when isocitrate is varied (Figs. 21, 22). It is therefore clear that, at least at pH 6.5 in the presence of AMP, the reaction mechanism is either ordered or follows a dead-end Rapid Equilibrium Random mechanism.

In the replots of slopes and intercepts versus inhibitor concentrations (Figs. 15, 18, 22) intercepts were always linear. However, the possibility exists in all three cases that the slope replot is parabolic, owing to the rather large errors obtained when the data was fitted to a straight line. This is borne out by the inconsistency of the calculation of K_{iq} (α-ketoglutarate inhibition constant) from Figures 16 and 17. The K_{iq} value from Fig. 16 was 80 mM but from Fig. 17 this value comes out to be 139 mM. This suggests that α-ketoglutarate may combine with the enzyme-NAD complex in a dead-end manner as well as combining as a product inhibitor. Similar deviations occur in the calculation from Fig. 22, suggesting that the case may be actually S-parabolic I-linear noncompetitive inhibition.

Isocitrate dehydrogenase had been previously shown (Sanwal et al., 1963, 1964) to exhibit allosteric effects at its pH optimum of 7.6, similar to other allosteric enzymes (Gerhart and Pardee, 1964; Changeux, 1963). At pH 7.6 NAD gives linear double reciprocal plots (Fig. 24), but the plots with isocitrate are markedly curved (Fig. 23) and show no relationship to the initial velocity rate equation described previously. When these curves are fitted to a parabola, significant fits are obtained, but the coefficient b is negative, which is impossible for a parabola. According to the theory of multi-reactant enzyme kinetics developed by Cleland (1963a,b,c,d) parabolic curves would be obtained for an ordered mechanism without alternate pathways if the varied substrate participated twice in the reaction sequence and if the points of addition of varied substrate were connected by reversible steps. However, the data represented in Fig. 14 are still consistent with the idea that isocitrate binds at the allosteric site and at the active site. A three point attachment (assuming two allosteric sites) is inconsistent with the data because of the insignificant fits obtained to equation (25).

The linear double reciprocal plots obtained when NAD is

varied against several fixed concentrations of isocitrate suggest that NAD perhaps binds only once during the reaction sequence. When reduced NAD was used as a product inhibitor, competitive inhibition was obtained, as at pH 6.5. Replots of slopes against NADH were also linear giving a K_{ir} value of 0.02 mM, which is similar to that obtained at pH 6.5. It is very likely that as at pH 6.5, NAD and NADH both bind to the free enzyme form at pH 7.6.

The formulation of a kinetic model for allosteric effects is made easier if certain parameters of this effect can be clearly defined in quantitative terms. Specifically, it is useful to know (in order to distinguish between partial and total allosterism) whether the various kinetic constants change at all in the presence of an allosteric effector. On the assumption that this is a total allosteric mechanism (no activity unless a substrate or modifier is bound at the allosteric site), the results from Fig. 27 were fitted to equation (34). The reciprocal plots of $1/v - v^{o}$ versus 1/isocitrate were linear as predicted but the replot of K_{app} against isocitrate was shown to be curved (Fig. 25). It is clear that the simple relationship expected from equation (34) was not obtained. The dissociation constant of isocitrate from

the allosteric site cannot be determined owing to the curvature of the K_{app} replot. Combination at the active site appears to influence combination at the allosteric site. However, since the double reciprocal plots are linear (Fig. 27), this does indicate a combination of only one molecule of citrate at the allosteric site. If more than one combined, the reciprocal plots would be parabolas or curves of even more complex nature.

When initial velocity studies were performed in the presence of saturating citrate, the double reciprocal plots of NAD versus several fixed isocitrate concentrations yielded straight lines (Fig. 27). However, the replots of slopes and intercepts were linear (Fig. 28) indicating that the allosteric site was saturated (by citrate) and only one molecule of isocitrate combines with the enzyme. Product inhibition by NADH with NAD varied was competitive (Fig. 29) indicating that the kinetic mechanism had not been altered.

It is clear from the data that NAD binds at only one site on the enzyme surface both in the presence and the absence of allosteric effects. Binding at places other than the active site would be recognizable kinetically by a curvature of reciprocal plots when NAD was the varied substrate (Figures 10,

17, 24) or the curvature of the replots of slopes or intercepts against the reciprocal of NAD when isocitrate was the varied substrate. Cleland (1963a) has already shown that reciprocal plots for substrates, activators or inhibitors, which bind at places other than the active site, or those resulting from some Random mechanisms, are 2/1 functions, such as

$$\frac{1}{v} = \frac{a + b\left(\frac{1}{s}\right) + c\left(\frac{1}{s}\right)^2}{d + e\left(\frac{1}{s}\right)}$$

(where a, b, c, d and e are functions of other reactant concentrations), or more complex curves. The same argument applies to the binding of isocitrate in the absence of allosteric effects at pH 6.5. It is nearly certain that isocitrate binds only at the active site when the allosteric site is inactive (pH 6.5) or is saturated by modifier (pH 7.6). Similarly, citrate binds only at one place when the allosteric site is operative at pH 7.6. The binding of citrate must be only at the allosteric site because citrate shows no effect on the velocity of the reaction at pH 6.5 (Sanwal et al., 1963).

The curved double reciprocal plots obtained with isocitrate as varied substrate at pH 7.6 (Fig. 23) suggest that

isocitrate binds at two different sites and that there is a reversible connection between the points of binding of the substrate in the reaction pathway. The question now arises whether the binding of the two molecules of isocitrate, one presumably at the allosteric site and another at the active site, is a prerequisite for the release of products (Total Allosterism, Mechanism 37),

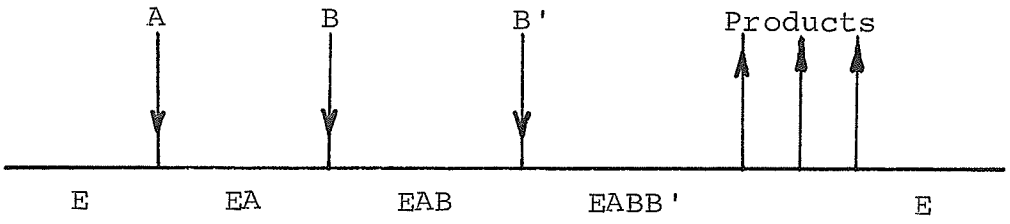

..... (37)

(where B' represents binding of B at the allosteric site and B represents binding at the active site), or, there is activity with isocitrate bound only at the active site, but more activity with another molecule of isocitrate bound also at the allosteric site (Partial Allosterism, Mechanism 38)

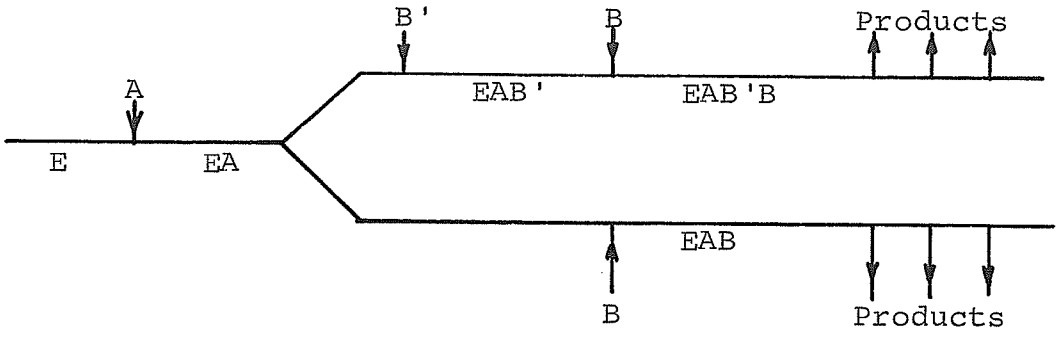

Assuming that the conversion of EA to the EAB' form is slow compared with other catalytic steps in reaction mechanisms 37 and 38, rate equations for these mechanisms can be derived. The form of the rate equation for mechanism 37 is obtained by multiplying the proper initial velocity equation by the factor $(B/K_1 + B)$ where K_1 is the allosteric constant for isocitrate, and equals $(EA)(B')/(EAB')$.

In terms of K_m and V_{max}, this is

$$v = V \left(\frac{B}{K_B + B}\right)\left(\frac{B}{K_1 + B}\right)$$

or, in the standard reciprocal form:

$$\frac{1}{v} = \frac{K_b K_1}{V}\left(\frac{1}{B}\right)^2 + \left(\frac{K_1 + K_b}{V}\right)\left(\frac{1}{B}\right) + \frac{1}{V} \qquad \ldots\ldots\ldots (39)$$

which is an equation for a parabola.

For mechanism 38, the rate equation is the sum of activities of EA and EAB' forms.

$$v = V_1 \left(\frac{B}{K_{b1} + B}\right)\left(\frac{K_1}{K_1 + B}\right) + \frac{V_2 B^2}{(K_{b2} + B)(K_1 + B)}$$

(where V_1 and K_{b1} are maximum velocity and Michaelis constants

for the EA form, and V_2 and K_{b2} are constants for the EAB' form) or, in standard reciprocal form (40)

$$\frac{1}{v} = \frac{1 + (K_1 + K_{b1} + K_{b2})(\frac{1}{B}) + (K_1K_{b1} + K_1K_{b2} + K_{b1}K_{b2})(\frac{1}{B})^2 + K_1K_{b1}K_{b2}(\frac{1}{B})^3}{V_2 + (V_1K_1 + V_2K_{b1})(\frac{1}{B}) + V_1K_1K_{b2}(\frac{1}{B})^2} \quad \ldots\ldots (40)$$

Equation (40) is a 3/2 function, the curves of which, unlike a parabola, have an asymptote, and the curve tends to be concave up if $V_2 > V_1$ and $K_{b1} > K_{b2}$. Both equations (39) and (40) reduce to the classical Michaelis-Menten equation when the allosteric site is unoperational (at pH 6.5) or is saturated with modifier (at pH 7.6). The curves obtained in Fig. 23 show no relationship to equation (40) indicating that mechanism 38 is not operating. These curves also did not fit the parabola indicating that the curves must be at least 3/1 or more complex functions. The data from Figures 23 and 25 suggest a rate equation of the type:

$$v = \frac{AB^2 + AB^3 + ABM + AB^2M}{\text{constant} + A + AM + AB + B + M + ABM + AB^2 + B^2 + BM + AB^2M + AB^3 + B^3 + B^2M} \quad \ldots\ldots (41)$$

(where A and B have the usual meaning, and M is the modifier). This equation is derived from the assumption that

1) the enzyme exhibits total allosterism

2) the allosteric combinations do not affect adsorption or release of A

3) the mechanism of the reaction is:

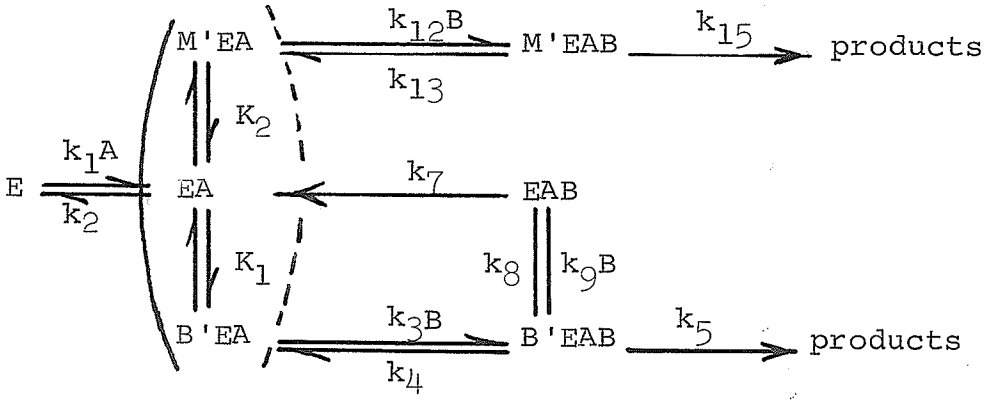

..... (42)

(where E is free enzyme, B is isocitrate, M is citrate, B' and M' denote binding at the allosteric site, $K_1 = (EA)(B')/(EAB')$ and $K_2 = (EA)(M')/(M'EA)$.

The distribution equations for the steady state are:

$$\frac{d\,(EA + M'EA + B'EA)}{dt} = k_1A\,(E) - k_2\,(EA + M'EA + B'EA)$$

$$+ k_7\,(EAB) + k_4\,(B'EAB) + k_{13}\,(M'EAB) - k_{12}B\,(M'EA)$$

$$- k_3B\,(B'EA) = 0$$

$$\frac{d\,(EAB)}{dt} = k_8\,(B'EAB) - (k_7 + k_9B)(EAB) = 0$$

$$\frac{d\,(B'EAB)}{dt} = k_3B\,(B'EA) + k_9B\,(EAB) - (k_4 + k_5 + k_8)(B'EAB) = 0$$

$$\frac{d\,(M'EAB)}{dt} = k_{12}B\,(M'EA) - (k_{13} + k_{15})(M'EAB) = 0$$

$$E_t = E + (EA + B'EA + M'EA) + EAB + B'EAB + M'EAB$$

This mechanism is consistent with the data of Fig. 23 and Fig. 25 in that the reciprocal plots (at pH 7.6) when isocitrate is varied are expected to be 3/1 functions while plots of NAD as the varied substrate are linear. Similarly, when citrate is varied at several levels of isocitrate (pH 7.6) the plots of $1/v - v^o$ versus 1/citrate (Fig. 26) are expected

to be linear and the replot (Fig. 25) of K_{app} is expected to be a 3/2 function of isocitrate. It may be mentioned in passing that although all the equations for initial velocity data at pH 7.6 are derived assuming an ordered mechanism, similar equations would result if the mechanism were dead-end Rapid Equilibrium.

2) Reaction Mechanism in the Absence of AMP

It is seen from Fig. 30 that the double reciprocal plots at pH 6.5 for NAD, linear in the presence of AMP, become non-linear in its absence. Saturation by isocitrate makes these plots linear, suggesting that the reaction may be random. If there were one binding site each for NAD and isocitrate and the mechanism was random, i.e., both NAD and isocitrate were able to bind to the free enzyme form and that these addition steps became partially rate limiting, the following mechanism would be proposed:

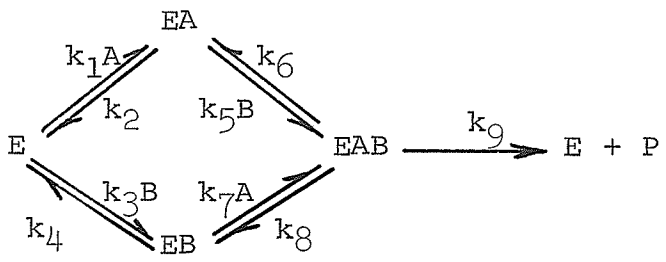

..... (43)

By a steady state derivation of the initial velocity equation, using the method of King and Altman (1956), the following rate equation is obtained:

$$v = \frac{k_q E_t \left[k_5 k_7 (k_1 A + k_3 B)\, AB + (k_1 k_4 k_5 + k_2 k_3 k_7)\, AB \right]}{\text{constant} + aA^2B + bAB^2 + cA^2 + dB^2 + eAB + fA + gB} \quad \ldots\ldots\ldots (44)$$

(where a, b, ...g are combination of constants). When one substrate is held constant and the other is varied this equation in the reciprocal form is a 2/1 function.

Since there are square terms in A and B in the numerator, the double reciprocal plots are expected to be non-linear. When isocitrate (B) is saturating, equation (44) reduces to:

$$v = \frac{k_q E_t A}{(k_8 + k_9)/k_7 + A}$$

and when NAD (A) is saturating, equation (44) reduces to:

$$v = \frac{k_9 E_t B}{(k_6 + k_9)/k_5 + B}$$

Both of these equations conform to the Michaelis-Menten formulation and will plot as straight lines in double reciprocal form.

However, when curves given in Fig. 30 are fitted to a 2/1 function, insignificant fits are obtained. It is apparent from log-log plots (Fig. 31) that the n value is approximately 3. It can be readily shown that the value of n obtained from equation (22) gives a minimum for the power to which substrate concentration occurs in the rate equation derived by steady-state methods. It is at once clear that the rate equation for the curves of Fig. 30 must have A^3 terms in the numerator. This is possible if one assumes that in the absence of AMP at pH 6.5 the allosteric binding site for isocitrate becomes operative (possibly due to a conformational change), and NAD can bind before and after binding of isocitrate, as given in Mechanism 45.

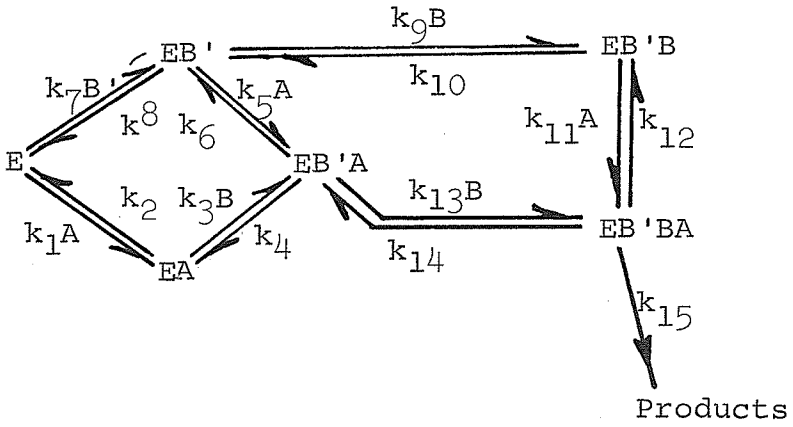

..... (45)

(where B' is binding of B at the allosteric site). The initial velocity equation for this mechanism is

$$v = \frac{aAB^2 + bAB^3 + cAB^4 + dA^2B^2 + eA^2B^3}{\text{constant} + fB + gA + hAB + iB^2 + jB^3 + kB^4 + lAB^2 + mAB^3 + nAB^4 + oA^2 + pA^2B + qA^2B^2 + rA^2B^3} \quad \ldots\ldots\ldots (46)$$

The curves given by this mechanism are impossible to fit, but regardless of how random the mechanism, the plots for isocitrate will always be curved when NAD is saturating. This is shown in Fig. 32. The curve obtained at 5 mM NAD (25 x K_m) shows very significant fits to equation (24), but the value of the constant b is negative, which means that the curve is most likely a 3/1 or greater function defined by an equation of the type:

$$v = \frac{B^2 + B^3}{\text{constant} + B + B^2 + B^3} \quad \ldots\ldots\ldots (47)$$

This is the type of equation we had previously obtained on the basis of the experiments done at pH 7.6 in the presence of AMP (Equation 41).

The rate equation (41) reduces to this form in the absence of modifier (M) and the mechanism of the reaction reduces to:

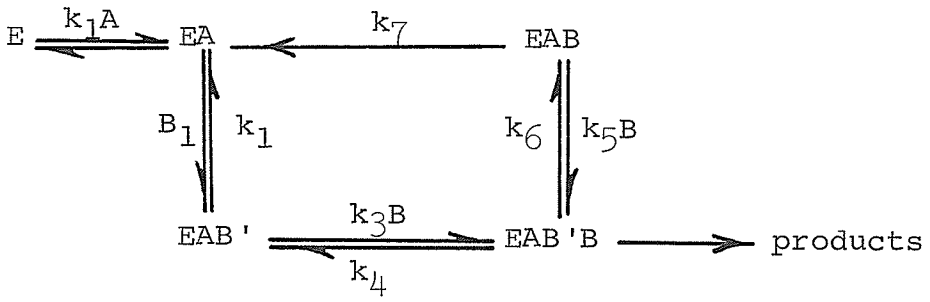

..... (48)

If this mechanism holds at pH 6.5 in the absence of AMP, one would expect the curves to be 3/1 or more complex functions in the presence of nearly saturating concentrations of NAD.

The finding that citrate activated the reaction in the absence of AMP (Fig. 34) is very important because it constitutes evidence that isocitrate combines at a regulatory site instead of causing site interactions on a tetramer. If the allosteric site is saturated with citrate, so that most of the enzyme is present in the form of enzyme-citrate complex, and the concentration of either substrate is varied at fixed concentrations of the other, the data should conform to equation (35) provided that the reaction is Random and the

concentration of the non-varied substrate is not saturating. This is indeed the case (Figures 35, 36) at low concentrations of non-varied substrate. At higher concentrations the lines become straight (Figures 35, 36) in accordance with either Mechanism 43 or 45. These observations are again consistent with a Random Mechanism.

Inhibition by NADH in the absence of AMP at pH 6.5 is noncompetitive (Fig. 37) further supporting the Random mechanism. The activation of the reaction by AMP also appeared to be Random (Fig. 38) as the double reciprocal plots are initially non-linear but become linear at saturation by the changing fixed substrate, analogous to Fig. 30.

In conclusion, the striking fact emerges that the reaction mechanism is apparently either dead-end Rapid Equilibrium Random or Ordered in the presence of AMP but is Random in the absence of AMP. It is therefore quite probable that the conformational state in which enzyme exists in the absence of AMP is different than in its presence. That the rate of binding of a ligand to a single protein in each of its two conformational states can be quite different has already been demonstrated by Antonini et al., (1963) for hemoglobin. Ullman et al. (1964) have given convincing evidence that AMP

causes conformational changes by binding to phosphorylase b. It is thus quite conceivable that the NAD site and the allosteric site for isocitrate are both exposed in the conformational state that the enzyme assumes in the absence of AMP and the binding of these substrates is independent of each other and diffusion limited. In the AMP activated conformational state two possibilities are explicit depending upon the choice of a mechanism. If an ordered reaction is assumed it is quite likely that in the presence of AMP only the NAD site is exposed and the rate of binding of the coenzyme is rapid. Binding of NAD is perhaps necessary to "unfold" the allosteric isocitrate site (thereby ordering the sequence of addition of substrates) by a further conformational change in a manner implicit in the "induced fit" hypothesis of Koshland (1963). If a dead-end Rapid Equilibrium mechanism is assumed, it is possible that the binding of both substrates to the enzyme become non-rate limiting in the presence of AMP.

A recent investigation of the NAD-specific isocitrate dehydrogenase from Baker's yeast (Sanwal and Miller, 1966, unpublished) has indicated that the mechanisms proposed in this work are completely applicable to that system. The recent work

of Cennamo *et al.* (1967) pertaining to the NAD-specific isocitrate dehydrogenase of Baker's yeast also suggests the possibility of a Random mechanism for the addition of reactants, in support of our kinetic interpretations.

RESULTS (CONT'D)

Binding Studies

The kinetic analysis of the isocitrate dehydrogenase reaction can only be taken as an indication of the type of mechanism involved. In order to determine the true mechanism of the reaction, binding studies were attempted utilizing the techniques of equilibrium dialysis, spectrofluorometric analysis and gel filtration previously described. For such an analysis, stoichiometric amounts of highly purified enzyme were required. Owing to the low yields of isocitrate dehydrogenase from Neurospora crassa cells (10 mg enzyme from approximately 6 kg wet weight of cells) however, it became extremely difficult to do extensive binding studies and none could be attempted with ligands like NAD (K_m approximately .25 mM) which would have necessitated the use of high concentrations of the enzyme. In what follows, however, reproducibility of the results has been ascertained by using enzyme preparations made at different times.

Molecular Weight Determinations

Schachman (1959) demonstrated that the sedimentation

constants of two kinds of macromolecules were related to their respective molecular weights according to the following equation:

$$\frac{S_1}{S_2} = \left(\frac{MW_1}{MW_2}\right)^{2/3} \qquad \ldots\ldots (49)$$

(where S is the sedimentation constant and MW is the molecular weight).

Martin and Ames (1961) demonstrated that molecular weights of protein mixtures could be determined by a measurement of sedimentation velocity after centrifugation in a sucrose gradient. The distance (D) a protein travelled from the meniscus was a direct measure of its sedimentation velocity and S_1/S_2 equalled D_1/D_2. Substituting in equation (49),

$$\frac{D_1}{D_2} = \left(\frac{MW_1}{MW_2}\right)^{2/3} \qquad \ldots\ldots\ldots (50)$$

(where D is the distance of travel from the meniscus).

Thus it is possible to determine the molecular weight by means of a reference run with another protein of known molecular weight in sucrose density gradients. Utilizing the

method of Martin and Ames (1961), molecular weight determinations of isocitrate dehydrogenase were carried out as previously described with malic dehydrogenase (MW 40,000) and alcohol dehydrogenase (MW 150,000) as reference proteins. Isocitrate dehydrogenase was thus estimated to have a molecular weight of 105,000-110,000 (Fig. 39).

The molecular weight was found unaltered using protein concentrations from 0.05 mg to 2.5 mg indicating that the enzyme did not aggregate in the concentration range used for subsequent binding studies. Further experiments indicated that the molecular weight was unaltered in the presence of saturating concentrations of the substrates and effectors of the enzyme (tested individually).

The sedimentation constant was determined by means of the analytical ultracentrifuge as previously described in Methods. Isocitrate dehydrogenase exhibited an $S_{20,w}$ value of 5.8 which was identical to that obtained by the density gradient method. A contaminant peak representing 10-20% of the total protein exhibited an $S_{20,w}$ value of 20.2. Despite persistent efforts to remove the contaminating peak by various means such as rechromatography on columns, various physical treatments or gel elution chromatography on Sephadex columns,

Fig. 39. Molecular weight determination of isocitrate dehydrogenase using malic dehydrogenase (MW 40,000) and alcohol dehydrogenase (MW 150,000) as reference proteins.

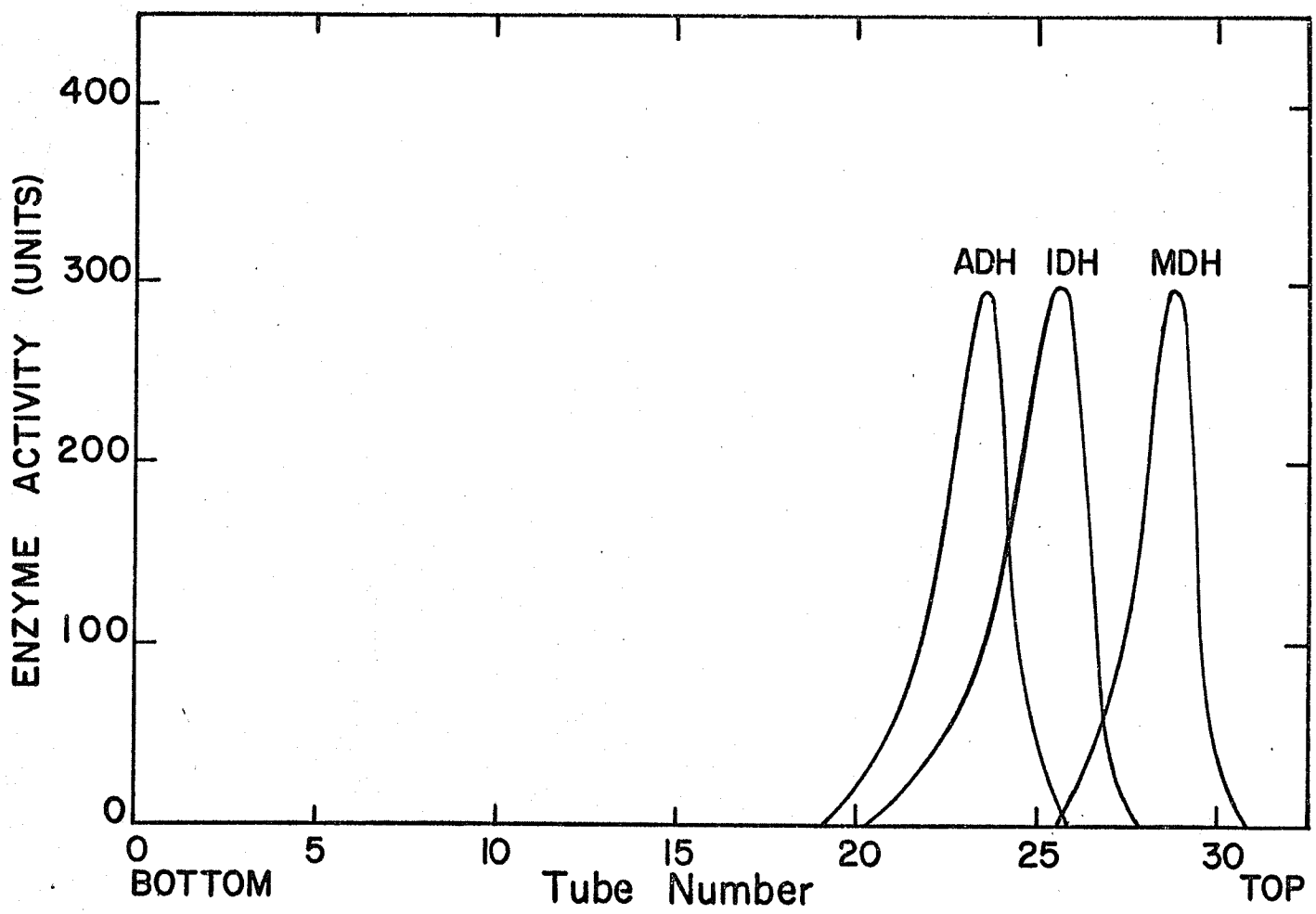
ENZYME ACTIVITY (UNITS)
400
300
200
100
0
ADH
IDH
MDH
0
5
10
15
20
25
30
BOTTOM
Tube Number
TOP

no success was obtained. All treatments led to an irreversible denaturation of the enzyme. In all binding experiments, therefore, the actual concentration of enzyme was calculated after accounting for the presence of the contaminant.

Binding Studies with NADH

The binding of NADH to isocitrate dehydrogenase was measured by the spectrofluorometric technique described in Methods. Two-four mg of isocitrate dehydrogenase were routinely used for each fluorometric titration. The enzyme was titrated with 0.005 ml increments of NADH under the conditions described previously. Preliminary experiments revealed that the E-NADH complex exhibited a different fluorescent peak from enzyme (E) or NADH alone (Fig. 40). A typical titration curve of isocitrate dehydrogenase with NADH is presented in Fig. 41. The results were analyzed according to the equation of Stockell (1959):

$$\frac{S}{P} = \frac{K_S}{E_o - p} + n \qquad \ldots\ldots\ldots (32)$$

Fig. 40. Fluorescent emission spectrums of isocitrate dehydrogenase (E), isocitrate dehydrogenase-NADH complex (E-NADH) and free NADH, at an excitation wavelength of 340 mμ.

All experiments were performed in phosphate buffer, 0.05 M, pH 6.5, at 23-25° C.

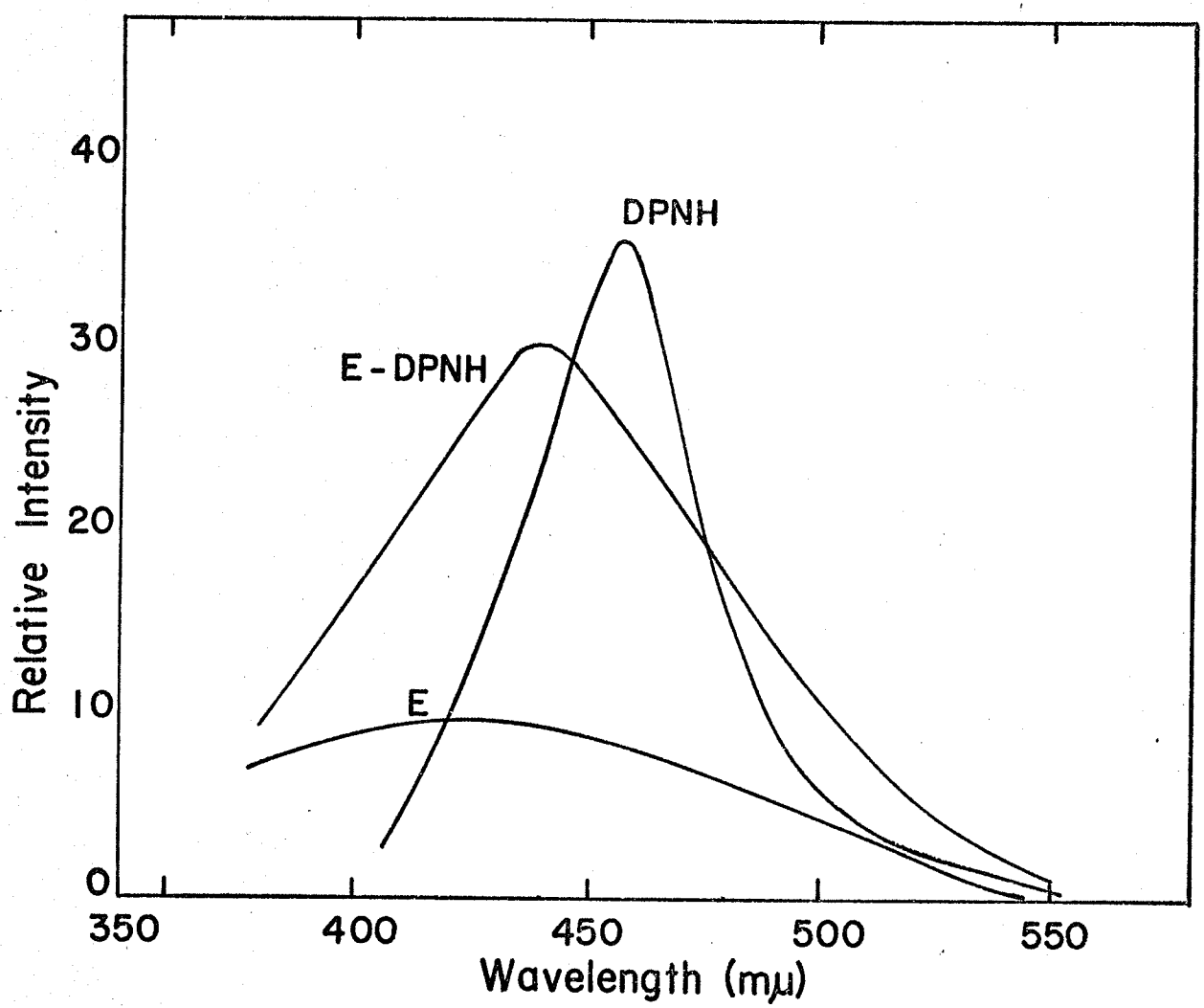
40
30
20
10
0
Relative Intensity
DPNH
E - DPNH
E
350
400
450
500
550
Wavelength (mμ)

Fig. 41. Fluorescent emission spectrums of isocitrate dehydrogenase at various stages of titration with NADH.

0, 2, 6, 10, 20 represent the number of 0.005 ml increments of NADH added. Intermediate spectrums have been omitted for clarity. All experiments were performed in phosphate buffer, 0.05 M, pH 6.5, at 23-25° C. Excitation wavelength was 340 mμ. Dotted line indicates shift in wavelength during conversion of E to E-NADH complex.

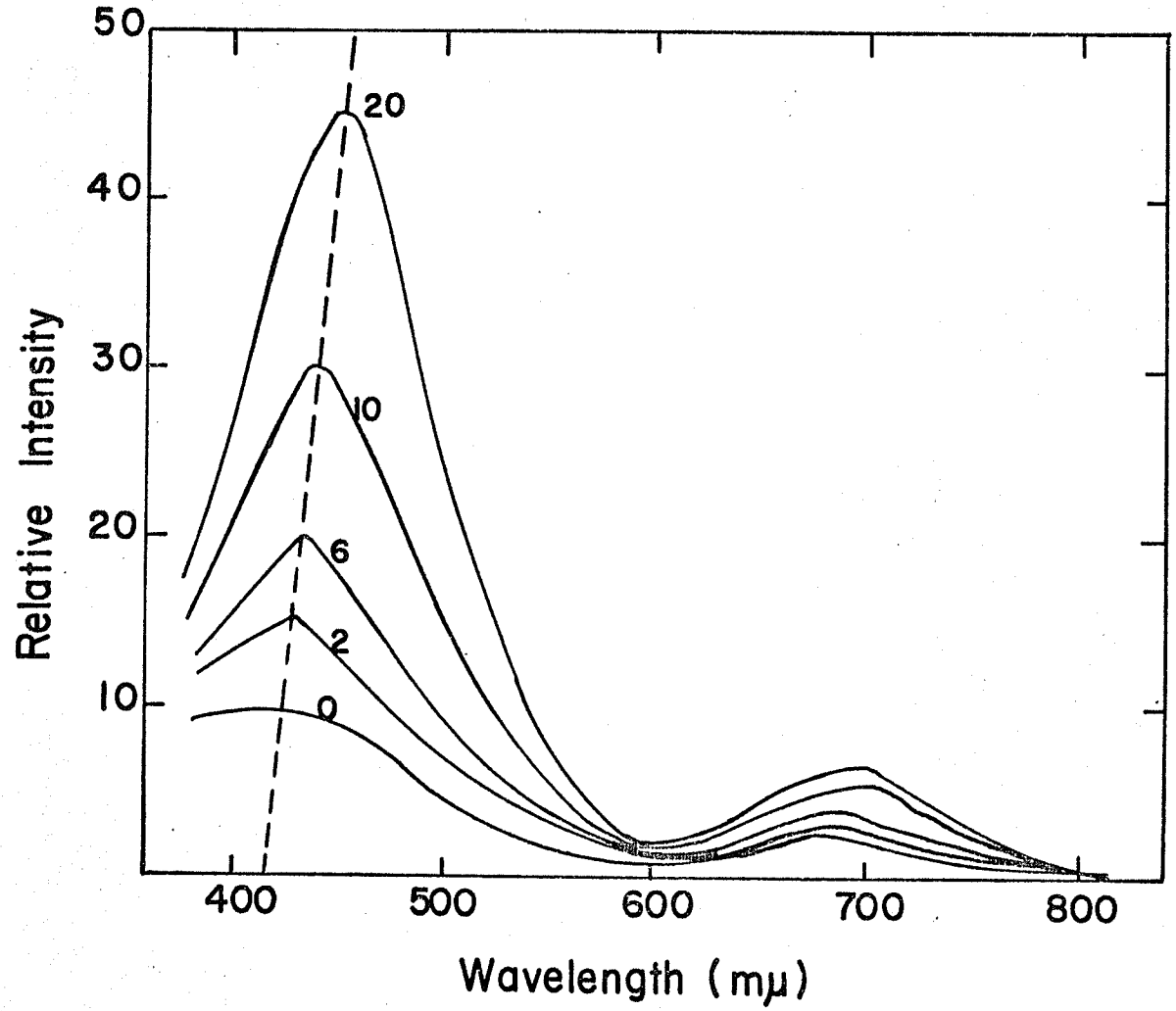
50
40
30
20
10
Relative Intensity
20
10
6
2
0
400
500
600
700
800
Wavelength (mμ)

which was discussed in detail previously. Plotting S/p as a function of $1/E^{\circ} - p$ (Fig. 42) indicated an n value of approximately 1.4. The standard error of this value is high ($\pm$ 0.2) due to experimental difficulty in the determination of the value p. However, four separate sets of titrations of the enzyme made at different times gave results identical to those presented in Fig. 42. In view of the fact that the NADH shares the adenine moiety with AMP, a possibility existed that non-specific binding of NADH at the AMP site could occur in addition to binding at its own site. Titration of isocitrate dehydrogenase with NADH in the presence of saturating concentrations of AMP (1 mM), however, did not alter the shape of the plots or the extrapolated n value.

The binding of NADH, typified by Fig. 42, indicated two, independent, equivalent binding sites (see, Fig. 4).

The number of binding sites was also determined by the method of gel filtration described previously. The number of moles of substrate bound was determined from the amount of NADH absent in the "trough" compared to an equal volume of the base line eluate (Fig. 43). This difference represents the amount of NADH bound to the enzyme. The n value ranged

Fig. 42. Data of Fig. 41 drawn in the form of the Stockell plot (equation 32).

The line has been fitted by the method of least squares. The extrapolated value of n was approximately 1.4. The shape of the plot may be compared with Fig. 4.

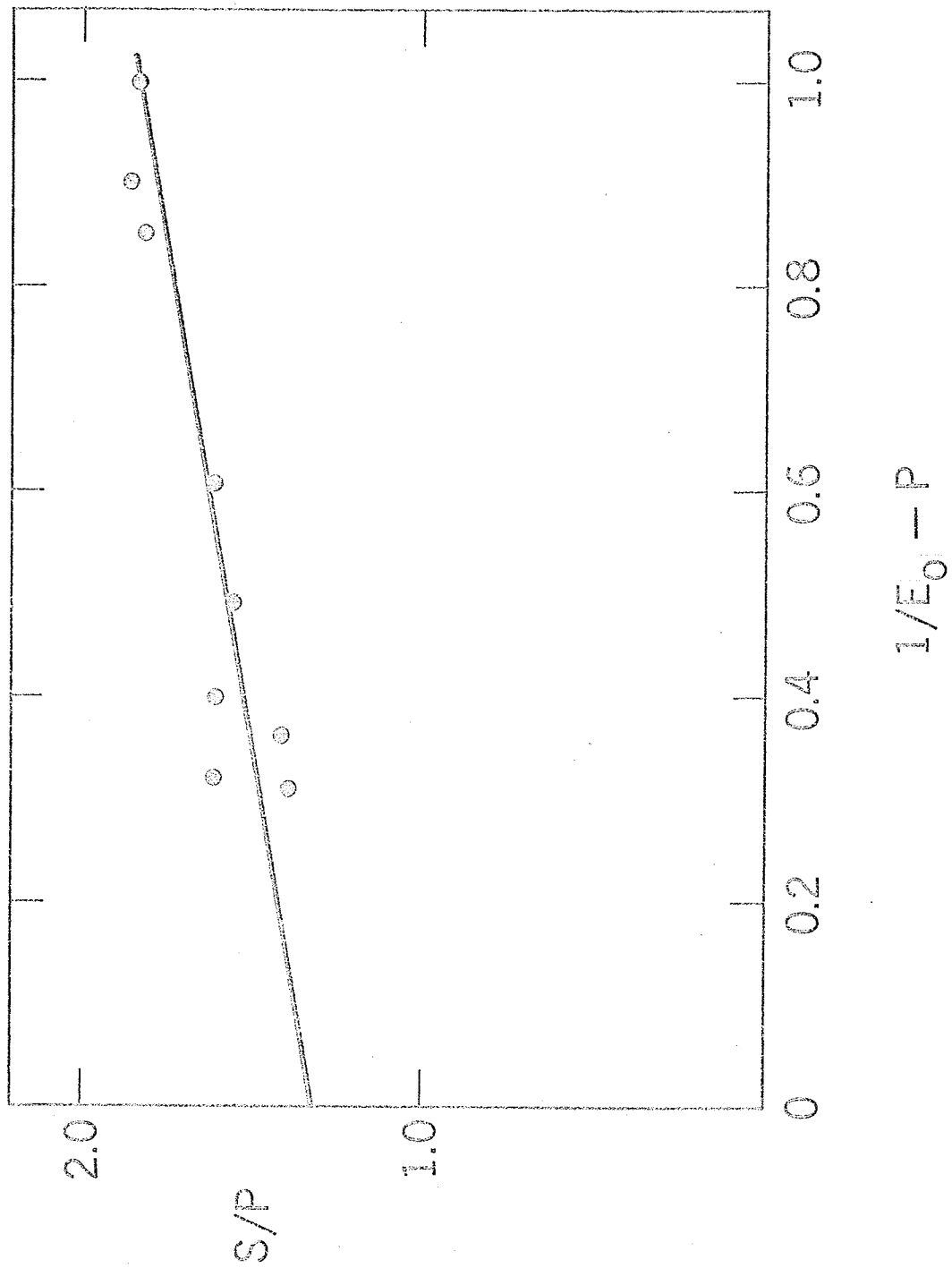
2.0
1.0
S/p
0
0.2
0.4
0.6
0.8
1.0
1/E₀ — P

from 2.0-2.3 in several experiments attempted at different enzyme concentrations.

Binding of AMP to Isocitrate Dehydrogenase

The binding of H^3-AMP to isocitrate dehydrogenase was measured by equilibrium dialysis as previously described in Methods. In different experiments 2-4 mg of enzyme was used for each dialysis cell and AMP was varied from 0.1 K_m to 10 K_m in the substrate compartments. A typical binding curve for AMP is presented in Fig. 44. It will be seen that the curve deviates considerably from a rectangular hyperbola. This is more clearly seen (Fig. 45, 46) when the binding data are plotted according to either the Klotz equation (30) or in the form of a Scatchard plot (equation 31).

The data of Figures 45 and 46 indicate either 'negative cooperativity' between identical binding sites for AMP (i.e., binding of one molecule of AMP hinders binding of a second molecule of AMP, or the presence of non-

Fig. 43. Elution profile of the 340 mμ absorbancy accompanying the passage of isocitrate dehydrogenase through a column of Sephadex G-25 gel which was equilibrated with NADH, as described in the text.

All experiments were performed in phosphate buffer, 0.05 M, pH 6.5, at 23-25° C.

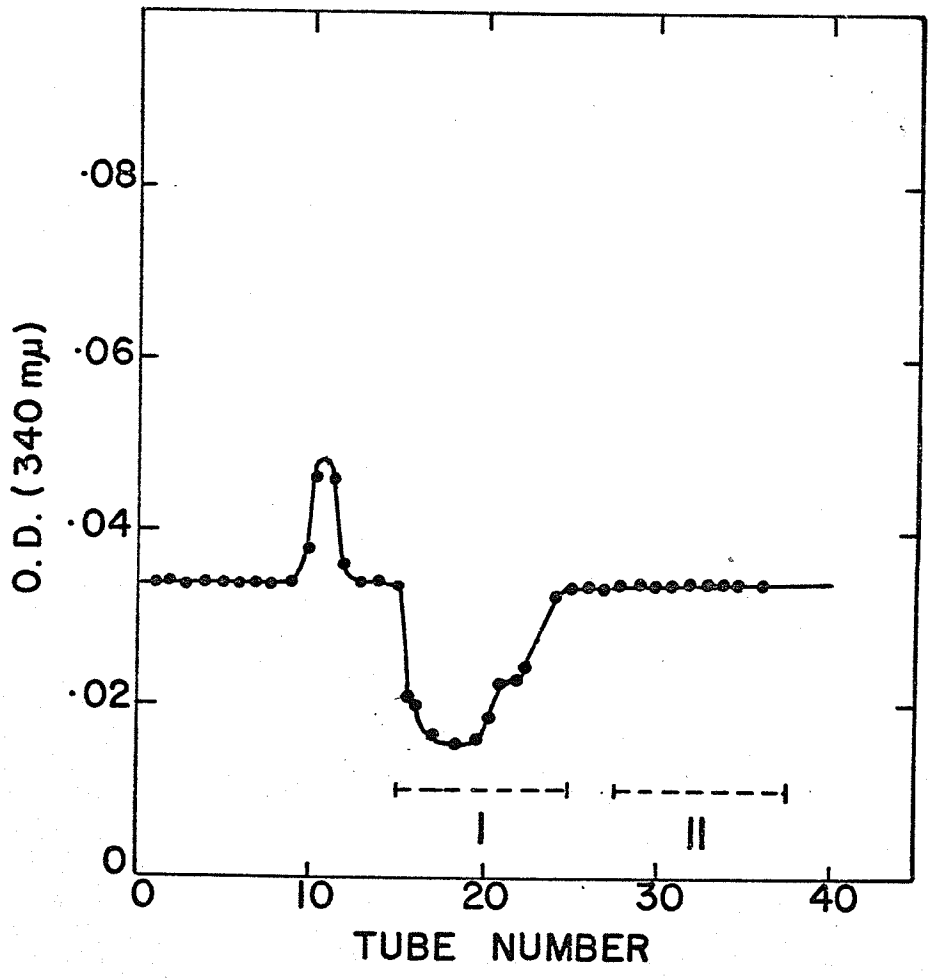
·08
·06
·04
·02
0
O.D. (340 mμ)
0
10
20
30
40
TUBE NUMBER
I
II

Fig. 44. Plot of the binding of AMP to isocitrate dehydrogenase at several concentrations of AMP. All points were determined by equilibrium dialysis for 12 hours as described in the text.

All experiments were performed in phosphate buffer, 0.05 M, pH 6.5, at 4° C.

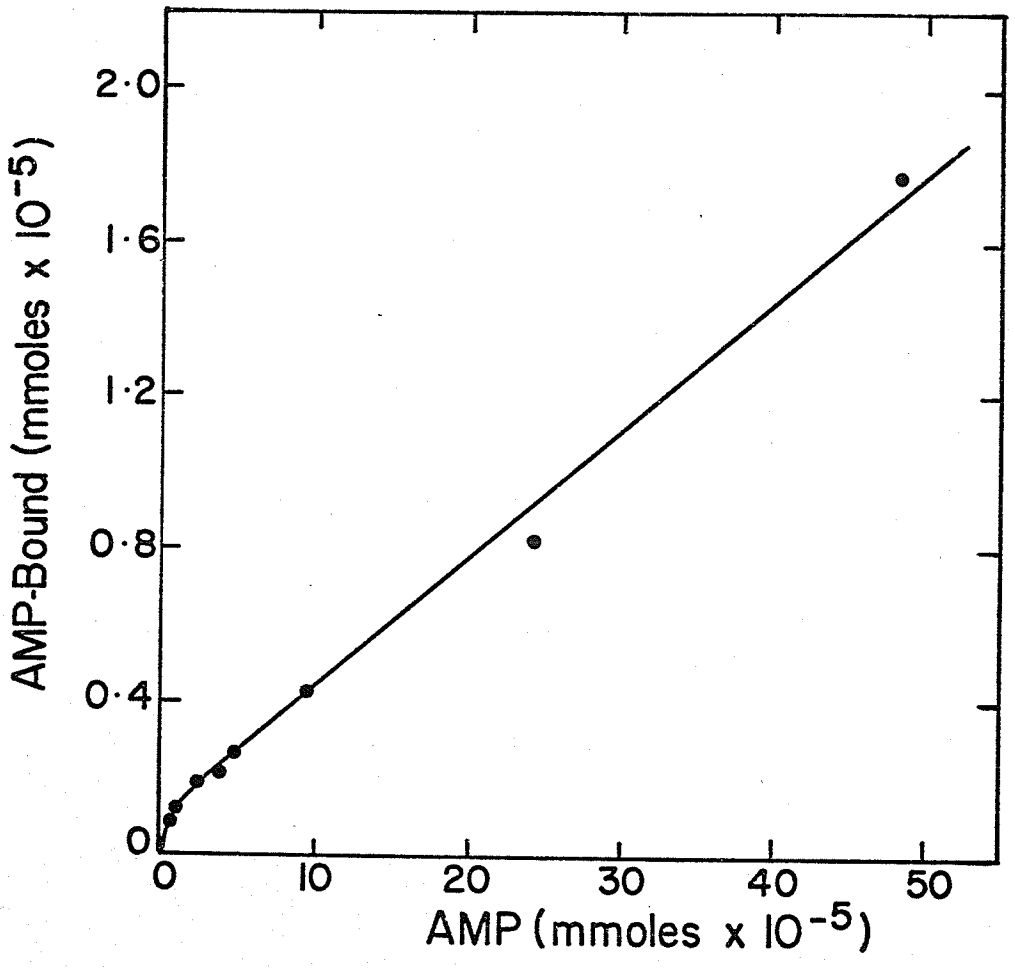
AMP-Bound (mmoles x 10^{-5})
2·0
1·6
1·2
0·8
0·4
0
0
10
20
30
40
50
AMP (mmoles x 10^{-5})

Fig. 45. Data from Fig. 44 drawn in the form of the Scatchard plot (equation 31). The solid and open dots represent two individual experiments with different enzyme preparations.

The lines have been fitted by eye. Shape of the plot may be compared with Fig. 3.

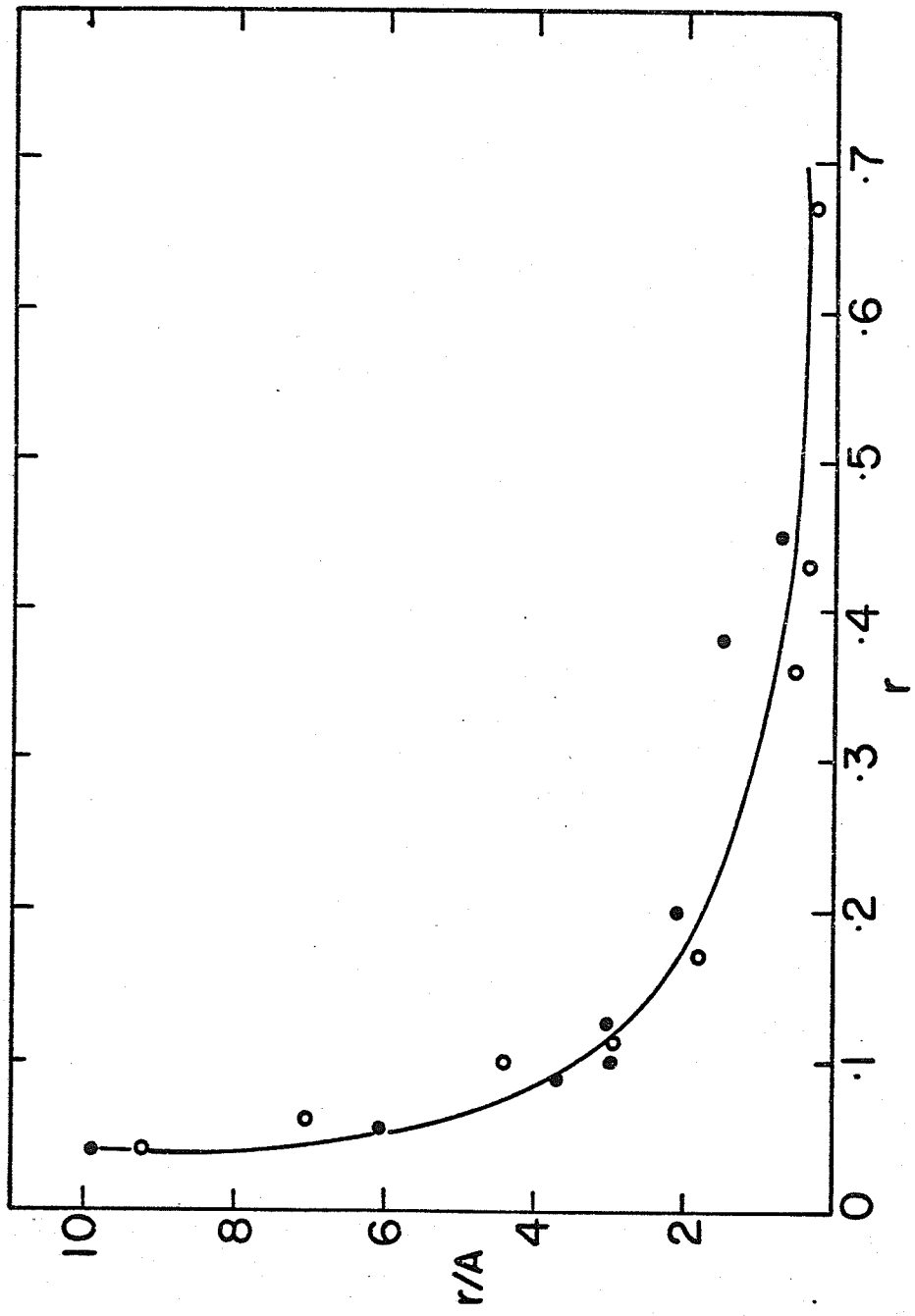
r/A
r
0
2
4
6
8
10
.1
.2
.3
.4
.5
.6
.7

Fig. 46. Data from Fig. 44 drawn in the form of equation (30). The value of n, determined by extrapolation, was approximately 2.

The line has been fitted by eye.

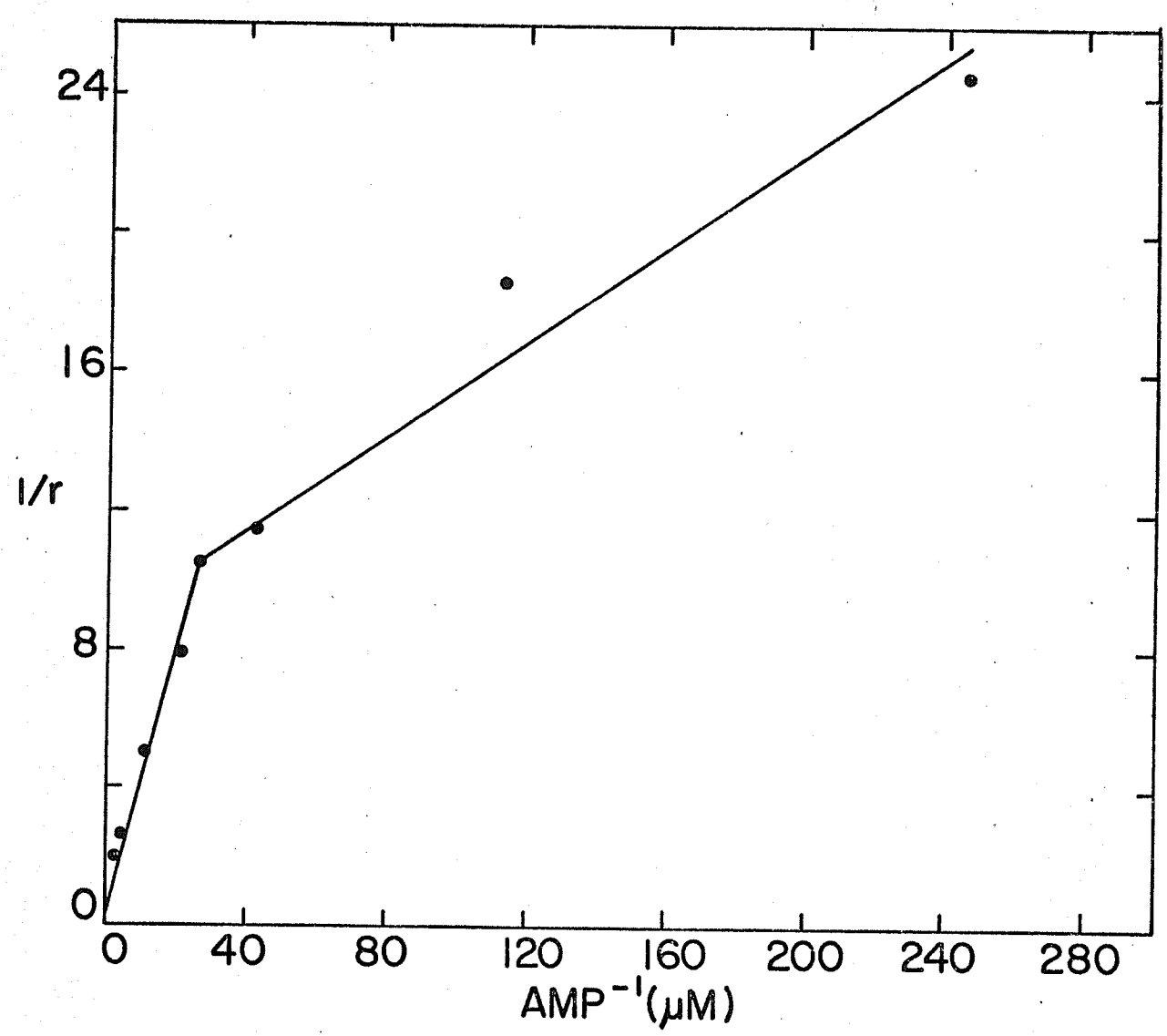
24
16
8
0
1/r
0
40
80
120
160
200
240
280
AMP⁻¹(μM)

identical binding sites for this ligand on the enzyme surface. The reciprocal plot (Fig. 46) allows the determination of an n value of approximately 2 by extrapolation to infinite AMP concentration.

It is difficult to decide from the data whether the binding sites for AMP are identical in the absence of interactions or entirely non-identical. If the presumed interactions are considered to be electrostatic in nature an approximate correction can be made according to Debye-Huckel theory assuming the enzyme to be globular with an uniform distribution of charges on the surface (Scatchard et al., 1950). The Scatchard equation can be modified for electrostatic interaction:

$$\frac{re^{2wr}}{(A)} = k(n - r) \qquad \ldots\ldots (51)$$

(where, e^{2wr} is the interaction parameter). The parameter w can be calculated from the equation:

$$w = \frac{\epsilon^2}{DRkT}\left(1 - \frac{KR}{1 + Ka}\right) \qquad \ldots\ldots\ldots (52)$$

(where ϵ = protonic charge; D = dielectric constant; R = radius in cms of the enzyme molecule (evaluated from a molecular weight of 105,000, partial specific volume = 0.73 by substitution in $4\ R^3/3 = Mv/N$); k = Boltzmann constant; T = absolute temperature; K = reciprocal distance of the ionic atmosphere (3.286×10^7 ionic strength); a = distance of the closest approach of anionic group of AMP + R).

In Fig. 47 the binding data for AMP (from Fig. 45) are replotted after correcting for electrostatic interactions. The non-linear curve suggests that the binding sites are perhaps non-identical, but it does not rule out the possibility that other kinds of interactions (e.g., hydrophobic) may occur between the sites. Indeed, when attempts were made to fit the curve presented in Fig. 45 by the successive approximation method of Scatchard et al., (1957), reasonable fits could not be made on the basis of the presence of two sites with different intrinsic dissociation constants. It seems likely, therefore, that some kind of negative interactions do exist between the two non-identical AMP binding sites.

It may be recalled that in the kinetic studies presented earlier, there was no suggestion of the presence of two non-identical AMP sites. Since the binding studies were done at

Fig. 47. Data from Fig. 45 corrected for electrostatic interaction. $\underline{W}$ was determined, with certain assumptions, as described in the text.

The lines have been fitted by eye.

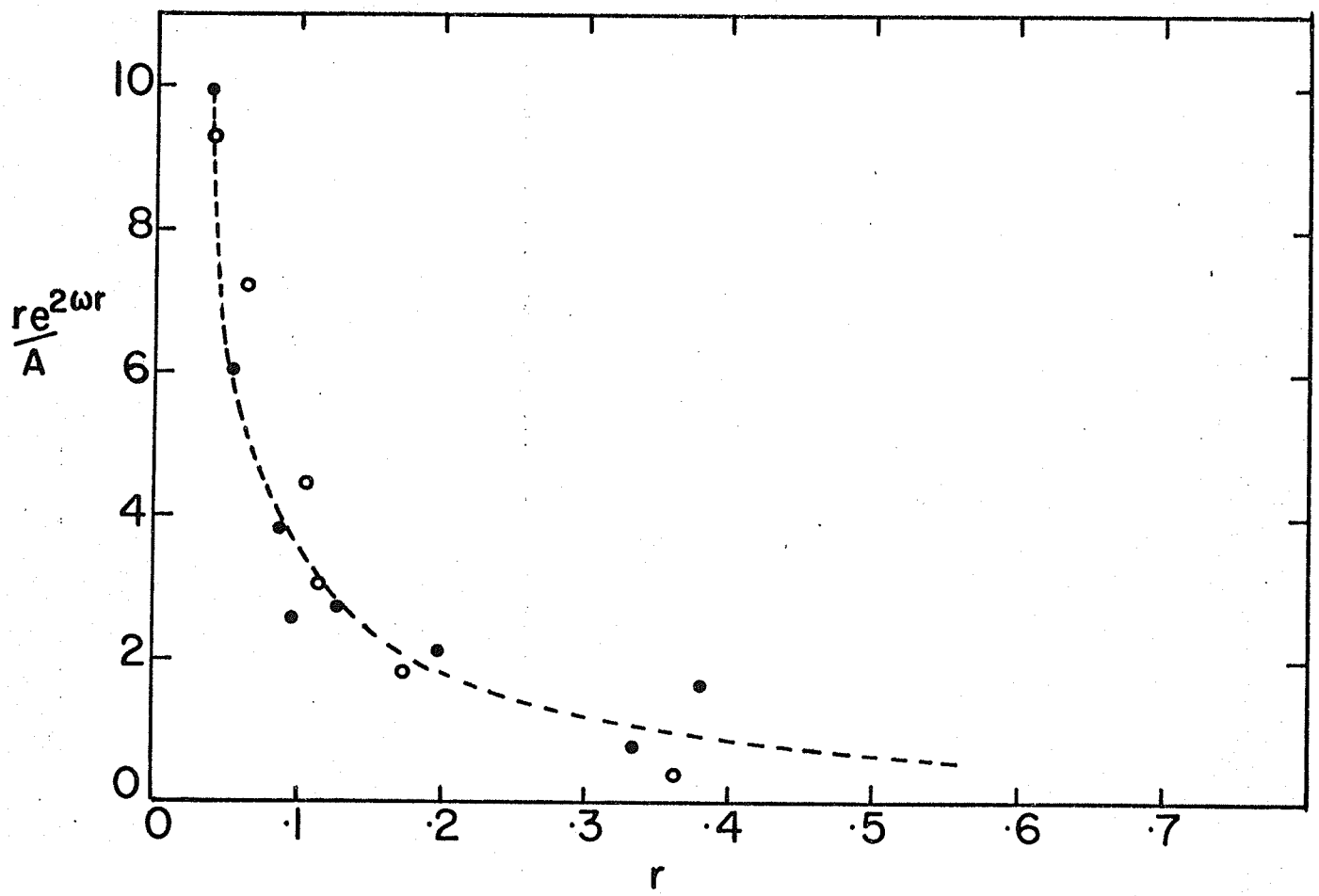
10
8
6
4
2
0
$\frac{re^{2\omega r}}{A}$
0
·1
·2
·3
·4
·5
·6
·7
r

4° C whereas the kinetic analysis was carried out at 25° C, a possible reason for the discrepancy could be the effect of temperature on the thermodynamic or kinetic constants. To rule out this possibility, kinetic analysis using AMP as the variable activator and isocitrate as the changing fixed substrate (at saturating concentrations of NAD) was carried out at 4° C. The results were found to be identical with the results obtained at 25° C, presented in Fig. 38.

Binding of Citrate to Isocitrate Dehydrogenase

The binding of citrate-5,6-C^{14} was examined by equilibrium dialysis as previously described. Two-four mg of enzyme was used in the protein compartment with citrate concentrations varying from 0.1 K_m to 10 K_m in the substrate compartments of the cells. A typical sigmoidal binding curve for citrate is presented in Fig. 48. The data when replotted according to equation (31), indicate a positive cooperative binding (Fig. 49) between citrate molecules, i.e., the binding of one molecule of citrate seems to facilitate the binding of the second molecule. Extrapolation of the line to r/A = 0 yielded an n value of approximately 1.9 indicating a minimum of 2 binding sites for citrate.

Fig. 48. Plot of the binding of citrate to isocitrate dehydrogenase at several fixed concentrations of citrate. All data was obtained by equilibrium dialysis for 12 hours as described in the text.

All experiments were performed in phosphate buffer, 0.05 M, pH 6.5, at 4° C.

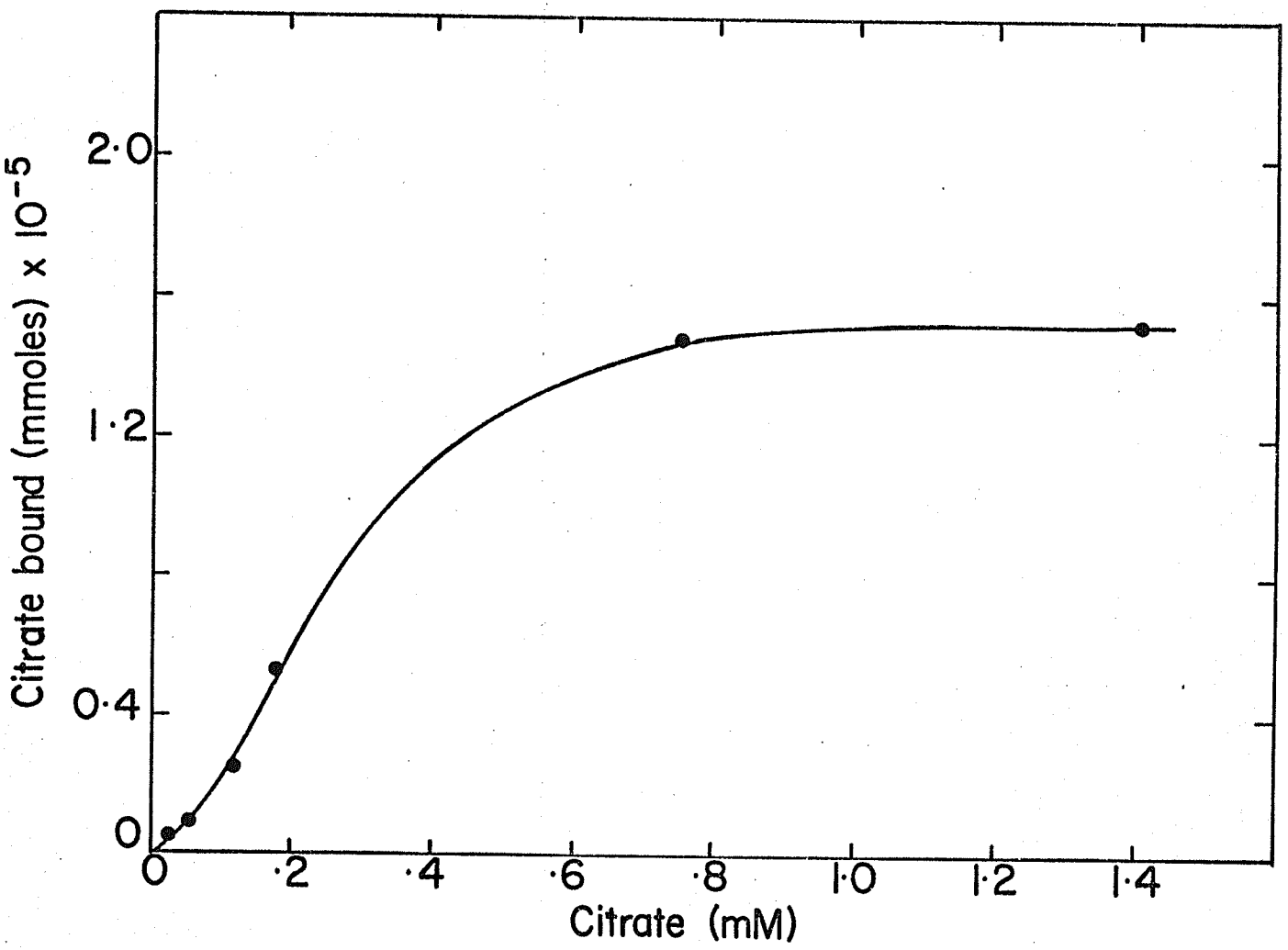
Citrate bound (mmoles) x 10^{-5}
2·0
1·2
0·4
0
0
·2
·4
·6
·8
1·0
1·2
1·4
Citrate (mM)

Fig. 49. Data of Fig. 48 drawn in the form of the Scatchard plot (equation 31). The lines have been fitted by eye and n has been determined by extrapolation to be approximately 1.9. The shape of the plot may be compared with Fig. 3.

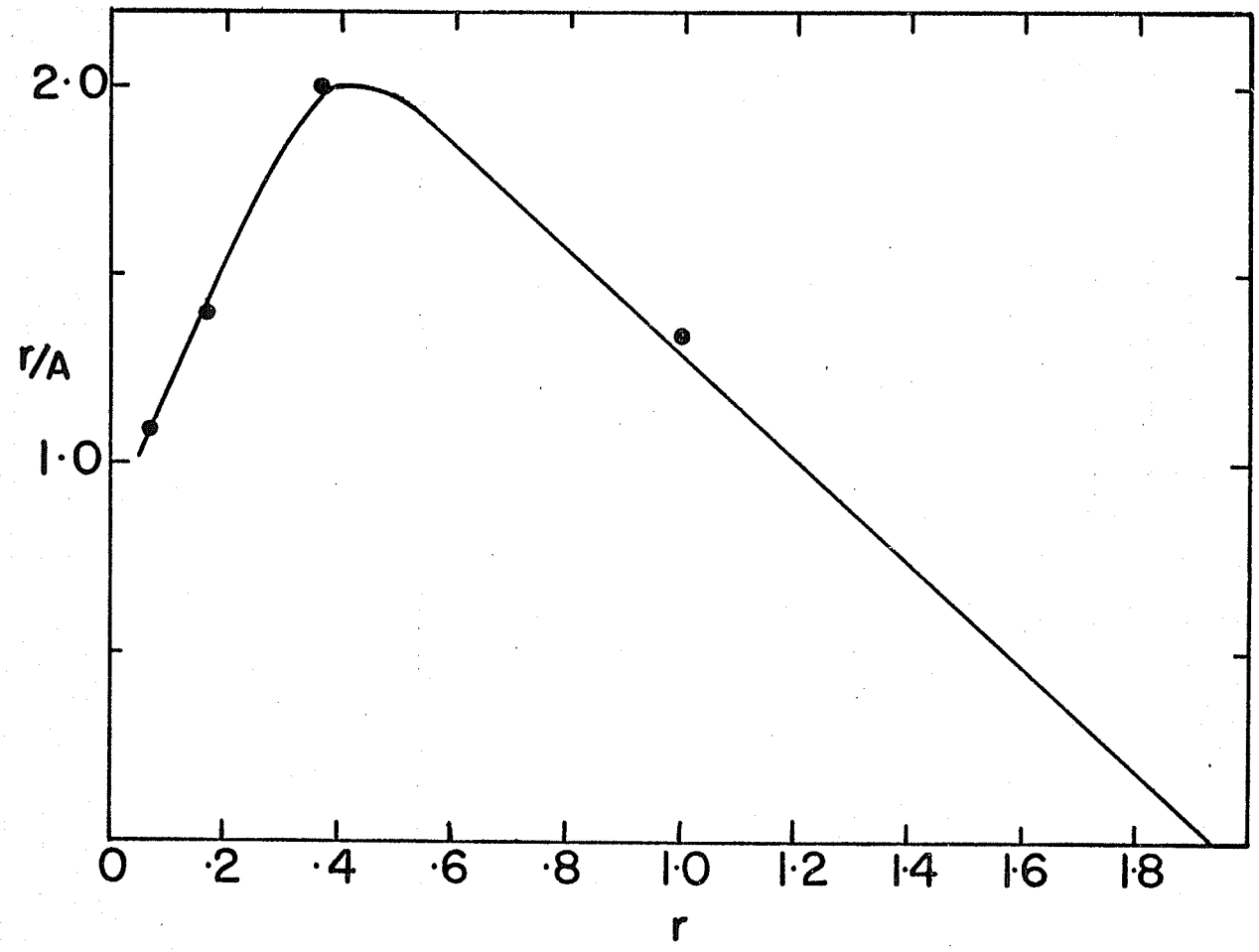
2·0
r/A
1·0
0
·2
·4
·6
·8
1·0
1·2
1·4
1·6
1·8
r

Binding of Isocitrate to Isocitrate Dehydrogenase

The binding of isocitrate-5,6-C^{14} was examined by equilibrium dialysis as described previously. In the range of 0.1 K_m to 10 K_m, a sigmoid binding curve was obtained (Fig. 50). The same data plotted according to equation (30) demonstrated a complex relationship between the isocitrate binding sites (Fig. 51). The n value obtained was approximately 4. The curve presented in Fig. 51 could possibly be generated if one assumes that isocitrate binds to two sets of non-identical sites (each set with 2 sites) and that in each set there is positive cooperativity of binding.

Viewed in this way, section I of Fig. 51 may represent cooperativity between the set of identical sites having a much greater affinity for isocitrate. Similarly, section II may represent binding to another set of sites of lesser affinity for the ligand and section III may represent a combination of both these effects.

To get some indication whether isocitrate competed with citrate for some of the binding sites, or, whether it influenced citrate binding, the binding of citrate-5,6-C^{14} was

Fig. 50. Plot of the binding of isocitrate to isocitrate dehydrogenase at several fixed concentrations of isocitrate. All data was obtained by equilibrium dialysis for 12 hours at 4° C, as described in the text.

All experiments were performed in phosphate buffer, 0.05 M, pH 6.5.

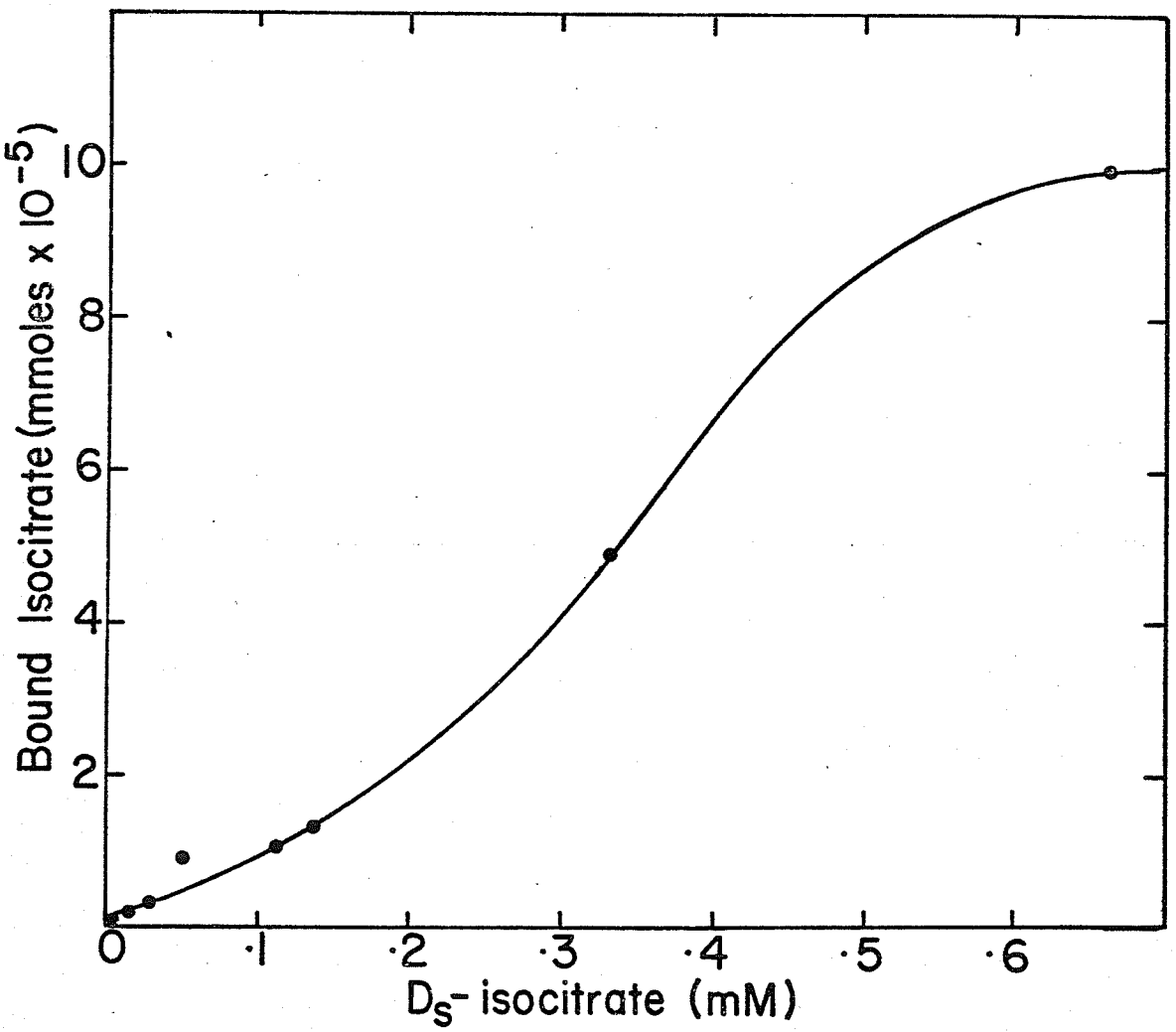
Bound Isocitrate (mmoles x 10^{-5})
10
8
6
4
2
0
·1
·2
·3
·4
·5
·6
D_S- isocitrate (mM)

Fig. 51. Data from Fig. 50 plotted according to equation (30). The line has been fitted by eye. The portions of the line I, II, and III are discussed in the text.

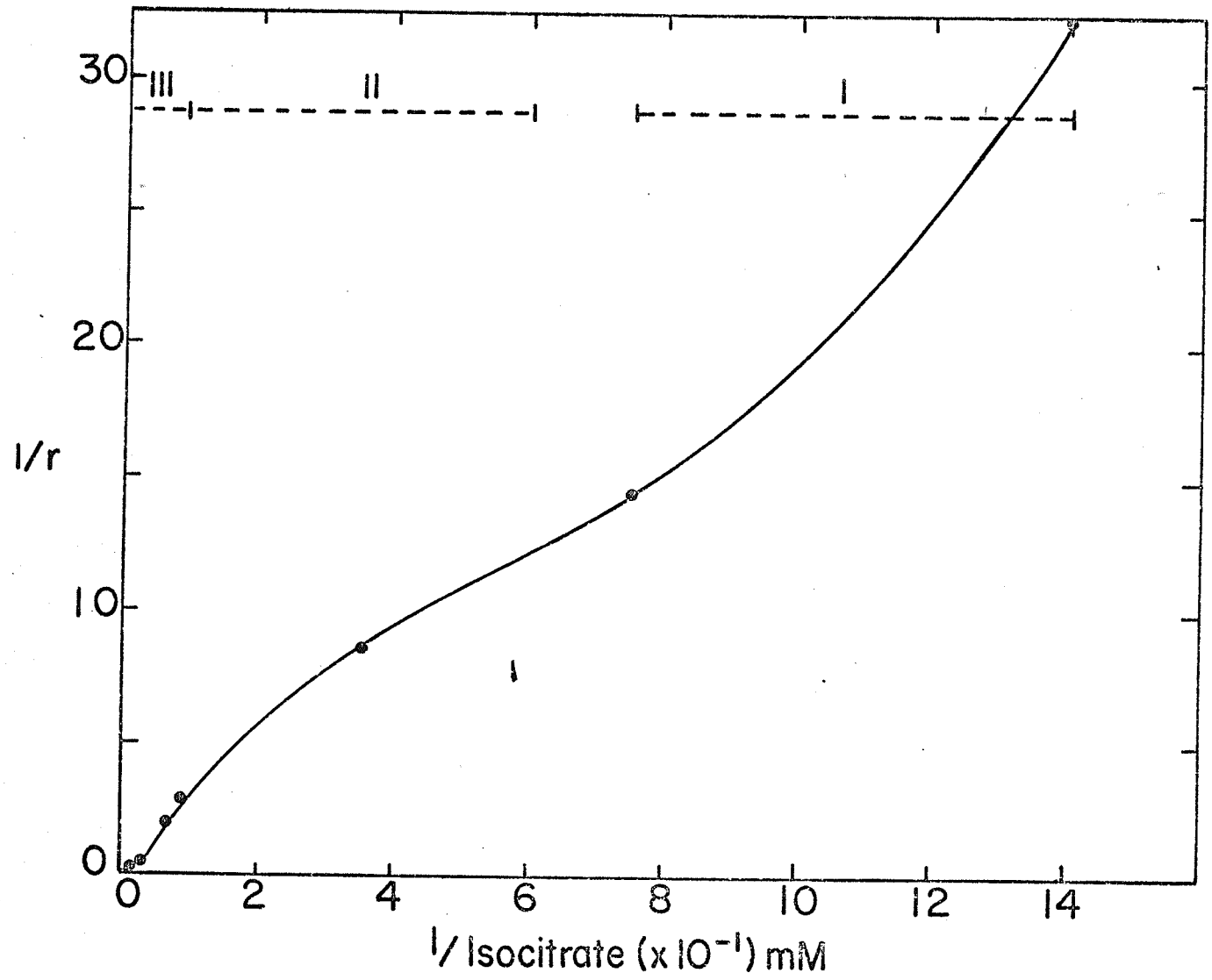
30
20
10
0
III
II
I
1/r
0
2
4
6
8
10
12
14
1/ Isocitrate (x 10⁻¹) mM

tested in the presence of cold isocitrate. The data presented in Table 5 indicated that isocitrate competed for some of the citrate binding sites.

Further experiments (using one fixed concentration of ligand and enzyme) indicated that the binding of citrate, isocitrate, AMP and NADH to isocitrate dehydrogenase was independent of the Mg^{++} ion (tested from 0 to 5 mM).

Table 5. Effect of cold isocitrate on the binding of citrate-5-6-C^{14} to isocitrate dehydrogenase.

citrate-C^{14}	isocitrate	citrate bound (mmoles)
.24 mM	-	$.94 \times 10^{-5}$
.24 mM	-	$.86 \times 10^{-5}$
.24 mM	.6 mM	$.64 \times 10^{-5}$
.24 mM	.6 mM	$.62 \times 10^{-5}$

DISCUSSION

DISCUSSION

From the results of the binding studies and the kinetic analysis presented earlier, a model for the subunit construction and mode of action of isocitrate dehydrogenase from Neurospora can be proposed (Fig. 56). The model is as follows:

1. The enzyme is composed of two non-identical subunits, one of which is productive (P subunit) and another non-productive (N subunit). As implied by the terminology, only the P subunit is capable of releasing the products.

2. Each of the subunits consists of two identical monomers. Thus, the enzyme is quasi-tetrameric.

3. Each monomer of the P subunit has one catalytic site each for NAD, AMP, and isocitrate while each monomer of the N subunit has one 'regulatory' site each for isocitrate and AMP. The isocitrate binding sites on this subunit are also capable of binding citrate.

4. The isocitrate and AMP binding sites on the N and P subunits are non-identical.

5. Kinetically, the enzyme follows a Random mechanism, and,

in general, binding of effectors and substrates change certain rate constants without changing the maximal velocity. This is possibly brought about by an intra- or intersubunit conformational change triggered by the binding of various ligands. Magnesium is required not for the binding of the substrates or effectors, but only for the activation of the ternary complex.

Before discussing the merits of this model, a few comments on the limitations of the experimental material and approach seem to be in order, since in the formulation of the model heavy reliance has been placed on the accuracy of the experimental binding data. In the equilibrium dialysis method (Peacocke and Skerrett, 1956), provided that the Donnan effects are at a minimum, the value of $\underline{r}$,

$$\underline{r} = \frac{C_i V_L - C_f V_T}{P V_E} = \frac{C_i - C_f (x + 1)}{P_x}$$

(where C_i and C_f are initial and final concentrations of unbound ligand, V_L and V_E are the volumes in the ligand compartment and enzyme compartment and V_T is the total volume, $x = V_E/V_L$) is subject to certain errors. If $\emptyset$ is one of the variables in the above equation, then the relative error

(Δ r/r) in r due to an error Δ $\emptyset$ is equal to the relative error, Δ $\emptyset/\emptyset$, multiplied by the coefficient ($C_f V_T / rPV_E$). For C_f, C_i and P these are, ($1 + C_f V_T / rPV_E$), ($1 + C_f / rP$), and 1 respectively. For maximum accuracy the coefficients should be as small as possible, and this occurs when the ratio of bound to total ligand is larger than at least 0.1. Using this criterion for reliability, considerable weight can be assigned to the values of r of up to 0.35 in the binding of AMP to the enzyme (Fig. 45). The value of n (2-4) obtained by extrapolation may or may not be a true value for the number of AMP binding sites. However, curvature of the Scatchard plots much before r attains the value of 0.35 (Fig. 45) shows that the AMP binding sites are non-identical. It may be pointed out here that non-linear Scatchard plots may be generated for identical binding sites, if, there is charge interaction (AMP is charged at all pH values above 2.5; see, Alberty et al., 1951) between bound molecules, or, if there is any significant amount of polymerization of either the ligand or the enzyme at higher concentrations. All these possibilities have been ruled out earlier. While AMP does show a tendency to 'stack' at higher concentrations (Van Holde and Rossetti, 1967), polymerization becomes significant only

at molarities higher than 0.01.

The binding of NADH to isocitrate dehydrogenase presented in the form of the Stockell plot (Fig. 42) seems to occur at two equal sites. It is reasonably certain that there are only two NADH binding sites on the enzyme surface. This is indicated by the results not only of spectrofluorometric titrations, but also of equilibration on Sephadex G-25. As used here, the latter method should give high values of binding since the column acts as an "infinite" source of NADH against which the enzyme is equilibrated with the result that even relatively weak binding will be detected. In all fairness it may be mentioned, however, that the value of n derived from the Stockell plots or Sephadex dialysis varies somewhat depending upon the molecular weight assigned to the enzyme. The effect of the value given to the molecular weight on the number of binding sites found by Sephadex dialysis is much more pronounced. The same uncertainties discussed above apply to the n values obtained for the binding of citrate (Fig. 49) and isocitrate (Fig. 51), although, it is clear that the number of binding sites for isocitrate are higher than those for citrate and NADH.

Contrary to the finding with NADH and AMP, citrate and,

partly, the isocitrate binding sites show positive cooperativity. This type of cooperativity can be interpreted in only one way, viz., that binding of one molecule of the ligand facilitates the binding of a second one (without any regard to the chemical identity or non-identity of the sites). The question that is of immediate importance is whether this cooperativity (for citrate molecules) is intra- or inter-protomeric, or, put in other words, are the cooperating sites present on the same subunit (monomer) or on different ones? This question, indeed, cannot be answered unless certain assumptions are made regarding the degree of polymerization of the enzyme, for which experimental data are not available. If the enzyme is considered to be a dimer constituted of two non-identical monomers, the two citrate binding sites would have to be on the same monomer. Alternatively, if the enzyme is considered to be a tetramer, which is more likely (Fig. 56), it would have to be assumed that each of the 2 identical N monomers bind citrate in a cooperative manner. The data for isocitrate binding (Fig. 51) are consistent with the assumption that the enzyme is tetrameric with two isocitrate molecules binding cooperatively on the P monomers, and two cooperatively on the N monomers. The data presented in Table

5 indicate that citrate and isocitrate may share the same binding sites on the N monomers, although it is equally possible that both of the ligands may have separate and distinct sites which affect each other by a conformational change.

Considering the totality of the kinetic and binding data, certain obvious difficulties of interpretation now arise if the enzyme is considered to be quasi-tetrameric. Taking the binding of NAD first, how can the presence of only two binding sites for this ligand be reconciled with the suggestion that the enzyme is tetrameric? It may be noted that an assumption runs through this discussion, namely, that the NADH binding sites are the same as the NAD binding sites, although due to the high dissociation constant of NAD (about 0.5 mM) it has not been feasible to undertake binding studies with this ligand directly. No apologies, however, need be offered for the assumption that NAD and NADH binding sites are identical. This is an unambiguous conclusion drawn from the kinetic studies. The possible presence of only two ligand binding sites in a tetrameric enzyme is not unique to isocitrate dehydrogenase. A few enzymes are, indeed, known which seem to have a smaller number of binding sites than

peptide chains, as, for example, beef liver glutamate dehydrogenase (Frieden, 1964), phosphorylase b (Madsen and Cori, 1957), and yeast UDP-galactose-4-epimerase (Darrow and Rodstrom, 1966). The case of the last named enzyme is particularly instructive. Here, one equivalent of NAD (or NADH) is bound per dimer, the monomers of which must exist in heterologous (using the terminology of Monod et al., 1965) association. The importance of heterologous associations, from the viewpoint of the mechanism of cooperativity (cf. Monod and Koshland's models) is that such associations allow monomers (identical or non-identical) to assume different conformations, and hybrid states predicted by Koshland's model are possible instead of only the two states permitted for isologous associations in Monod's model. Should the isocitrate dehydrogenase subunits be in heterologous association, cooperativity of the citrate as well as that of isocitrate molecules can easily be due to an induced conformational change communicated through the zones of association of the subunits.

As visualized in the model (Fig. 56), there is no positive cooperativity between the bound AMP molecules and consequently, AMP is unable to change the homotropic interactions of isocitrate by indirect means, as is postulated in

Monod's model. This contention is consistent with the binding as well as the kinetic data. AMP at saturating levels does not change the sigmoidality of the isocitrate plots at pH 7.5, although it does change the velocity of the reaction. It seems likely that this is caused by a 'direct' effect of AMP on the conformational state of isocitrate binding sites on individual monomers, and a concommitant change of the various associated rate constants of the reaction. It has been shown earlier that the enzymic reaction follows a Random mechanism in the absence of AMP but changes to an ordered or Rapid Equilibrium Random in its presence. In view of the binding data, it is now clear that the reaction must be Rapid Equilibrium Random. The question which remains to be answered is: How does a Random reaction become Rapid Equilibrium Random, or, paraphrased, how and under what conditions do non-linear reciprocal plots generated by a Random mechanism become linear? This question is a part of a more general question: Why does the heterogeneity of the ligand binding sites (for AMP and isocitrate) revealed by thermodynamic binding studies not clearly discernible in kinetic analysis?

To answer these questions some properties of the Random

rate equation can be examined. Consider two ligands X and Y which bind in a random manner, or, two molecules of the same ligand, X and X' which bind at chemically distinct binding sites (one productive and another non-productive) in such a way that only certain rate constants are altered but V_{max} remains the same for EX and EXX' complexes:

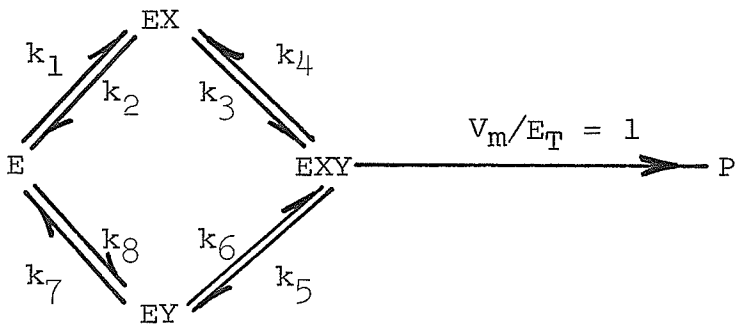

or,

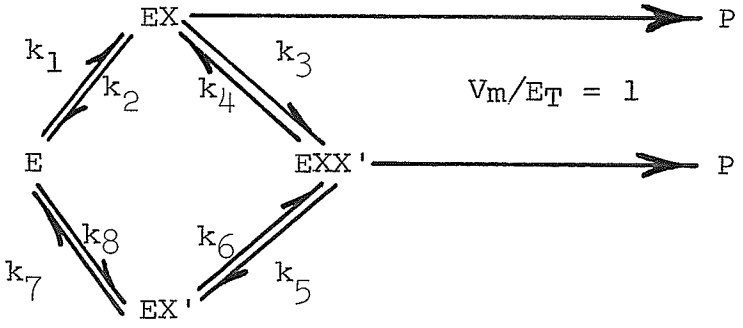

The reciprocal plots generated by these mechanisms have the form:

$$\frac{1}{v} = \frac{a + b\,(1/x) + c\,(1/x)^2}{1 + d\,(1/x)}$$

(where a, b, c and d are groupings of rate constants). These curves are hyperbolas with non-horizontal asymptotes given by:

$$\frac{1}{v} = (c/d)\,(1/x) + (bd - c)/d^2$$

If $cd^2 + a < bd$ the plot is convex up, if $cd^2 + a > bd$ it is concave down, and if $cd^2 + a = bd$, the curve reduces to a straight line.

The whole problem is then reduced to finding conditions under which $cd^2 + a$ becomes equal to bd. This can happen in a number of ways, i.e.,

1. If k_4 and k_5 are not greater than V_m/E_T and $k_2 = k_7$; $k_8/k_3 = k_5/(k_4 + k_5)$; $k_1/k_6 = k_4/(k_4 + k_5)$. The rate equation is then identical to equation (33).

2. If k_4 is $> V_mE_T$ but k_5 is $< V_mE_T$, the curve becomes straight if k_1 becomes equal to k_6. If opposite conditions prevail, i.e., k_5 is $> V_mE_T$ and $k_4 < K_mE_T$, the curve becomes straight if k_8 equals k_3.

3. If both k_4 and k_5 are $>> V_m/E_T$, the curve becomes straight, if, $(k_1/k_6)\,(k_5 + 2k_7) + (k_8/k_3)\,(k_4 + 2k_2) >> V_m/E_T$.

This is the traditional Rapid Equilibrium Random mechanism.

The cases discussed above serve to explain the actual kinetic data for more complicated situations. Considering the data of Fig. 38, for instance, if AMP binds to two heterogenous sites and the reaction is non-random, the double reciprocal plots should be 2/1 functions at all concentrations of isocitrate. Should the reaction be Random, however, the curves should be 3/2, 4/3, or more complicated functions (depending upon the concentration of NAD), but in all cases should be reduced to 2/1 functions at saturating levels of isocitrate. The curves of Fig. 38 indeed are functions more complex than 2/1 at lower isocitrate concentrations, but become straight lines at high concentrations. This can possibly be if isocitrate modifies the rate constants in such a way that $cd^2 + a$ becomes equal to bd.

Surprisingly, the positive cooperativity seen in the binding of citrate (Fig. 49) is not noted kinetically in the double reciprocal plot of $1/v - v_o$ versus 1/citrate (Fig. 26). On the basis of the binding behaviour these lines should have been curved. Similarly, the positive cooperativity of the active isocitrate sites on the P subunit indicated by the binding data is not discernable in the primary plots of the

kinetic results. However, replots of K_{app} from Fig. 26 do indicate such cooperativity.

As pointed out in preceeding paragraphs, there is a fair amount of agreement between the model (Fig. 56) and the experimental results, although the clarification of the detailed enzymic mechanism would have to await further experimental work. Despite the agreement, mentioned above, it is possible that the results could be explained on the basis of other models, and it seems worthwhile to examine these. Comparing the results with the allosteric model of Monod et al. (1965) it is evident that there are numerous discrepancies between the experimental data and the theory for this model to be valid in the case of isocitrate dehydrogenase. If one assumes that the enzyme exists primarily in the T state, the sigmoidality of NAD, isocitrate and AMP could be explained on the basis that these ligands stabilize the R state. However, the prediction of this model is that in the presence of saturating concentrations of all other ligands, the sigmoidality of the variable ligand should vanish. This is the case only for NAD and AMP. The rate-concentration curves for isocitrate always remain sigmoidal. For Monod's model to be applicable here one would have to

invoke non-exclusive binding (Rubin and Changeux, 1966), i.e., consider that the enzyme is present in solution not exclusively in the T state but also partly in the R state (see, Historical), or, if it is present mostly in the T state, the constant $\underline{c}$ of equations (4) and (5) is large. If the number of binding sites (n) is known, the theory of non-exclusive binding predicts that (equations 11, 12 and 13) the Hill coefficient ($\overline{n}$) will vary fundamentally depending upon the value of L (equation 12) and c. For a tetramer with L low (about 10^2) and c = 0, experimental $\overline{n}$ will be much less than n, but will reach 1 in the presence of saturating activator or inhibitor; for L values high (say, $> 10^5$) and c = 0, experimental $\overline{n}$ will be nearly equal to n and will reach 1 in the presence of saturating effectors (this is the ideal case). However, if $c > 10^{-3}$, the $\overline{n}$ value may or may not equal n, but it can never reach 1. With this analysis in mind, one can examine the behaviour of the curves when NAD is the variable substrate. The value of n is 2 and $\overline{n}$ approximates the same number. Saturation by isocitrate produces $\overline{n}$ values of 1. Thus, non-exclusive binding does not seem important here. This being so, equations (8), (16) and (17) should be applicable. Figs. 52 and 53 show that the expected linear

Fig. 52. Data from Fig. 30 plotted according to equation (17) assuming an n value of 2 for NAD. The lines have been fitted by eye.

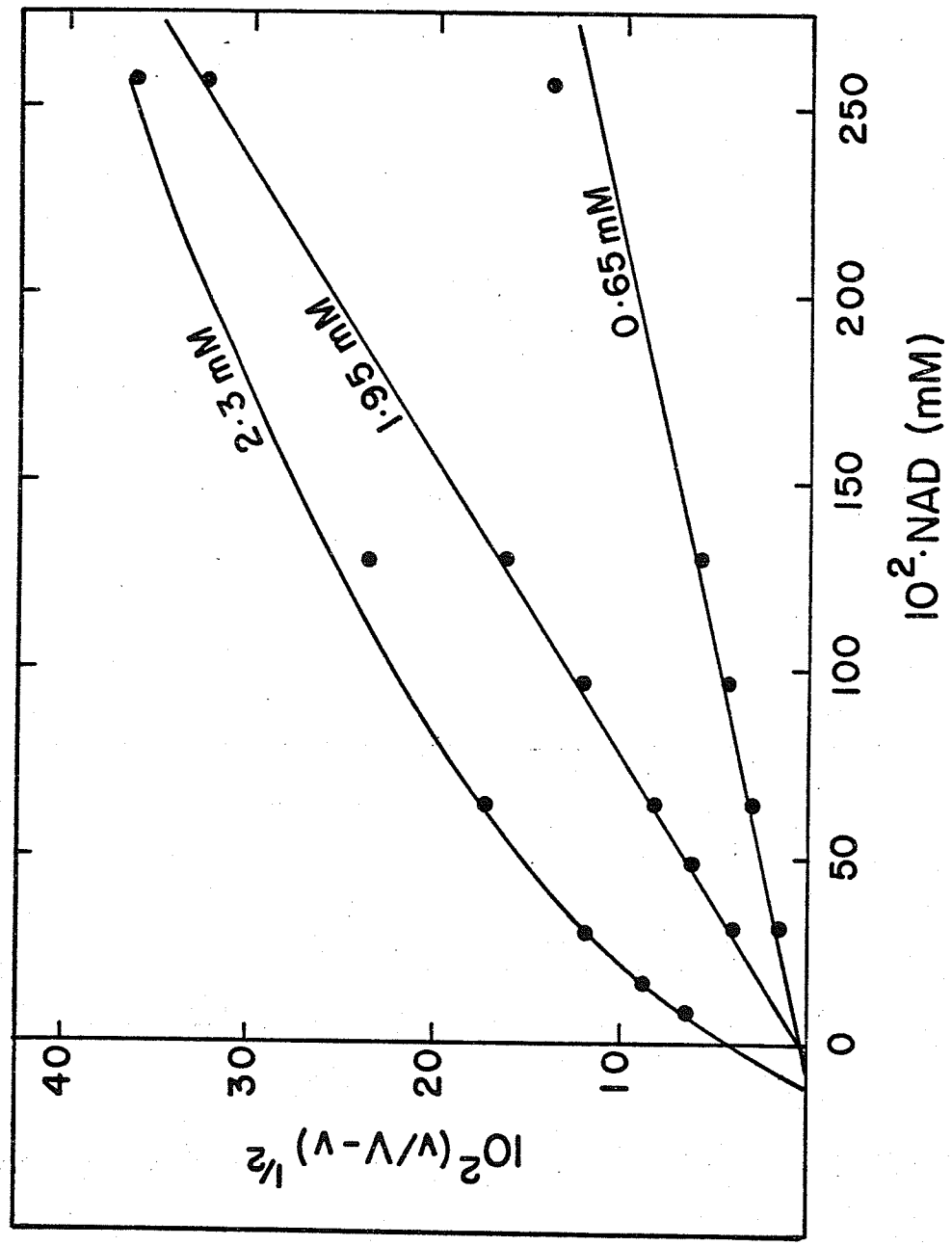
$10^2(v/V-v)^{1/2}$
10^2.NAD (mM)
0
10
20
30
40
50
100
150
200
250
2·3 mM
1·95 mM
0·65 mM

Fig. 53. Data from Fig. 30 plotted according to equation (17) assuming an n value of 4 for NAD. The lines have been fitted by eye.

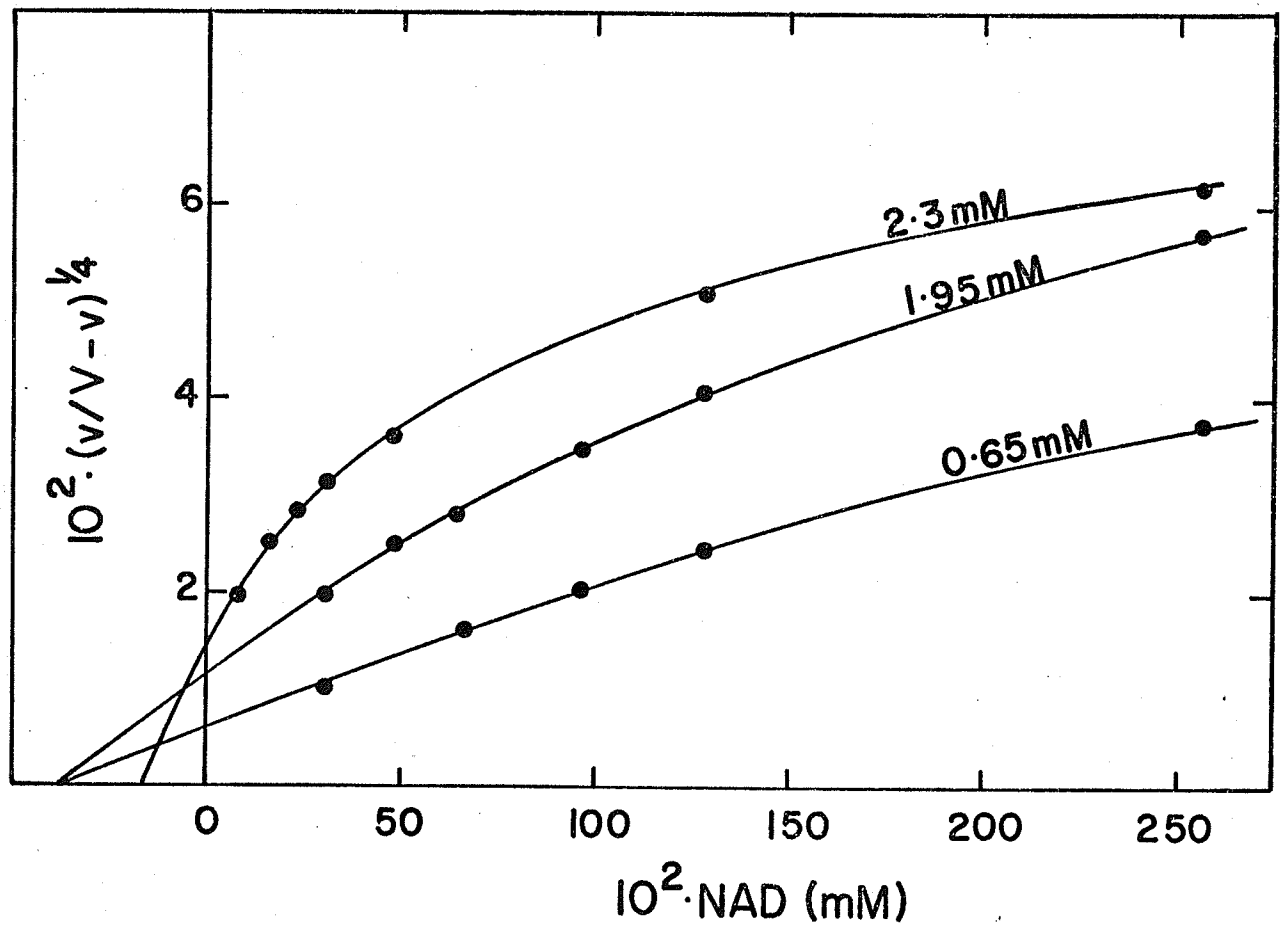
$10^2 \cdot (v/V-v)^{1/4}$
6
4
2
0
50
100
150
200
250
$10^2 \cdot$NAD (mM)
2·3mM
1·95mM
0·65mM

relationship is not fulfilled and different K_{NAD} values are obtained at different concentrations of isocitrate. The case of AMP is also similar (Figs. 54 and 55). If non-exclusive binding does not occur, this behaviour can only mean that the binding of the two ligands is not independent of one another, as postulated by the theory of allosteric transitions.

It is pertinent to point out here that the model presented for isocitrate dehydrogenase earlier does not account for all the complexities of the binding and kinetic behaviour. Unexplained in detail is the binding curve of isocitrate and the effect of pH (from the structural point of view) on the kinetics of the enzyme. In this regard, the model may only be considered as an oversimplified approximation.

Fig. 54. Data from Fig. 38 plotted according to equation (17) assuming an n value of 2 for AMP. The lines have been fitted by eye.

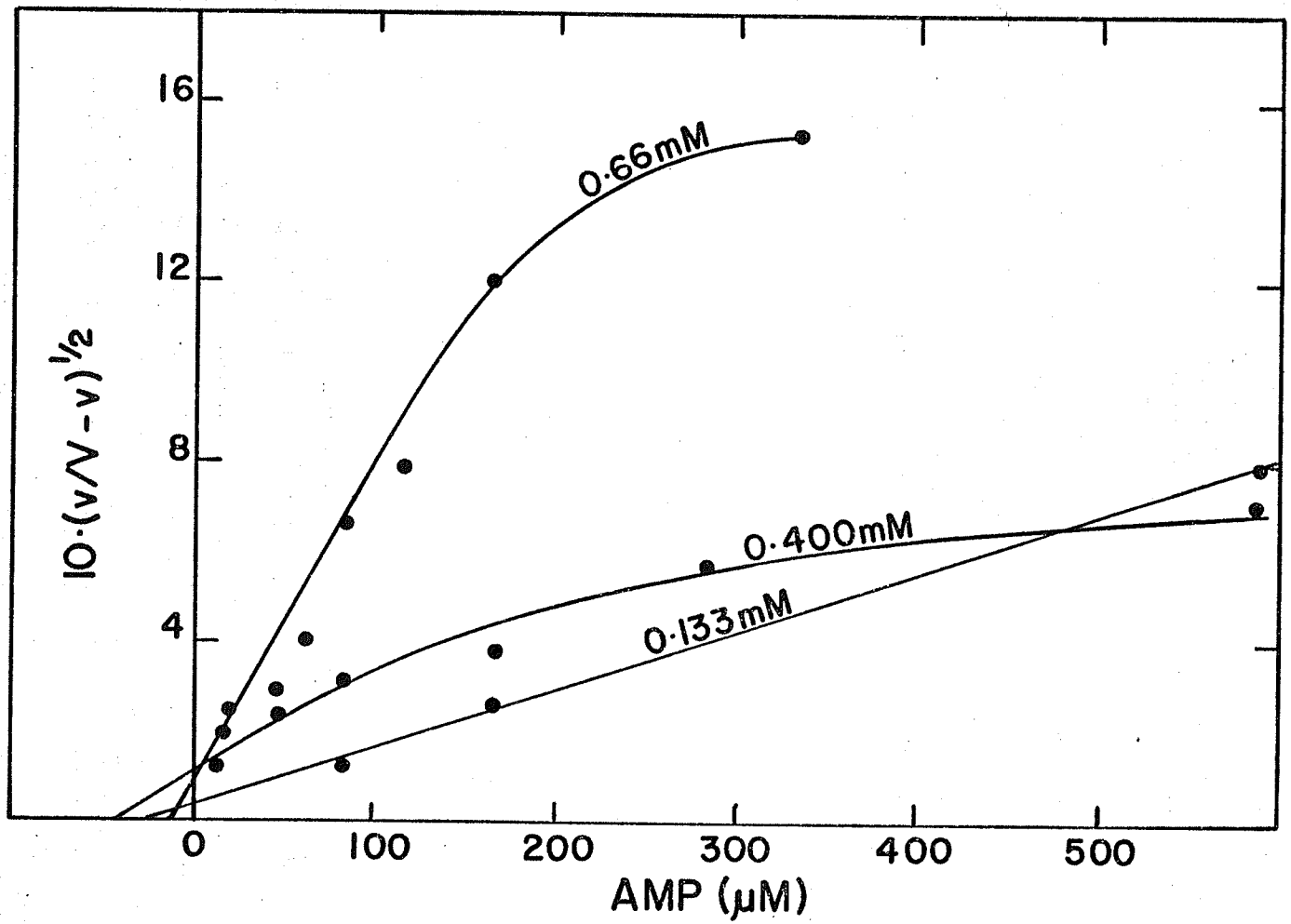
16
12
8
4
0
100
200
300
400
500
10·(v/V-v)^1/2
AMP (μM)
0·66mM
0·400mM
0·133mM

Fig. 55. Data from Fig. 38 plotted according to equation (17) assuming an n value of 4 for AMP. The lines have been fitted by eye.

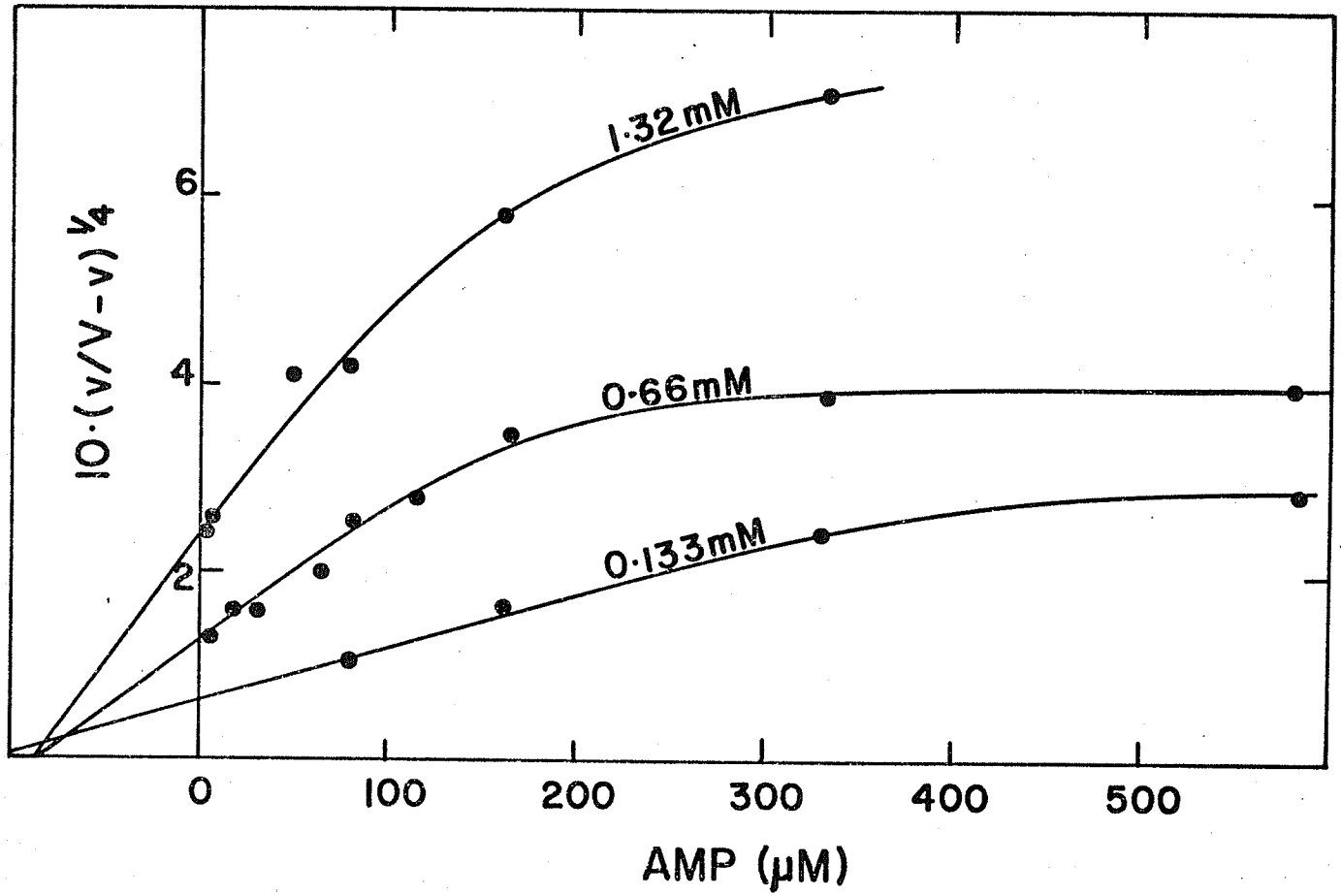
1·32 mM
0·66 mM
0·133 mM
10·(v/V-v) ¼
6
4
2
0
100
200
300
400
500
AMP (μM)

Fig. 56. A proposed model for the isocitrate dehydrogenase molecule.

A is AMP, D is NAD, C is citrate and I is isocitrate. P and N refer to the productive and non-productive subunit, respectively.

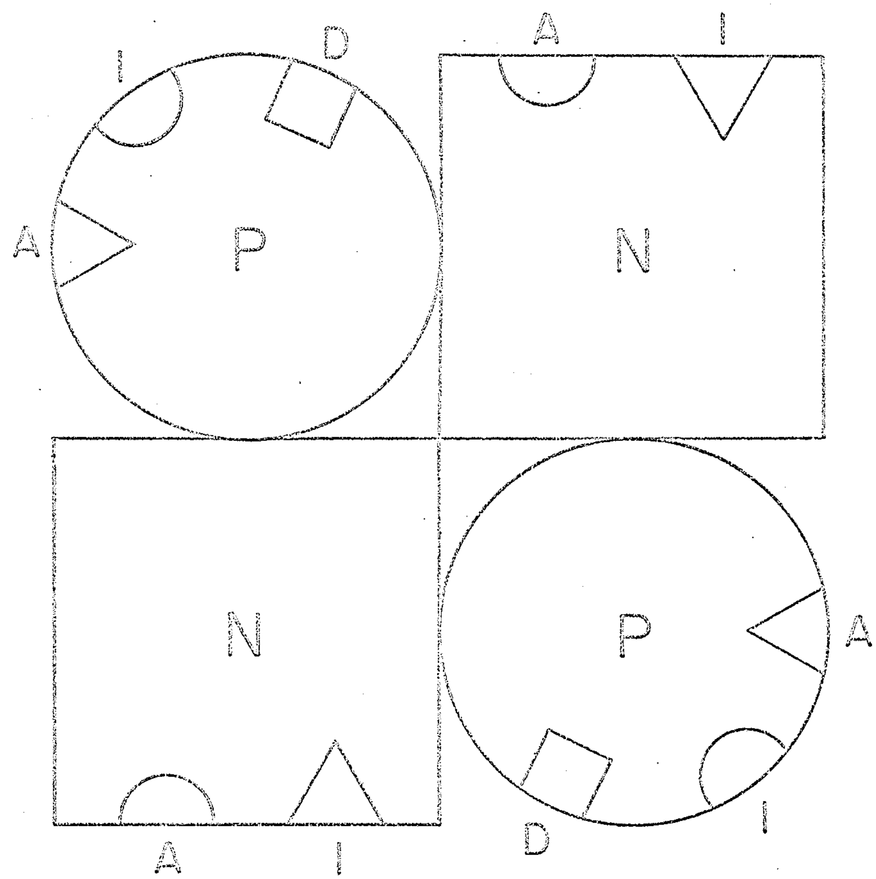
I
D
A
I
A
P
N
N
P
A
A
I
D
I

REFERENCES

REFERENCES

Adair, G. S. (1925). The hemoglobin system. VI. The oxygen dissociation curve of hemoglobin. J. Biol. Chem., 63: 529.

Adler, E., von Euler, H., Gunther, G., and Plass, M. (1939). CXXVI - Isocitric dehydrogenase and glutamic acid synthesis in animal tissues. Biochem. J., 33: 1028.

Alberty, R. A., Smith, R. M., and Bock, R. M. (1951). The apparent ionization constants of adenosinephosphates and related compounds. Jour. Biol. Chem., 193: 425.

Algranati, I., and Cabib, E. (1962). Uridine diphosphate d-glucose-glycogen glucosyltransferase from yeast. J. Biol. Chem., 237: 1007.

Anderson, S. R., and Weber, G. (1965). Multiplicity of binding by lactate dehydrogenase. Biochemistry 4: 1948.

Antonini, E., Wyman, J., Moretti, R., and Rossi-Fanelli, A. (1963). The interaction of bromthymol blue with

hemoglobin and its effect on the oxygen equilibrium. Biochim. Biophys. Acta, 71: 124.

Atkinson, D. E., and Walton, G. M. (1965). Kinetics of regulatory enzymes. E. coli phosphofructokinase. J. Biol. Chem., 240: 757.

Atkinson, D. E., Hathaway, J. A., and Smith, E. C. (1965). Kinetics of regulatory enzymes. Kinetic order of the yeast DPN-isocitrate dehydrogenase reaction and a model for the reaction. J. Biol. Chem., 240: 2682.

Atkinson, D. E. (1966). Regulation of enzyme activity. Ann. Reviews Biochem., 35: 85.

Blangy, D. (1967). Ph.D. dissertations. Pasteur Institute, Paris, France.

Brown, W. E. L., and Hill, A. V. (1923). The oxygen-dissociation curve of blood, and its thermodynamical basis. Proc. Roy. Soc., B, 94: 297.

Cennamo, C., Boll, M., and Holzer, H. (1964). Uber threoninedehydratase aus Saccharomyces cerevisiae.

Biochem. Zeitchrift, 340: 125.

Cennamo, C., Montecuccoli, G., and Bonaretti, G. (1967). Anion and substrate inhibition and kinetic behaviour of NAD-specific isocitrate dehydrogenase from Baker's yeast. Biochim. Biophys. Acta, 132: 232.

Chan, M. F., Stachow, C. S., and Sanwal, B. D. (1965). The allosteric nature of NAD-specific isocitric dehydrogenase from Aspergilli. Can. J. Biochem., 43: 111.

Changeux, J. P., (1961). The feedback control mechanism of biosynthetic L-threonine deaminase by L-isoleucine. Cold Spring Harbor Symp. Quant. Biol. 26: 313.

Changeux, J. P. (1963). Allosteric interactions on biosynthetic L-threonine deaminase from E. coli K12. Cold Spring Harbor Symp. Quant. Biol., 28: 497.

Changeux, J. P., Gerhart, J. C., and Schachman, H. K., (1967). J. Mol. Biol. (in press).

Chen, R. F., and Plaut, G. W. E. (1963). Activation and inhibition of DPN-linked isocitrate dehydrogenase of

heart by certain nucleotides. Biochemistry 2: 1023.

Chen, R. F., Brown, D. M., and Plaut, G. W. E. (1964). DPN-linked isocitrate dehydrogenase of bovine heart. Structural changes associated with activation by ADP. Biochemistry 3: 552.

Cleland, W. W. (1963a). The kinetics of enzyme-catalyzed reactions with two or more substrates or products. I. Nomenclature and rate equations. Biochim. Biophys. Acta, 67: 104.

Cleland, W. W. (1963b). The kinetics of enzyme-catalyzed reactions with two or more substrates or products. II. Inhibition - nomenclature and theory. Biochim. Biophys. Acta, 67: 173.

Cleland, W. W. (1963c). The kinetics of enzyme-catalyzed reactions with two or more substrates or products. III. Prediction of initial velocity and inhibition patterns. Biochim. Biophys. Acta, 67: 188.

Cleland, W. W. (1963d). Computer programmes for processing enzyme kinetic data. Nature 198: 463.

Cohen, M., Cohen, G. N., and Monod, J. (1953). L'effect inhibiteur specifique de la methionine-synthase chez Escherichia coli. Compte. Rend., 236: 746.

Dalziel, K. (1957). Initial steady-state velocities in the evaluation of enzyme-coenzyme-substrate reaction mechanisms. Acta Chem. Scand. 11: 1706.

Daniel, E., and Weber, G. (1966). Cooperative effects in binding by serum albumin. I. The binding of 1-anilino-8-naphthalene-sulfonate: Fluorimetric titrations. Biochemistry 5: 1893.

Darrow, R. A., and Rodstrom, R. (1966). Subunit association and catalytic activity of uridine diphosphate galactose-4-epimerase from yeast. Proc. Natl. Acad. Sci. 55: 205.

Datta, P., Gest, H., and Segal, H. (1964). Effect of feedback modifiers on the state of aggregation of homoserine dehydrogenase of rhodospirillum rubrum. Proc. Natl. Acad. Sci. U. S. 51: 125.

Datta, P., and Gest, A. (1964). Alternate patterns of end-product control in biosynthesis of amino-acids of the

aspartic family. Nature 203: 1259.

Davies, D. D. (1955). The oxidation of d-isocitrate by pea seedling mitochondria. J. Exptl. Botany, 6: 212.

Dische, Z. (1940). Sited in Adv. in Enzymology 28: 41. Bull. Soc. Biochim. France, 23: 1140.

Ernster, L., and Navazio, F. (1957). Studies on TPN-linked oxidations. I. Pathways of isocitrate oxidation in rat liver mitochondria. Biochim. Biophys. Acta, 26: 408.

Fairclough, G. F., and Fruton, J. S. (1966). Peptide-protein interactions as studied by gel filtration. Biochemistry 5: 673.

Freundlich, M., and Umbarger, H. E. (1963). The effect of analogues of threonine and of isoleucine on the properties of threonine deaminase. Cold Spring Harbor Symp. Quant. Biol., 28: 505.

Frieden, C. (1957). The calculation of an enzyme-substrate dissociation constant from the overall initial velocity for reactions involving two substrates. J. Am. Chem.

Soc., 79: 1894.

Frieden, C. (1964). Relationship between subunit structure and activity for beef liver glutamic dehydrogenase. Brookhaven Symp. Biol., No. 17: 98.

Frieden, C. (1964). Treatment of enzyme kinetic data. I. The effect of modifiers on the kinetic parameters of single substrate enzymes. J. Biol. Chem., 239: 3522.

Frieden, C., and Colman, R. F. (1967). Glutamate dehydrogenase concentration as a determinant in the effect of purine nucleotides on enzymatic activity. J. Biol. Chem., 242: 1705.

Gerhart, J. C., and Pardee, A. B. (1962). The enzymology of control by feedback inhibition. J. Biol. Chem., 237: 891.

Gerhart, J. C., and Pardee, A. B. (1964). Aspartate transcarbamylase - an enzyme designed for feedback inhibition. Fed. Proc. 23: 727.

Gerhart, J. C., and Schachman, H. K. (1965). Distinct subunits for the regulation and catalytic activity of

aspartate transcarbamylase. Biochemistry 4: 1054.

Gorini, L., and Maas, W. K. (1956). The potential for the formation of a biosynthetic enzyme in Escherichia coli. Biochim. Biophys. Acta, 25: 208.

Gross, S. R., and Webster, R. E. (1963). Some aspects of interallelic complementation involving leucine biosynthetic enzymes of Neurospora. Cold Spring Harbor Symp. Quant. Biol., 28: 543.

Hathaway, J. A., and Atkinson, D. E. (1963). The effect of adenylic acid on yeast nicotinamide adenine dinucleotide isocitrate dehydrogenase, a possible metabolic control mechanism. J. Biol. Chem., 238: 2875.

Helmreich, E., and Cori, C. F. (1964). The role of adenylic acid in the activation of phosphorylase. Proc. Natl. Acad. Sci. U. S. 51: 131.

Hummel, J. P., and Dreyer, W. J. (1962). Measurement of protein-binding phenomena by gel filtration. Biochim. Biophys. Acta, 63: 530.

Kaplan, N. O., Swartz, M. N., Frech, M. E., and Ciotti, M. M.

(1956). Phosphorylative and nonphosphorylative pathways of electron transfer in rat liver mitochondria. Proc. Natl. Acad. Sci. U. S. 42: 481.

King, E. L., and Altman, C. (1956). A schematic method of deriving the rate laws for enzyme-catalyzed reactions. J. Phys. Chem., 60: 1375.

Kirschner, K., Eigen, M., Bittman, R., and Voigt, B. (1966). The binding of nicotinamide-adenine dinucleotide to yeast D-glyceraldehyde-3-phosphate dehydrogenase. Temperature-jump relaxation studies on the mechanism of an allosteric enzyme. Proc. Natl. Acad. Sci. U. S. 56: 1661.

Klotz, I. M., Walker, F. M., and Pivan, R. B. (1946). The binding of organic ions by proteins. J. Am. Chem. Soc., 68: 1486.

Kornberg, A., and Pricer, Jr., W. E. (1951). Di and tri-phosphopyridine nucleotide isocitric dehydrogenases in yeast. J. Biol. Chem., 189: 123.

Kornfield, S., Kornfield, R., Neufeld, E., and O'Brien, P. J.

(1964). The feedback control of sugar nucleotide biosynthesis in liver. Proc. Natl. Acad. Sci. U. S. 52: 371.

Koshland, Jr., D. E. (1963). Correlation of structure and function in enzyme action. Science 142: 1533.

Koshland, Jr., D. E., Nemethy, G., and Filmer, D. (1966). Comparison of experimental binding data and theoretical models in proteins containing subunits. Biochemistry 5: 365.

Krebs, H. (1964). The Croonian Lecture. Gluconeogenesis. Proc. Roy. Soc., 159: 545.

Lowry, O. H., Rosebrough, N. J., Farr, A. L., and Randall, R. J. (1951). Protein measurement with the Folin phenol reagent. J. Biol. Chem., 193: 265.

Lowry, O. H., Schulz, D. W., and Passonneau, J. V., (1967). The kinetics of glycogen phosphorylases from brain and muscle. J. Biol. Chem., 242: 271.

Madsen, N. B. (1964). Allosteric properties of phosphorylase

b. Biochem. Biophys. Res. Commun., 15: 390.

Madsen, N. B., and Cori, C. F. (1957). The binding of adenylic acid by muscle phosphorylase. J. Biol. Chem., 224: 899.

Maeba, P., and Sanwal, B. D. (1965). Feedback inhibition of phosphoenolpyruvate carboxylase of Salmonella. Biochem. Biophys. Res. Commun., 21: 503.

Maeba, P., and Sanwal, B. D. (1966). The allosteric threonine deaminase of Salmonella. Kinetic model for the native enzyme. Biochemistry 5: 525.

Maley, G. F., and Maley, F. (1964). The purification and properties of deoxycytidylate deaminase from chick embryo extracts. J. Biol. Chem., 239: 1168.

Mansour, T. E., and Mansour, J. M. (1962). Effects of serotonin and adenosine 3'-5'-phosphate on phospho-fructokinase from the liver fluke Fasciola hepatica. J. Biol. Chem., 237: 629.

Martin, R. G., and Ames, B. N. (1961). A method for

determining the sedimentation behaviour of enzymes: Applications to protein mixtures. J. Biol. Chem., 236: 1372.

Martin, R. G. (1962). The first enzyme in histidine biosynthesis. The nature of feedback inhibition by histidine. J. Biol. Chem., 237: 257.

Melo, A., and Glaser, L. (1965). The nucleotide specificity and feedback control of thymidine diphosphate D-glucose pyrophosphorylase. J. Biol. Chem., 240: 398.

Monod, J., Changeux, J. P., and Jacob, F. (1963). Allosteric proteins and cellular control systems. J. Mol. Biol., 6: 306.

Monod, J., Wyman, J., and Changeux, J. P. (1965). On the nature of allosteric transitions: A plausible model. J. Mol. Biol., 12: 88.

Myer, Y. P., and Schellman, J. A. (1962). The interaction of ribonuclease with purine and pyrimidine phosphates. I. Binding of adenosine-5'-monophosphate to ribonuclease. Biochim. Biophys. Acta, 55: 361.

Neufeld, E. F., and Hall, C. W. (1965). Inhibition of UDP-D-glucose dehydrogenase by UDP-D-xylose: a possible regulatory mechanism. Biochem. Biophys. Res. Commun., 19: 456.

Ochoa, S. (1948). Biosynthesis of tricarboxylic acids by carbon dioxide fixation. III. Enzymatic mechanisms. J. Biol. Chem., 174: 133.

Passonneau, J. V., and Lowry, O. H. (1962). Phosphofructokinase and the pasteur effect. Biochem. Biophys. Res. Commun., 7: 10.

Peacocke, A. R., and Skerrett, J.N.H. (1956). The interaction of amino acridines with nucleic acids. Trans. Faraday Soc., 52: 261.

Patte, J. C., and Cohen, G. N. (1964). Interactions cooperatives effecteur-effecteur chez deux enzymes allosterique inhibees de maniere non competitive. C. R. Acad. Sci. 259: 1255.

Ranakrishnan, C. V., and Martin, S. M. (1955). Isocitric dehydrogenase in Aspergillus niger. Arch. Biochem.

Biophys., 55: 403.

Rao, M.R.R. (1955). Ph.D. dissertation, University of Illinois.

Reiner, J. M. (1959). Behaviour of enzyme systems. Minneapolis, Minn., Burgess.

Roberts, R. B., Abelson, P. H., Cowie, D. V., Bolton, E. T., and Britten, R. J. (1955). Studies on the biosynthesis in Escherichia coli. Carnegie Institute, Washington, D.C., Publ. No. 607.

Rosen, O. M., Copeland, P. L., and Rosen, S. M. (1966). The subunit structure of fructose-1,6-diphosphatase. Proc. Natl. Acad. Sci. U. S. 55: 1156.

Rossetti, G. P., and Von Holde, K. E. (1967). Association of adenosine-5'-phosphate in aqueous solutions. Biochem. Biophys. Res. Commun., 26: 717.

Rubin, M. M., and Changeux, J. P. (1966). On the nature of allosteric transitions: Implications of non-exclusive ligand binding. J. Mol. Biol., 21: 265.

Salas, M., Vinuela, E., Salas, J., and Sols, A. (1964). Muscle fructose-1,6-diphosphatase. Biochem. Biophys. Res. Commun., 17: 150.

Sanwal, B. D., and Lata, M. (1961). The occurrence of two different glutamic dehydrogenases in Neurospora. Can. J. Microbiol., 7: 319.

Sanwal, B. D., Zink, M. W., and Stachow, C. S. (1963). Control of DPN-specific isocitric dehydrogenase activity by precursor activation and end product inhibition. Biochem. Biophys. Res. Commun. 12: 510.

Sanwal, B. D., Zink, M. W., and Stachow, C. S. (1964). Nicotinamide adenine dinucleotide-specific isocitric dehydrogenase. J. Biol. Chem., 239: 1597.

Sanwal, B. D., and Stachow, C. S. (1965). Allosteric activation of nicotinamide-adenine dinucleotide specific isocitrate dehydrogenase of Neurospora. Biochim. Biophys. Acta, 96: 28.

Sanwal, B. D., Stachow, C. S., and Cook, R. A. (1965). A kinetic model for the mechanism of allosteric activation of

nicotinamide-adenine dinucleotide specific isocitrate dehydrogenase. Biochemistry 4: 410.

Sanwal, B. D., Maeba, P., and Cook, R. A. (1966). Interaction of macroions and dioxane with the allosteric phospho-enolpyruvate carboxylase. J. Biol. Chem., 241: 5177.

Sanwal, B. D., and Cook, R. A. (1966). Effect of adenylic acid on the regulatory nicotinamide-adenine dinucleotide specific isocitrate dehydrogenase. Biochemistry 5: 886.

Sanwal, B. D., and Maeba, P. (1966a). Regulation of the activity of phosphoenolpyruvate carboxylase by fructose diphosphate. Biochem. Biophys. Res. Commun., 22: 194.

Sanwal, B. D., and Maeba, P. (1966b). Phosphoenolpyruvate carboxylase: Activation by nucleotides as a possible compensatory feedback effect. J. Biol. Chem., 241: 4557.

Scarano, E., Geraci, G., Polzella, A., and Campanile, E. (1963). The enzymatic aminohydrolysis of 4-aminopyrimidine deoxyribonucleotides. IV. On the possibility of the occurrence of an allosteric site on

2'-deoxyribosyl-4-amino-pyrimidone-2,5'-phosphate aminohydrolase. J. Biol. Chem., 238: 1556.

Scarano, E., Geraci, G., and Rossi, M. (1964). On the regulatory properties of deoxycytidylate aminohydrolase. Biochem. Biophys. Res. Commun., 16: 239.

Scatchard, G., Scheinberg, I. H., and Armstrong, S. H., Jr., (1950). Physical chemistry of protein solutions. IV. Combination of human serum albumin with Cl^-. J. Am. Chem. Soc., 72: 535.

Scatchard, G., Coleman, J. S., and Shen, A. L. (1957). Physical chemistry of protein solutions. VII. The binding of small anions to serum albumin. J. Am. Chem. Soc., 79: 12.

Schachman, H. K. (1959). Ultracentrifugation in Biochemistry, Academic Press, Inc., New York, New York.

Sober, H. A., Gutter, F. J., and Wychoff, M. M. (1956). Chromatography of proteins. II. Fractionation of serum protein on anion-exchange cellulose. J. Am. Chem. Soc., 78: 756.

Stadtman, E. R., Cohen, G. N., Le Bras, G., and de Robichon-Szulmajster, H. (1961). Feedback inhibition and repression of aspartokinase activity in Escherichia coli and Saccharomyces cerevisiae. J. Biol. Chem. 236: 2033.

Stadtman, E. R. (1966). Allosteric regulation of enzyme activity. Adv. in Enzymology 28: 41.

Stockell, A. (1959). The binding of diphosphopyridine nucleotide by yeast glyceraldehyde-3-phosphate dehydrogenase. J. Biol. Chem., 234: 1286.

Sturani, E., Datta, F., Hugues, M., and Gest, H. (1963). Regulation of enzyme activity by specific reversal of feedback inhibition. Science 141: 1053.

Takata, K., and Pogell, B. M. (1965). Allosteric inhibition of rat liver fructose-1,6-diphosphatase by AMP. J. Biol. Chem., 240: 651.

Traut, R. R., and Lipmann, F. (1963). Activation of glycogen synthetase by glucose-6-phosphate. J. Biol. Chem., 238: 1213.

Ullman, A., Vagelos, P. R., and Monod, J. (1964). The effect

of AMP upon the association between bromthymolblue and muscle phosphorylase b. Biochem. Biophys. Res. Commun., 17: 86.

Umbarger, H. E., (1956). Evidence for a negative feedback mechanism in the biosynthesis of isoleucine. Science 123: 848.

Vagelos, P. R., Alberts, A. W., and Martin, D. B. (1963). Studies on the mechanism of activation of acetyl-CoA carboxylase by citrate. J. Biol. Chem., 238: 533.

Velick, S. F. (1958). Fluorescence spectra and polarization of glyceraldehyde-3-phosphate and lactic dehydrogenase coenzyme complexes. J. Biol. Chem., 233: 1455.

Vogel, H. J. (1956). A convenient growth medium for Neurospora (Medium N). Microbial Genetics Bull., 13: 42.

Wratten, C. C., and Cleland, W. W. (1963). Product inhibition studies on yeast and liver alcohol dehydrogenases. Biochemistry 2: 935.